KfK 3457
August 1984
(1. Ex.)

Experimental Determination of the Atmospheric Dispersion Parameters at the Karlsruhe Nuclear Research Center for 160 m and 195 m Emission Heights

Part 2: Evaluation of Measurements

P. Thomas, K. Nester
Hauptabteilung Sicherheit
Projekt Nukleare Sicherheit

Kernforschungszentrum Karlsruhe

KERNFORSCHUNGSZENTRUM KARLSRUHE

Hauptabteilung Sicherheit

Projekt Nukleare Sicherheit

KfK 3457

Experimental Determination of the Atmospheric Dispersion Parameters at the Karlsruhe Nuclear Research Center for 160 m and 195 m Emission Heights

Part 2: Evaluation of Measurements

P. Thomas
K. Nester

Kernforschungszentrum Karlsruhe GmbH, Karlsruhe

Kernforschungszentrum Karlsruhe GmbH
ISSN 0303-4003

Abstract

Experiments are carried out at the Kernforschungszentrum Karlsruhe in order to determine the atmospheric diffusion of pollutants. The influence on atmospheric diffusion by conditions specific to the site will be investigated.

For evaluation of the measurements the diffusion is assumed to be a steady-state process. A two-dimensional Gaussian distribution is used as the theoretical approximation of the concentrations. The dependence of the dispersion parameters σ_y and σ_z on the downwind distance is described by a power function. A least squares fit is applied to calculate the horizontal and vertical dispersion parameters and the normalized diffusion factor with the respective errors from the measured wind velocity, emission rate and concentration distribution. The dispersion parameters determined are assigned to stability classes by the measured standard deviation of the vertical wind direction.

The reported dispersion parameters are derived from 18 experiments with mostly two sampling periods of 30 min duration each. In 17 experiments two different tracers were released simultaneously at 160 m and 195 m height, in one experiment three different tracers were released. The results of the individual experiments have been combined and smoothed to a set of dispersion parameters for the stability classes A to F.

In Part 1 of this report the diffusion experiments are described and the measured data are presented in detail. The results of earlier experiments performed at the Kernforschungszentrum Karlsruhe for emission heights of 60 m and 100 m have been published already.

Experimentelle Bestimmung der atmosphärischen Ausbreitungsparameter für Emissionshöhen von 160 m und 195 m am Kernforschungszentrum Karlsruhe

Teil 2: Auswertung der Meßergebnisse

Zusammenfassung

Am Kernforschungszentrum Karlsruhe werden Experimente durchgeführt, um die Ausbreitung von Schadstoffen in der Atmosphäre zu erforschen. Standortspezifische Einflüsse sollen dabei untersucht werden.

Mittels der Methode der kleinsten Fehlerquadrate werden aus der gemessenen Konzentrationsverteilung die horizontalen und vertikalen Ausbreitungsparameter und der normierte Ausbreitungsfaktor mit den zugehörigen Fehlerbreiten ermittelt. Für die Konzentration wird eine zweidimensionale Gaußverteilung zugrunde gelegt. Die Ausbreitung wird als stationär angenommen. Ein Potenzansatz beschreibt die Abhängigkeit der Ausbreitungsparameter von der Quelldistanz. Die Zuordnung der ermittelten Ausbreitungsparameter zu Ausbreitungskategorien erfolgt über die gemessene Standardabweichung der vertikalen Windrichtung.

Die angegebenen Ausbreitungsparameter stammen von 18 Experimenten mit zumeist zwei Sammelperioden von 30 min Dauer. In 17 Experimenten wurden jeweils zwei verschiedene Tracer, in einem Experiment jeweils drei verschiedene Tracer simultan in 160 m und 195 m Höhe freigesetzt. Die Ergebnisse der Einzelversuche wurden zusammengefaßt und geglättet und ergaben einen vollständigen Satz von Ausbreitungsparametern für die Ausbreitungskategorien A bis F.

Im ersten Teil dieses Berichtes werden die Ausbreitungsexperimente beschrieben und die Meßergebnisse in Form von

Tabellen und Abbildungen dargestellt. Die Ergebnisse früherer Experimente am Kernforschungszentrum mit 60 m und 100 m Emissionshöhen wurden bereits veröffentlicht.

1. Introduction

Conventional and nuclear facilities release pollutants into the atmosphere during routine operation and in case of accidents. To assess the resulting impact on the health of the population living in the environment of the facility, atmospheric diffusion calculations must be performed. Although the Gaussian plume model is the simplest solution of the diffusion equation, it is used in numerous theoretical diffusion studies, especially when a large number of individual cases have to be treated [1,2]. This model has been incorporated also in regulatory guides [3,4] because of its simplicity of application and the restricted number of input data required. It is a disadvantage of the Gaussian model that many effects influencing diffusion are not taken into account directly. They have to be introduced into this model by the dispersion parameters. To get reasonable estimates of the concentration field using the Gaussian plume model, it is necessary to consider carefully the influences of topography, atmospheric stability, source height and sampling time by choosing an appropriate system of dispersion parameters. Such systems have been developed theoretically [5,6]. Another approach consists in the determination of the dispersion parameters from diffusion experiments performed under various meteorological and topographical conditions.

At the Kernforschungszentrum Karlsruhe (KfK) the dispersion parameters have been determined experimentally as a function of the downwind distance, source height, and stability class. The detailed measured data of experiments with emission heights of 160 m and 195 m have been compiled in [7]. They comprise emission and concentration data of the tracers as well as comprehensive information about the meteorological conditions up to a height of 200 m for each diffusion experiment. In this report the data of [7] are evaluated by a least squares fit to deduce dispersion parameters. Finally, these parameters are pooled and smoothed to establish a set of dispersion parameters for stability classes A to F.

The results of the dispersion experiments performed at the KfK at source heights of 160 m and 195 m provide a valuable contribution to the knowledge of dispersion parameters over terrain with major surface roughnesses. They complete the results of the Karlsruhe diffusion experiments performed at tracer release heights of 60 m and 100 m [8,9]. The effect of source height on the dispersion parameters can be deduced from these experiments.

2. Evaluation Technique

The concentration distributions measured at ground level in the diffusion experiments are used to determine the dispersion parameters. For this purpose, the least squares technique is applied to fit the double Gaussian function to the concentrations measured. Because of the emission technique used and the physical and chemical properties of the tracers droplet or particle formation is not anticipated. The deposition of the tracers has been neglected because these effect is small as compared to the error of measurement.

2.1 The Double Gaussian Function

The double Gaussian function describing the concentration C(x,y) close to the ground level at the field point P(x,y) downwind of the source reads

$$C(x,y) = \frac{\chi\ (x,y)\ \dot{A}_O}{u} = \frac{\dot{A}_O}{\pi\ u\ \sigma_y(x)\ \sigma_z(x)} \exp\left[-\frac{y^2}{2\ \sigma_y^{\,2}(x)} - \frac{H^2}{2\ \sigma_z^{\,2}(x)}\right] \qquad (1)$$

This follows from the diffusion equation for steady-state conditions, constant emission rate and reflection of the tracer at ground level, where

$\dot{A}_O$	emission rate in g/s,
u	mean wind velocity in m/s,

$\chi\ (x,y)$ normalized diffusion factor in m^{-2},

x downwind distance in m,

y crosswind distance in m,

H emission height in m,

σ_y, σ_z horizontal and vertical dispersion parameters, resp., in m.

The foot of the source coincides with the origin of the Cartesian coordinate system.

2.2 Dispersion Parameters

The dispersion parameters σ_y and σ_z describe the horizontal and vertical distributions, respectively, of the concentration perpendicular to the transport direction. They are functions of the downwind distance x.

For this dependence on x, the power functions

$$\sigma_y = \sigma_{oy}\, x^{p_y}, \quad \sigma_z = \sigma_{oz}\, x^{p_z} \tag{2}$$

are chosen.

2.3 Least Squares Method

The measured tracer concentrations C_i determined at field points with the coordinates x_i and y_i are available from the experiments. A weighting factor g_i is assigned to each measured tracer concentration.

The four coefficients σ_{oy}, p_y, σ_{oz}, p_z must be found to fit the function C(x,y) of Eq. (1) to the measured C_i in such a way that the sum of the square deviations

$$Q = \sum_{i=1}^{n} g_i \, (C(x,y) - C_i)^2 \qquad (3)$$

becomes minimum. n is the number of tracer concentrations.

This yields four equations determining the four coefficients σ_{oy}, p_y, σ_{oz}, p_z. Since the function C(x,y) is not a linear function of the coefficients, an approximation technique with iterative improvement must be applied to solve the four equations.

The least squares fit yields also the errors in the coefficients and the errors in any function of the coefficient, hence, the errors in the dispersion parameters σ_y and σ_z. These errors qualify the least squares fit and, hence, the reliability of the deduced dispersion parameters. The errors are due to differences existing between the measured concentration distribution and the theoretical double Gaussian function. Compared with these differences, the errors in measurement are hardly significant. The evaluation technique is described in detail in [8,9].

2.4 Weighting Procedure and Initial Approximations

First computer runs showed a disadvantage of the evaluation technique. If different coefficients σ_{oy}, p_y, σ_{oz}, p_z were used as first approximations, the same concentration distribution gave rise to different dispersion parameters σ_y and σ_z. But these dispersion parameters showed good agreement at downwind distance with maximum concentration. The respective sums of least squares differed only slightly in most cases. To avoid this disadvantage a weighting procedure was chosen that preferred low concentration values at small and large downwind distances in the following manner:

$$g_i = C_{max}/C(x_i,0). \qquad (4)$$

C_{max} is the maximum value of all values $C(x_i,0)$ of Eq. (1). In Eqs. (1) and (4) the dispersion parameters σ_y, σ_z are inserted which have been determined in the previous step.

This weighting procedure was chosen because it is comparable with a separate evaluation of the concentration data of each zone, as performed by many authors (for example [10,11,12]).

2.5 Transport Direction

The best fit to the measured concentrations can be achieved if transport directions are chosen which differ slightly from that deduced from measurements of the wind direction. For this reason, several evaluation runs are carried out while varying the transport direction in steps of 1°. Again, that direction is deemed to be representative whose respective least squares sum ist smallest.

2.6 Wind Velocity

The wind velocity must be known for Eq. (1). For emission heights of 160 m and 195 m it is measured at 160 m and 200 m heights, respectively, of the meteorological tower and averaged over the sampling time. A corresponding wind velocity should be used in diffusion calculations together with the dispersion parameters from this report.

2.7 Experiments Suited for Evaluation

The concentrations measured in some of the sampling periods do not furnish physically meaningful dispersion parameters with the evaluation technique described in this paper. Reasons are that only the background concentrations or one wing of the cross-wind distribution are measured because of changes in the wind direction or that periods have been considered in which several zones show two concentration peaks or more than one peak occurs in the downwind direction. During these periods extremely non-steady state conditions prevail which are not described by the double Gaussian function.

3. Results of Individual Experiments

Table 1 shows the coefficients σ_{oy}, σ_{oz}, p_y, p_z as determined and the dispersion parameters σ_y and σ_z with the respective error widths at three downwind distances for all sampling periods suited for evaluation. The three distances roughly represent the shortest and the longest downwind distances of the sampling locations and that distance at which the maximum of concentration is found. The individual periods of one experiment are combined by forming the geometric mean value of the σ-parameters. These combined parameters are also indicated. In addition, Table 1 contains the stability class prevailing during the experiment and the mean transport directions θ and θ' deduced from wind measurements and from the least squares fit, respectively.

Figures 1 to 71 show the dispersion parameters σ_y and σ_z determined and the normalized diffusion factor χ as a function of the downwind distance x. All periods suited for evaluation of one experiment are combined. The error widths are indicated as shaded areas. If two tracers had been released simultaneously in one experiment, the results of both tracers are plotted to facilitate comparison.

The dispersion parameters of the experiments Nos. 52 to 67 have already been used to stablish a family of dispersion parameters for the stability classes A to F [13]. These dispersion parameters and normalized diffusion factors are plotted as dashed lines in Figs. 1 to 71 for comparison.

4. Determination of a Representative Set of Dispersion Parameters

4.1 Combination within the Same Stability Class

The dispersion parameters of each period which belong to the same stability class were combined by forming the geometrical mean value. To determine the stability class the standard deviation σ_ϕ of the vertical wind direction was used, which had been measured at 100 m height using a vector vane (Type 1053 III, Meteorology Research Inc.).

A classification scheme corresponding to the Pasquill-Gifford categories A to F was established. A frequency distribution of σ_ϕ and correlations between σ_ϕ, the temperature gradient, the wind speed and the radiation balance resulted in the following scheme:

Stability class	σ_ϕ in degrees
A	> 14.5
B	10.5 - 14.5
C	7.0 - 10.5
D	3.3 - 7.0
E	1.8 - 3.3
F	≤ 1.8

Because σ_ϕ is only measured at a few sites, we have developed statistically equivalent systems based on the meteorological parameters mentioned above and on the horizontal standard deviation σ_θ of the wind direction [14]. We have not tried until now to correlate σ_y and σ_z directly to σ_θ and σ_ϕ according to Pasquill [15] and Draxler [16].

The results of the combination have been compiled in Tab. 2. No experiments have been carried out for the stability classes E and F. From experience with tracers released at a height of 100 m it was anticipated that the ground level concentrations at most sampling positions would not exceed the detection limit during stable stratification. The exponents p_y and p_z are not monotonous functions of the stability classes. However, for practical application of the dispersion parameters going beyond the source heights and distances directly covered by the experiments, a monotonous function seems to be appropriate. This aim could be attained by a number of additional experiments. But this way is very time consuming and laborious. The more reasonable procedure consists in a suitable smoothing of the σ-curves.

4.2 Smoothing of the Dispersion Parameters

The evaluation of the individual experiments shows that the error band of the dispersion parameters is minimum around the concentration maximum. Therefore, in the smoothing process, it is attempted to preserve the position x_{max} and the normalized diffusion factor χ_{max} of this maximum:

$$x_{max} = \left(\frac{H}{\sigma_{oz}\sqrt{r}}\right)^{1/p_z} \tag{5}$$

$$\chi_{max} = \frac{1}{\pi\,\sigma_{oy}\,\sigma_{oz}} \left(\frac{\sigma_{oz}}{H}\sqrt{\frac{r}{e}}\right)^{r} \tag{6}$$

$$r = \frac{p_y + p_z}{p_z} \tag{7}$$

e = base of the natural logarithm

The general smoothing technique is performed in the following manner: Curves of p_y, p_z, x_{max} and χ_{max} are established as a function of σ_ϕ. These curves fit the results of the experiments for classes A to D. Then the curves are extrapolated to classes E and F using the dispersion parameters of the diffusion experiments at KfK with emission heights of 60 m and 100 m [17]. Finally, p_y, p_z, x_{max} and χ_{max} are taken from these curves at σ_ϕ-values, corresponding to the long term average σ_ϕ of each stability class B to F. In the case of class A the mean σ_ϕ-value from Tab. 2 was used instead of the long-term average. The latter leads to an extrapolation providing a lower diffusion factor.
From Eqs. (5) to (7) the factors σ_{oz} and σ_{oy} are calculated. The results are compiled in Tab. 3, and are plotted in Figs. 76 and 77.

4.2.1 Downwind Distance x_{max}

x_{max} is calculated for a source height of 180 m using the dispersion parameters from the experiments of the lower source heights [17]. In Fig. 72 x_{max} is plotted versus σ_ϕ (thin line). For comparison x_{max} evaluated from the experiments with source heights of 160 m and 195 m is also plotted in Fig. 72 using the data of Tab. 2 (full line).

x_{max} is influenced mainly by σ_z, which is a function of σ_ϕ. Therefore, it is possible to determine approximately the dependence of σ_ϕ on source height as indicated by arrows in Fig. 72. The relation of $\sigma_{\phi 1}$ and $\sigma_{\phi 2}$ is plotted in Fig. 73. For classes A and B σ_ϕ increases with the source height ($\sigma_{\phi 2} > \sigma_{\phi 1}$) whereas it decreases with the height under neutral and stable conditions ($\sigma_{\phi 2} < \sigma_{\phi 1}$). By an extrapolation of the curve to the origin in Fig. 73 x_{max} is determined for the stability classes E and F.

The height dependence of σ_ϕ during stable statification is given in [18]:

$$\sigma_{\phi 1} \approx \frac{\sigma_{w1}}{u} = f(H_1, L) = \frac{G(H_1)}{\ln(H_1/Z_o) + cH_1/L} \qquad (8)$$

$$\sigma_{\phi 2} \approx \frac{\sigma_{w2}}{u} = f(H_2, L) = \frac{G(H_2)}{\ln(H_2/Z_o) + cH_2/L} \qquad (9)$$

c	const.,
L	Monin-Obukhov stability length scale,
H_1, H_2	heights,
Z_o	roughness length,
u	wind speed,
σ_w	standard deviation of the vertical wind speed,
$G(H)$	height dependence of σ_w.

If we replace L in Eq. (8) using Eq. (9) the following relation between $\sigma_{\phi 1}$ and $\sigma_{\phi 2}$ is derived:

$$\sigma_{\phi 1} = \frac{\sigma_{\phi 2}}{b + a\,\sigma_{\phi 1}} \qquad (10)$$

The solid curve in Fig. 73 is extrapolated as a dashed line to the origin using Eq. (10). The values for a and b are 0.0542 and 0.549, respectively. This dashed line furnishes the extrapolation of x_{max} in Fig. 72 (dashed thick line).

4.2.2 Exponent p_z

In Fig. 72 the exponents p_z of the individual periods of the experiments are plotted versus σ_ϕ. The corresponding correlation coefficient of 0.55 demonstrates the weak correlation existing between p_z and σ_ϕ. The linear regression line is compared to the dashed line. The dashed line is derived in the following manner: For each class, A to D, $\sigma_{\phi 2}$ is taken from Fig. 73. The p_z-values corresponding to these $\sigma_{\phi 2}$ values are determined from the p_z/σ_ϕ-plot for the smaller source heights and plotted versus σ_ϕ in Fig. 74. This dashed line is well inside the scatter of the points in Fig. 74. It is used as a relation between p_z and σ_ϕ; this is consistent with an earlier evaluation of experiments Nos. 52 to 67 [13].

4.2.3 Exponent p_y

Figure 75 is the scatter plot of the exponent p_y versus σ_ϕ. The correlation coefficient of 0.26 is still weaker than between p_z and σ_ϕ. There is no pronounced relation between p_y and the stability classes. Therefore, the arithmetic mean value 0.82 of all p_y-values was chosen for all classes.

4.2.4 Maximum of the Normalized Diffusion Factor χ_{max}

In Fig. 72 the χ_{max}-values of classes A to D from Tab. 2 are plotted by a thick line as a function of σ_ϕ. In Fig. 72 the χ_{max}-values of the classes A and B are combined by calculating the geometric mean value of the dispersion parameters of all experiments performed for classes A and B.

The thick line has to be extrapolated to classes E and F. For this purpose, the thin line in Fig. 72 is constructed in the following manner: σ_y is taken from the results of the lower source heights [17]. σ_z is calculated using x_{max} from Fig. 72 (thick line) und p_z from Fig. 74 (dashed line) via Eq. (5). The difference of both χ_{max}-curves mainly reflects the influence of source height on σ_y, because both curves refer only to σ_z for the great source heights. It is assumed that the decrease in σ_y with height for stable conditions is proportional to that of class D. This furnishes the extrapolation of the thick line parallel to the thin line in Fig. 72.

5. Discussion of the Results

The results of the diffusion experiments are influenced mainly by the source height and by the structure of the surface in the invironment of the KfK, characterized by a roughness length of about 1.5 m. If comparisons with experimental results of other authors are performed, this fact has to be taken into account.

5.1 Vertical Dispersion Parameter σ_z

As expected, the vertical dispersion parameters decrease with increasing atmospheric stability. The σ_z-curves for classes A and B do not represent the real vertical spread of the plume. They are too steep. The σ_z-curve is only a least squares fit of the Gaussian distribution to the concentration field measured near ground level; it is determined by the large scale up and downward motions of the tracer in the convective boundary layer. These motions lead to a rather short source distance of the maximum ground level concentration, observed especially under class A conditions.

The downwind distances x_{max} of the maximum concentration calculated from the dispersion parameters of individual experiments within the same stability class agree better with each other than the dispersion parameters themselves. Therefore, this distance x_{max}, which is influenced most by σ_z, is used for a comparison with the dispersion parameters derived from diffusion experiments carried out in Brookhaven [19], St. Louis [10] and Jülich/Karlsruhe [20] (see Tab. 4). Only for the stability classes A to C the distance x_{max} calculated with the parameters of this report agrees well with the x_{max}-values determined from the dispersion parameters published in [10,20]. The Brookhaven experiments for all classes, however, give nearly the same x_{max} as derived from the Karlsruhe experiments with emission heights of 160 m and 195 m.

5.2 Horizontal Dispersion Parameter σ_y

The azimuthal distribution of the concentration field is influenced by variations in the wind direction and by the topography. Both effects are reflected more in the horizontal than in the vertical dispersion parameters. This is also obvious from the great error width of the σ_y-curves derived from the individual experiments.

One of the results of our experiments is the fact that the concentration distribution under stable atmospheric conditions is broader than in the case of neutral stability. This effect observed for release heights of 60 m and 100 m was extrapolated to the σ_y-parameters belonging to the greater source heights.

A comparison of σ_y-parameters with those from the experiments for smaller source heights shows a significant decrease with height. This reflects the reduced influence of the topography on the concentration distribution near ground level.

5.3 Normalized Diffusion Factor χ

The normalized diffusion factor χ summarizes the maximum pollutant burden to be expected from short-term emissions. Since σ_z has a stronger influence upon χ than σ_y, the error bands are small as compared to the σ_y-curves. The increase in σ_y with stability from D to F is reflected also in the χ_{max} values. For the classes E and F χ_{max} is much smaller than the corresponding values calculated with the St. Louis or the Brookhaven dispersion parameters (see Tab. 4).

6. Final Remarks

An evaluation of the experiments No. 52 up to 67 for source heights of 160 m and 195 m has already been published in [13]. We have compared the short-term and long-term diffusion factors around a

180 m heigh source. Calculated with this old set of dispersion parameters and the new one from Tab. 3. The results for both sets of σ-parameters are shown in Figs. 78 and 79.

The deviation of both curves in each figure is small as compared to the uncertainty of the evaluation. The differences in both sets of σ-parameters are not significant in practical applications.

10. References

[1] Der Bundesminister for Forschung und Technologie (Editor), Deutsche Risikostudie Kernkraftwerke, Verlag TÜV Rheinland, Köln (1980).

[2] N. C. Rasmussen, Reactor Safety Study - An Assessment of Accident Risks in US Commercial Nuclear Power Plants, United States Nuclear Regulatory Commission, WASH-1400 (NUREG-75/014), (1975).

[3] Der Bundesminister des Innern, Allgemeine Berechnungsgrundlagen für die Bestimmung der Strahlenexposition durch Emission radioaktiver Stoffe mit der Abluft, Köln (1977).

[4] NRC, Methods for Estimating Atmospheric Transport and Dispersion of Gaseous Effluents in Routine Releases from Light-Water-Cooled Reactors. Regulatory Guide 1.111, Washington, D. C. (1977).

[5] J. S. Irwin, Estimating Plume Dispersion - A Recommended Generalized Scheme, Preprints of Fourth Symposium on Turbulence, Diffusion and Air Pollution, Reno, Americ. Met. Soc., Boston (1979)

[6] J. C. Wamser et al., Darstellung und Anwendung eines verbesserten, universell gültigen Ausbreitungskriteriums, Staub-Reinhaltung der Luft, Vol. 40, Nr. 6 (1980).

[7] P. Thomas et al., Experimental Determination of the Atmospheric Dispersion Parameters at the Karlsruhe Nuclear Research Center for 160 m and 195 m Emission Heights. Part 1, Measured Data, KfK 3456 (1983).

[8] P. Thomas, K. Nester, Experimental Determination of the Atmospheric Dispersion Parameters over Rough Terrain. Part 2, Evaluation of Measurements, KfK 2286 (1976).

[9] P. Thomas, K. Nester, Experimental Determination of the Atmospheric Dispersion Parameters at the Karlsruhe Nuclear Research Center for 60 m and 100 m Emission Heights. Part 2, Evaluation of Measurements, KfK 3091 (1981).

[10] J. McElroy, A Comparative Study of Urban and Rural Dispersion, J. of Appl. Meteorol. 8, No. 1, pp. 19-31 (1969).

[11] S. E. Gryning, Elevated Source SF_6-Tracer Dispersion Experiments in the Copenhagen Area, Risø-R-446 (1981).

[12] M. Yersel, R. Goble, J. Morrill, Short Range Dispersion Experiments in an Urban Area, Atm. Env. 17, pp. 275-282 (1983).

[13] W. Hübschmann, K. Nester, P. Thomas, Auswertung von Ausbreitungsversuchen in Jahresbericht 1979 der Hauptabteilung Sicherheit, KfK 2939, p. 183 (1980).

[14] K. Nester, Statistically Equivalent Systems for the Determination of Dispersion Categories, Seminar on Radioactive Releases and their Dispersion in the Atmosphere Following a Hypothetical Reactor Accident, Risø (1980).

[15] F. Pasquill, Atmospheric Dispersion Parameters in Gaussian Plume Modeling, Part 2, Possible Requirements for Change in the Turner Workbook Values, EPA-600/4-76-030b, Washington, D. C. (1976).

[16] R. R. Draxler, Determination of Atmospheric Diffusion Parameters. Atmos. Environ., 10, 99-105 (1976).

[17] K. Nester, P. Thomas, Im Kernforschungszentrum Karlsruhe experimentell ermittelte Ausbreitungsparameter für Emissionshöhen bis 195 m, Staub-Reinh. Luft 39, pp. 291-295 (1979).

[18] S. R. Hanna, G. A. Briggs, R. P. Hosker, Jr., Handbook on Atmospheric Diffusion, Technical Information Center, U. S. Department of Energy (DOE/TIC-11223), (1982).

[19] I. A. Singer, M. E. Smith, An Improved Method of Estimating Concentrations and Related Phenomena from a Point Source Emission, J. of Appl. Meteorol. 5, pp. 631-639 (1966).

[20] H. Geiß, K. Nester, P. Thomas, K. J. Vogt, In der Bundesrepublik Deutschland experimentell ermittelte Ausbreitungsparameter für 100 m Emissionshöhe, JÜL-1707, KfK 3095 (1981).

Stab. class	No. of exp.	Tracer and emission height (m)	Period	θ	θ'	σ_y: σ_{oy}	σ_y: p_y	σ_z: σ_{oz}	σ_z: p_z	x (m)	σ_y (m)	$\frac{\Delta\sigma_y}{\sigma_y}$ (%)	σ_z (m)	$\frac{\Delta\sigma_z}{\sigma_z}$ (%)
A	57	CF_2Br_2 160 m	1	65°	68°	7.78	0.447	0.00157	1.92	100	61	66	11	34
										300	99	21	91	8
										2500	256	82	5379	61
			2	68°	73°	0.0532	1.23	0.212	1.15	100	16	46	43	108
										300	60	14	152	49
										2500	823	67	1756	83
			1+2			0.643	0.839	0.0182	1.54	100	31	40	22	41
										300	77	13	119	14
										2500	456	57	3111	56
		$CFCl_3$ 195 m	1	68°	74°	7.49	0.528	0.0531	1.37	100	85	75	29	45
										300	152	26	131	15
										2500	466	90	2376	82
			2	69°	72°	1.26	0.750	0.446	1.04	100	40	57	53	79
										300	91	19	165	35
										2500	444	79	1485	83
			1+2			3.07	0.639	0.154	1.20	100	58	47	39	39
										300	117	16	145	14
										2500	455	60	1841	60
B	52	CF_2Br_2 160 m	1	57°	50°	0.120	1.037	0.407	0.854	100	14	61	21	19
										600	91	19	99	8
										2000	319	24	277	24
			2	46°	49°	0.340	0.916	0.109	1.12	100	23	41	19	12
										600	119	9	141	8
										2000	359	27	543	19
			1+2			0.202	0.978	0.211	0.989	100	18	39	20	13
										600	105	10	118	7
										2000	342	21	388	18
		$CFCl_3$ 195 m	1	58°	54°	6.82	0.474	0.299	0.919	100	60	213	21	81
										600	141	60	107	27
										2000	250	73	323	92
			2	47°	50°	0.0854	1.05	0.154	1.06	100	11	54	20	29
										600	70	15	132	9
										2000	246	27	467	34
			1+2			0.763	0.762	0.215	0.990	100	26	89	21	48
										600	100	22	121	16
										2000	250	40	399	56
B	60	CF_2Br_2 160 m	1	224°	218°	7.68	0.630	0.00630	1.64	200	216	65	37	16
										400	335	31	117	16
										3500	1313	117	4089	86
		$CFCl_3$ 195 m	1	217°	211°	3.79	0.670	0.00767	1.62	200	132	66	41	14
										400	210	33	126	13
										3500	898	99	4228	74

Table 1: Determined dispersion parameters σ_y and σ_z

x: downwind distance

θ: mean transport direction from wind measurements

θ': mean transport direction from least squares fit

Stab. class	No. of exp.	Tracer and emission height (m)	Period	θ	θ′	σ_y: σ_{oy}	σ_y: p_y	σ_z: σ_{oz}	σ_z: p_z	x (m)	σ_y (m)	$\frac{\Delta\sigma_y}{\sigma_y}$ (%)	σ_z (m)	$\frac{\Delta\sigma_z}{\sigma_z}$ (%)
B	64	CF_2Br_2 160 m	1	281°	277°	0.0256	1.39	2.41	0.719	200	41	29	109	49
										500	146	17	211	29
										4800	3385	77	1071	80
			2	271°	283°	7.06	0.589	1.46	0.763	200	160	70	83	42
										500	274	36	168	44
										4800	1040	151	943	149
			1+2			0.425	0.990	1.88	0.741	200	81	30	95	33
										500	200	18	188	25
										4800	1874	81	1005	83
		$CFCl_3$ 195 m	1	286°	284°	1.14	0.802	0.0697	1.34	200	80	36	85	24
										500	167	21	292	20
										4800	1024	96	6076	89
			2	275°	274°	0.00170	1.95	1.25	0.705	200	51	63	52	11
										500	301	32	100	11
										4800	24501	69	492	48
			1+2			0.0440	1.38	0.295	1.02	200	66	43	66	12
										500	233	16	167	20
										4800	5291	92	1678	86
B	67	CF_2Br_2 160 m	1	276°	269°	0.00308	1.59	0.0474	1.19	200	14	45	26	9
										800	125	11	134	11
										3200	1127	38	697	30
		$CFCl_3$ 195 m	1	282°	270°	0.00118	1.63	0.0581	1.17	200	7	41	29	10
										800	65	11	145	9
										3200	622	33	733	27
C	55	CF_2Br_2 160 m	1	238°	236°	1.23	0.648	0.0310	1.15	300	49	27	21	8
										1600	146	5	145	7
										5000	306	16	536	15
			2	225°	232°	0.136	0.941	0.0187	1.19	300	29	37	17	8
										1600	140	6	123	4
										5000	411	19	481	11
			1+2			0.407	0.795	0.0240	1.17	300	38	23	19	7
										1600	144	5	135	5
										5000	355	12	511	11
		$CFCl_3$ 195 m	1	243°	236°	5.29	0.433	0.0210	1.20	300	62	60	20	16
										1600	129	11	150	11
										5000	211	33	589	27
			2	240°	232°	0.00171	1.50	0.0765	1.00	300	9	112	23	41
										1600	109	26	125	11
										5000	602	46	393	38
			1+2			0.0951	0.967	0.0401	1.10	300	24	47	21	14
										1600	119	11	134	8
										5000	359	23	470	19
C	62	CF_2Br_2 160 m	1	241°	251°	0.0101	1.39	0.0142	1.41	100	6	34	9	11
										700	90	7	141	5
										4900	1345	25	2179	19
			2	230°	247°	8.80	0.435	0.0744	1.12	100	65	141	13	42
										700	152	31	114	18
										4900	355	99	993	73
			1+2			0.298	0.913	0.0325	1.26	100	20	66	11	26
										700	118	15	125	12
										4900	697	51	1451	45
		$CFCl_3$ 195 m	1	245°	250°	0.110	1.03	0.0366	1.29	100	13	82	14	32
										700	95	18	166	15
										4900	713	66	2026	57
			2	229°	243°	1.26	0.704	0.0859	1.10	100	32	103	14	34
										700	127	28	116	14
										4900	501	64	985	54
			1+2			0.372	0.867	0.0561	1.19	100	20	73	13	25
										700	109	17	136	11
										4900	589	51	1381	43

Table 1 continued/1

Stab. class	No. of exp.	Tracer and emission height (m)	Period	θ	θ′	σ_y: σ_{oy}	σ_y: p_y	σ_z: σ_{oz}	σ_z: p_z	x (m)	σ_y (m)	$\frac{\Delta\sigma_y}{\sigma_y}$ (%)	σ_z (m)	$\frac{\Delta\sigma_z}{\sigma_z}$ (%)
C	66	CF_2Br_2 160 m	2	90°	76°	7,68	0.433	0.154	1.07	200	76	116	45	20
										500	113	52	119	39
										4000	279	145	1101	136
		$CFCl_3$ 195 m	2	65°	63°	0.0177	1.35	0.0104	1.47	200	23	54	25	29
										500	78	23	97	7
										4000	1290	66	2051	61
C	73	$CFCl_3$ 160 m	1	36°	38°	1.03	0.690	0.0139	1.30	150	33	241	9	72
										1000	121	52	108	24
										2700	239	74	393	65
			2	41°	36°	0.0129	1.29	0.575	0.760	150	8	56	26	14
										1000	97	17	109	10
										2700	351	30	232	21
			1+2			0.115	0.991	0.0894	1.03	150	16	77	15	41
										1000	108	20	109	14
										2700	289	33	301	40
		CF_2Br_2 195 m	1	43°	40°	0.126	0.980	0.00941	1.36	150	17	37	9	23
										1000	109	7	113	6
										2700	289	12	438	12
			2	47°	37°	5.06	0.477	0.0615	1.05	150	55	40	12	10
										1000	136	12	89	2
										2700	219	6	253	6
			1+2			0.797	0.728	0.0241	1.21	150	31	32	10	10
										1000	122	8	100	3
										2700	252	8	333	7
C	68	CF_2Br_2 160 m	1	246°	242°	9.50	0.411	0.221	0.864	250	92	58	26	19
										2200	225	16	171	21
										5400	325	32	371	35
			2	237°	242°	8.94	0.410	0.108	0.938	250	86	73	19	23
										2200	210	16	148	17
										5400	303	30	343	32
			1+2			9.22	0.411	0.155	0.901	250	89	45	22	14
										2200	217	11	159	13
										5400	314	22	357	23
		$CFCl_3$ 195 m	1	251°	243°	9.81	0.404	0.320	0.797	250	91	53	26	15
										2200	220	12	147	10
										5400	317	18	300	20
			2	241°	241°	3.33	0.552	1.29	0.591	250	70	72	34	17
										2200	233	20	122	12
										5400	383	24	207	21
			1+2			5.71	0.478	0.641	0.694	250	80	44	30	12
										2200	227	11	134	8
										5400	348	15	249	15
D	53	CF_2Br_2 160 m	1	199°	192°	3.01	0.484	0.00362	1.32	300	47	32	7	9
										2200	124	4	92	2
										5500	194	9	305	6
			2	210°	201°	0.288	0.907	0.0570	1.00	300	51	33	17	10
										2200	309	6	129	5
										5500	709	13	324	11
			1+2			0.933	0.695	0.0144	1.16	300	49	61	11	37
										2200	196	10	109	8
										5500	371	21	314	28
		$CFCl_3$ 195 m	1	205°	193°	5.20	0.581	3.56	0.429	300	143	141	41	20
										2200	455	38	97	10
										5500	775	43	143	18
			2	216°	201°	4.78	0.586	4.06	0.428	300	135	90	45	14
										2200	435	25	105	9
										5500	744	39	155	17
			1+2			4.99	0.584	3.80	0.426	300	140	80	43	12
										2200	447	22	101	7
										5500	763	30	149	13

Table 1 continued/2

Stab. class	No. of exp.	Tracer and emission height (m)	Period	θ	θ′	σ_y: σ_{oy}	σ_y: p_y	σ_z: σ_{oz}	σ_z: p_z	x (m)	σ_y (m)	$\frac{\Delta\sigma_y}{\sigma_y}$ (%)	σ_z (m)	$\frac{\Delta\sigma_z}{\sigma_z}$ (%)
D	58	CF_2Br_2 160 m	1	81°	80°	1.16	0.713	0.0417	1.13	300	68	34	26	12
										1200	183	10	125	9
										5600	546	29	717	29
			2	82°	81°	0.00416	1.46	0.0442	1.14	300	17	23	30	8
										1200	126	6	144	7
										5600	1182	22	833	22
			1+2			0.0695	1.09	0.0429	1.14	300	35	26	29	10
										1200	158	7	139	7
										5600	846	24	804	24
		$CFCl_3$ 195 m	1	82°	83°	4.84	0.546	4.07	0.439	300	109	46	50	9
										1200	232	21	91	6
										5600	539	23	180	16
			2	82°	78°	3.76	0.570	0.0126	1.35	300	97	39	28	14
										1200	214	10	181	10
										5600	515	41	1447	35
			1+2			4.27	0.558	0.226	0.895	300	103	32	37	10
										1200	223	10	129	7
										5600	527	23	511	23
D	61	CF_2Br_2 160 m	1	47°	47°	0.0430	1.09	0.392	0.740	400	30	20	33	3
										1800	152	8	101	4
										8400	815	13	314	9
			2	50°	49°	1.81	0.616	1.63	0.556	400	73	14	45	4
										1800	183	7	105	4
										8400	473	15	248	11
			1+2			0.279	0.853	0.799	0.648	400	46	15	39	3
										1800	167	7	103	3
										8400	621	12	279	8
D	63	CF_2Br_2 160 m	1	49°	51°	0.0633	0.987	0.00399	1.37	500	29	18	20	9
										1700	98	7	106	3
										9200	517	17	1075	17
			2	41°	43°	0.0135	1.26	0.0722	0.990	500	34	28	34	6
										1700	160	11	114	7
										9200	1344	28	609	19
			1+2			0.0292	1.12	0.0170	1.18	500	31	22	26	11
										1700	121	8	110	4
										9200	803	21	809	20
D	65	CF_2Br_2 160 m	1	31°	26°	3.35	0.423	0.262	0.807	250	35	469	23	460
										2000	83	159	121	77
										6000	133	60	294	364
			2	17°	29°	8.99	0.411	0.0543	1.05	250	87	51	18	13
										2000	205	9	160	12
										6000	322	27	507	25
			1+2			5.48	0.417	0.119	0.929	250	55	44	20	12
										2000	130	10	139	7
										6000	206	17	385	17
D	69	CF_2Br_2 160 m	1	31°	37°	5.14	0.461	0.294	0.757	600	98	53	37	14
										3200	212	13	132	15
										8400	330	27	274	30
			2	37°	37°	3.13	0.524	0.233	0.798	600	89	36	38	8
										3200	215	12	146	13
										8400	356	24	316	25
			1+2			4.01	0.492	0.262	0.777	600	93	30	38	7
										3200	213	8	139	10
										8400	343	18	294	19
		$CFCl_3$ 195 m	1	36°	35°	7.88	0.446	2.76	0.480	600	137	61	59	15
										3200	289	21	132	21
										8400	445	30	210	39
			2	42°	38°	9.27	0.430	1.99	0.533	600	145	80	60	17
										3200	298	27	147	29
										8400	452	46	245	53
			1+2			8.54	0.438	2.34	0.506	600	141	48	60	11
										3200	294	17	139	17
										8400	448	25	227	32

Table 1 continued/3

Stab. class	No. of exp.	Tracer and emission height (m)	Period	θ	θ'	σ_y: σ_{oy}	σ_y: p_y	σ_z: σ_{oz}	σ_z: p_z	x (m)	σ_y (m)	$\frac{\Delta\sigma_y}{\sigma_y}$ (%)	σ_z (m)	$\frac{\Delta\sigma_z}{\sigma_z}$ (%)
D	70	$CFCl_3$ 160 m	1	67°	68°	0.701	0.813	3.55	0.414	300	72	69	38	10
										2900	457	20	97	11
										5300	746	28	124	15
			2	61°	59°	0.00541	1.47	2.42	0.482	300	24	63	38	11
										2900	697	21	113	15
										5300	1671	30	151	21
			1+2			0.0616	1.14	2.93	0.448	300	42	49	38	8
										2900	559	16	105	10
										5300	1113	22	137	13
		CF_2Br_2 195 m	1	67°	64°	1.20	0.957	3.78	0.430	300	281	143	44	14
										2900	2462	43	116	20
										5300	4383	43	151	27
			2	61°	66°	0.197	1.03	3.95	0.410	300	71	96	41	12
										2900	736	25	104	9
										5300	1371	35	133	14
			1+2			0.487	0.994	3.86	0.420	300	141	83	42	9
										2900	1343	23	110	9
										5300	2446	28	142	13
D	72	$CFCl_3$ 160 m	1	67°	68°	0.0737	0.990	0.254	0.815	400	28	31	34	10
										2500	171	10	150	12
										8300	560	29	398	26
			2	65°	65°	4.88	0.460	2.02	0.496	400	77	70	39	16
										2500	178	26	98	15
										8300	308	40	177	32
			1+2			0.602	0.724	0.715	0.656	400	46	41	36	10
										2500	174	13	121	11
										8300	414	31	266	23
		$CFCl_3$ (JRC)* 160 m	1	67°	68°	6.25	0.417	0.215	0.824	400	76	26	30	7
										2500	163	5	136	7
										8300	270	15	364	26
			2	65°	68°	1.49	0.628	4.12	0.405	400	64	28	47	7
										2500	203	11	98	7
										8300	430	19	160	14
			1+2			3.06	0.522	0.941	0.615	400	70	22	37	5
										2500	182	7	115	6
										8300	340	12	241	12
		CF_2Br_2 195 m	1	71°	69°	0.00296	1.36	0.0599	0.981	400	10	33	21	17
										2500	125	9	130	4
										8300	640	21	420	16
			2	70°	66°	0.164	0.817	2.62	0.452	400	22	170	39	28
										2500	98	48	90	11
										8300	261	100	155	28
			1+2			0.0220	1.09	0.396	0.717	400	15	75	29	24
										2500	111	20	108	7
										8300	408	35	255	24
		SF_6 195 m	1	71°	66°	1.57	0.606	0.894	0.622	400	59	188	37	42
										2500	179	52	116	28
										8300	370	65	245	66
			2	70°	68°	0.993	0.622	1.80	0.509	400	41	88	38	20
										2500	129	32	97	11
										8300	272	96	179	26
			1+2			1.25	0.614	1.27	0.566	400	49	97	38	21
										2500	152	32	106	14
										8300	317	43	210	31

Table 1 continued/4

*Sampled and analysed by Joint Research Center Ispra

Stability class	σ_y		σ_z		σ_ϕ
	σ_{oy}	p_y	σ_{oz}	p_z	
A	1.406	0.739	0.0530	1.370	15.00
B	0.127	1.123	0.121	1.133	13.14
C	0.363	0.855	0.0590	1.115	8.56
D	1.040	0.705	0.487	0.710	6.31

Table 2: Experimentally determined dispersion parameters for emission heights of 160 and 195 m

Stability class	σ_y		σ_z		σ_ϕ
	σ_{oy}	p_y	σ_{oz}	p_z	
A	1.08	0.82	0.0253	1.50	15.0
B	0.667	0.82	0.0341	1.32	12.0
C	0.436	0.82	0.114	0.99	8.3
D	0.432	0.82	0.349	0.71	5.1
E*	0.637	0.82	0.556	0.55	2.5
F*	1.214	0.82	0.472	0.50	1.2

*extrapolated

Table 3: Smoothed and centered dispersion parameters for emission heights of 160 and 195 m

Stability class	Karlsruhe		Jülich/Karlsruhe [20]		St. Louis [10]		Brookhaven [19]	
	x_{max} in km	χ_{max} in m^{-2}	x_{max} in km	χ_{max} in m^{-2}	x_{max} in km	χ_{max} in m^{-2}	x_{max} in km	χ_{max} in m^{-2}
A	0.32	$0.830 \cdot 10^{-5}$	0.38	$0.246 \cdot 10^{-5}$	-	-	-	-
B	0.55	$0.850 \cdot 10^{-5}$	0.70	$0.356 \cdot 10^{-5}$	0.73	$0.595 \cdot 10^{-5}$	0.55	$0.741 \cdot 10^{-5}$
C	1.25	$0.635 \cdot 10^{-5}$	1.06	$0.486 \cdot 10^{-5}$	1.13	$0.490 \cdot 10^{-5}$	1.02	$0.663 \cdot 10^{-5}$
D	3.85	$0.235 \cdot 10^{-5}$	1.90	$0.380 \cdot 10^{-5}$	2.06	$0.390 \cdot 10^{-5}$	3.48	$0.497 \cdot 10^{-5}$
E	16.0	$0.450 \cdot 10^{-6}$	4.50	$0.122 \cdot 10^{-5}$	5.19	$0.346 \cdot 10^{-5}$	-	-
F	55.0	$0.820 \cdot 10^{-7}$	26.4	$0.54 \cdot 10^{-7}$	-	-	48.46	$0.140 \cdot 10^{-5}$

Table 4: Source distance x_{max} and amount χ_{max} of the maximum of the normalized diffusion factor for an emission height of 180 m

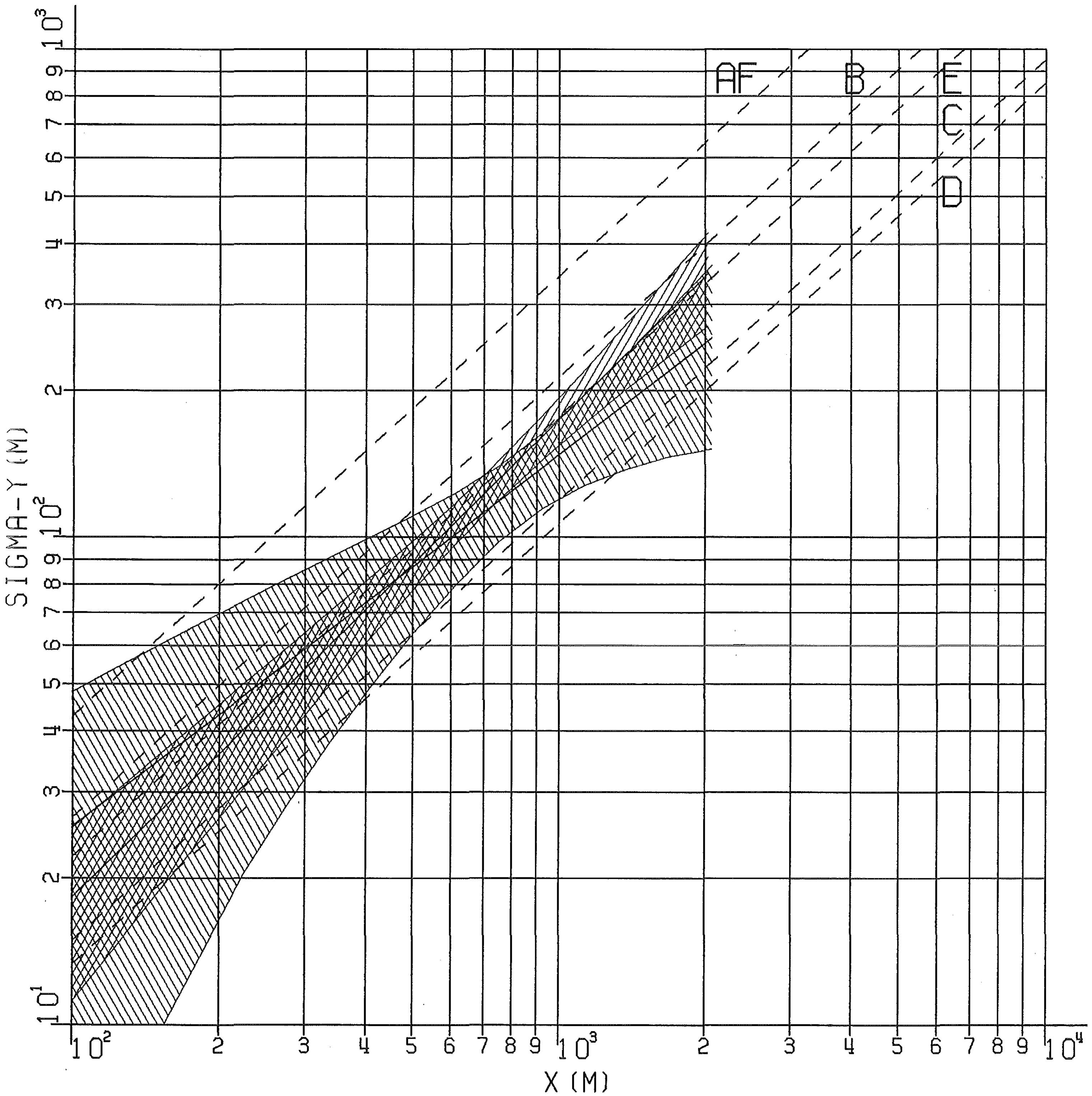

FIG. 1: HORIZONTAL DISPERSION PARAMETER
OF EXPERIMENT NO.52, PERIODS 1+2
H=160M, TRACER CF2BR2
H=195M, TRACER CFCL3
– – – – – COMBINED, SMOOTHED, AND CENTERED RESULTS

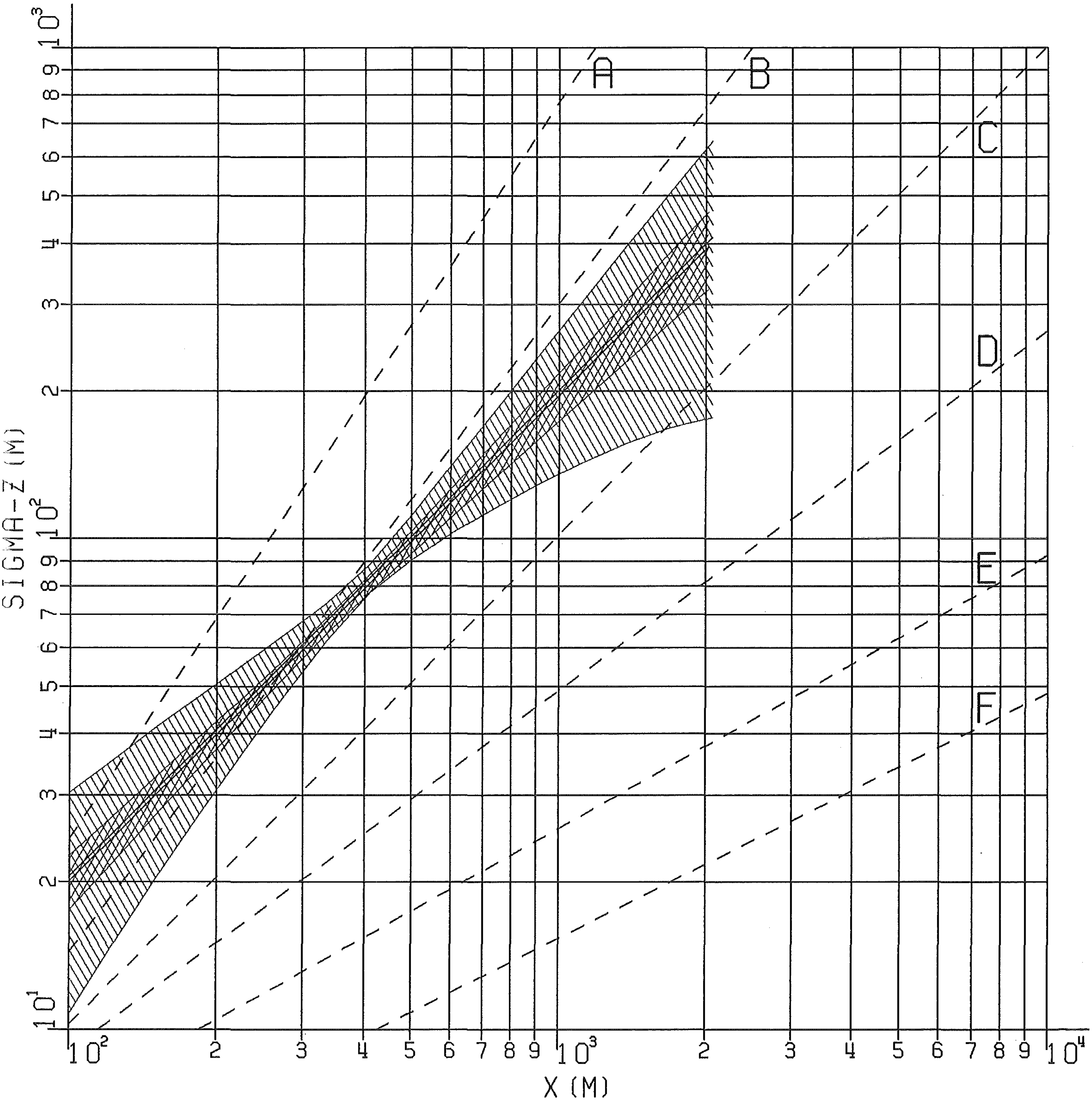

FIG. 2: VERTICAL DISPERSION PARAMETER
OF EXPERIMENT NO.52, PERIODS 1+2
H=160M, TRACER CF2BR2
H=195M, TRACER CFCL3
- - - - - COMBINED, SMOOTHED, AND CENTERED RESULTS

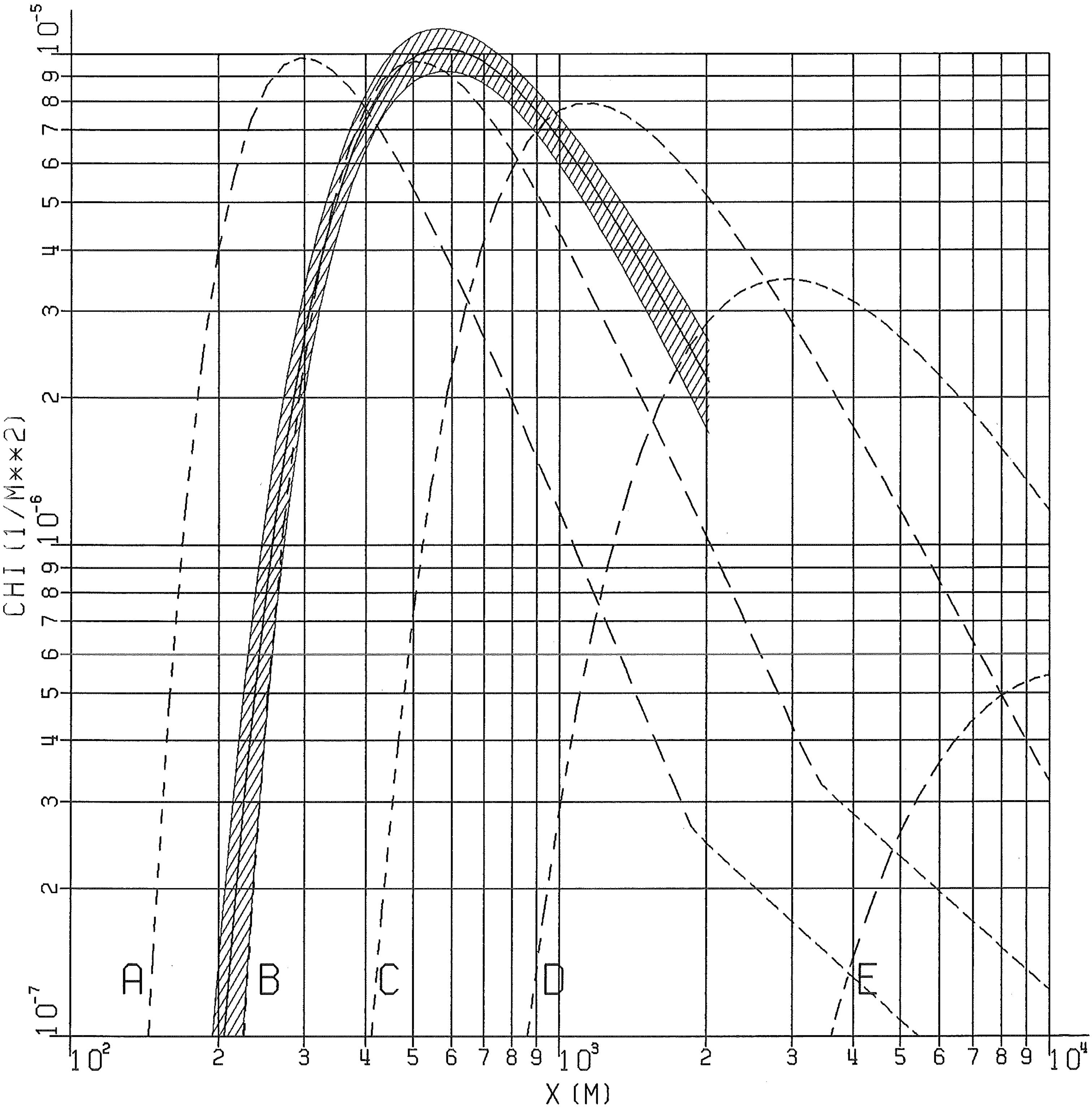

FIG. 3: NORMALIZED DIFFUSION FACTOR
OF EXPERIMENT NO.52, PERIODS 1+2
////////////// H=160M, TRACER CF2BR2
- - - - - COMBINED, SMOOTHED, AND CENTERED RESULTS

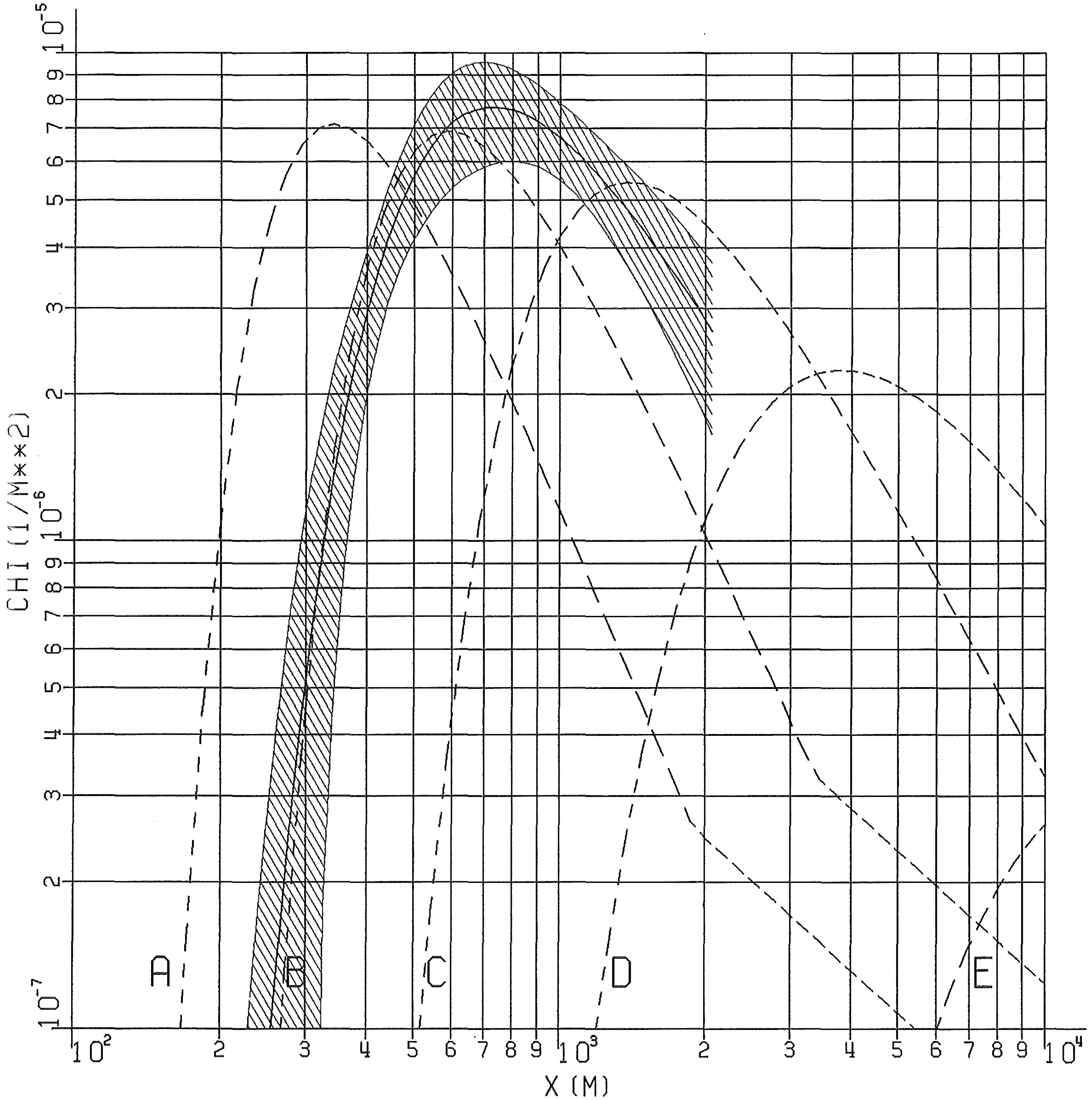

FIG. 4: NØRMALIZED DIFFUSIØN FACTØR
ØF EXPERIMENT NØ.52, PERIØDS 1+2
H=195M, TRACER CFCL3
- - - - - CØMBINED, SMØØTHED, AND CENTERED RESULTS

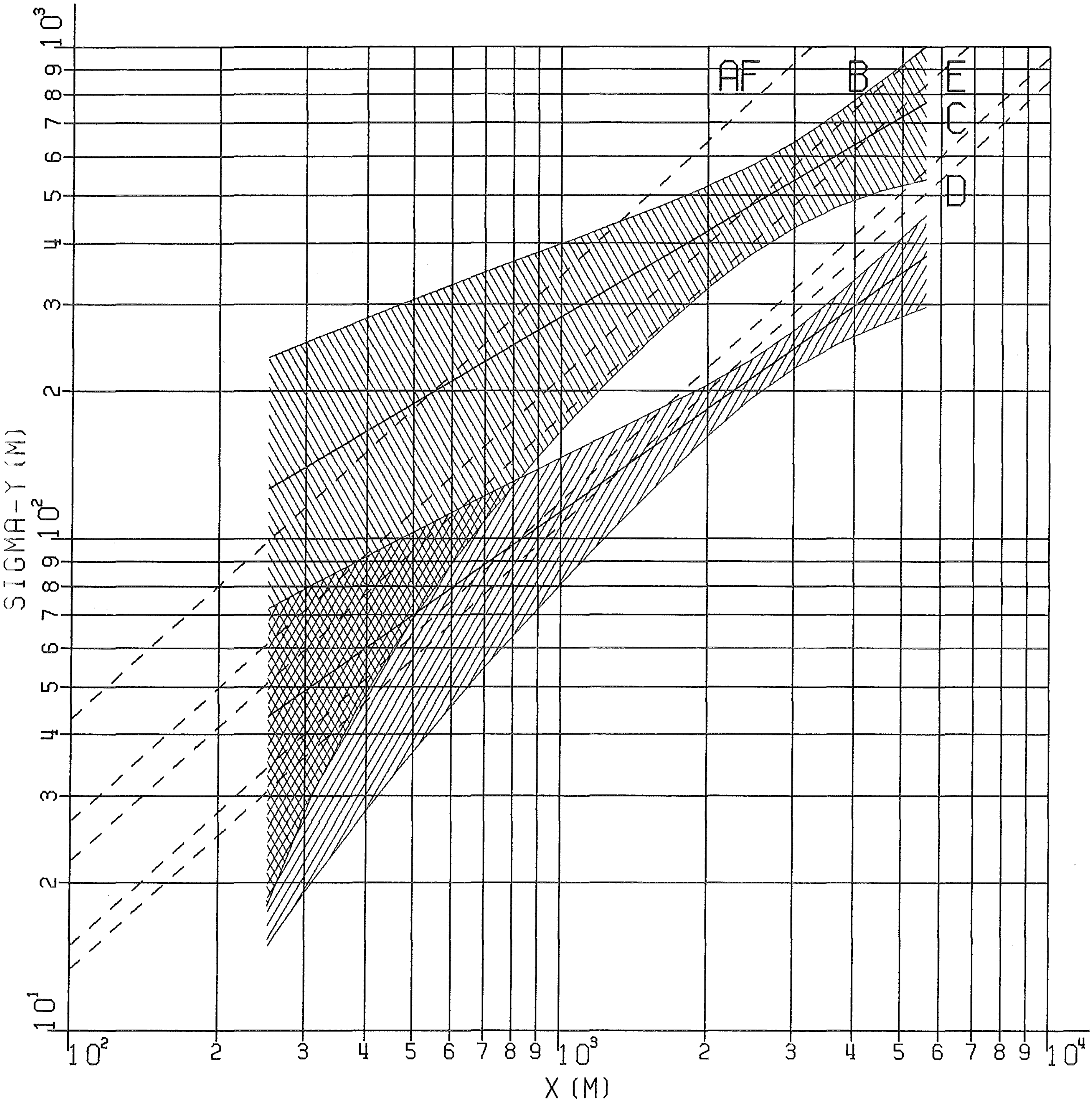

FIG. 5: HORIZONTAL DISPERSION PARAMETER
OF EXPERIMENT NO.53, PERIODS 1+2

H=160M, TRACER CF2BR2

H=195M, TRACER CFCL3

- - - - - COMBINED, SMOOTHED, AND CENTERED RESULTS

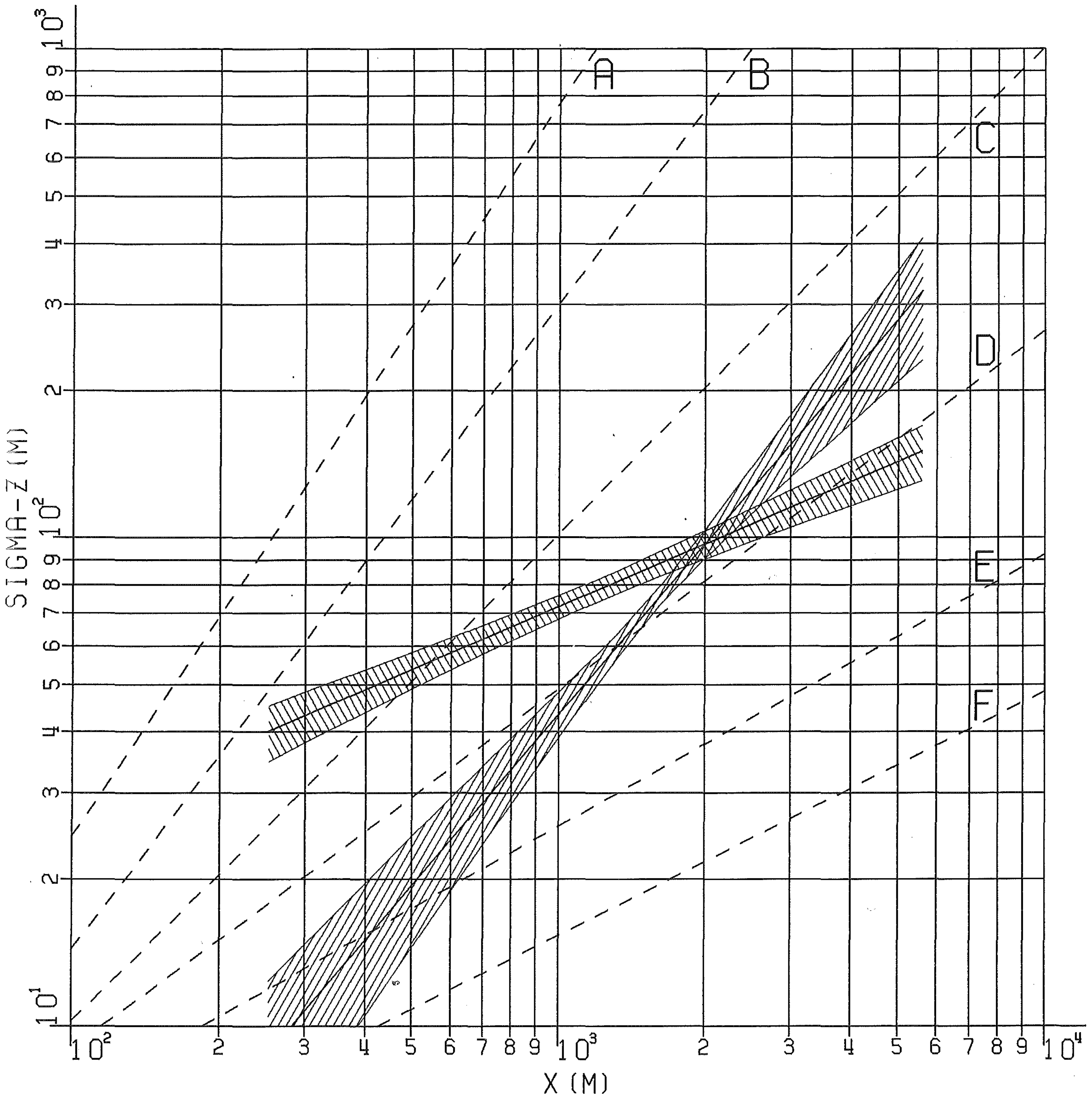

FIG. 6: VERTICAL DISPERSION PARAMETER
OF EXPERIMENT NO.53, PERIODS 1+2

//////////// H=160M, TRACER CF2BR2

\\\\\\\\\\\\ H=195M, TRACER CFCL3

– – – – – COMBINED, SMOOTHED, AND CENTERED RESULTS

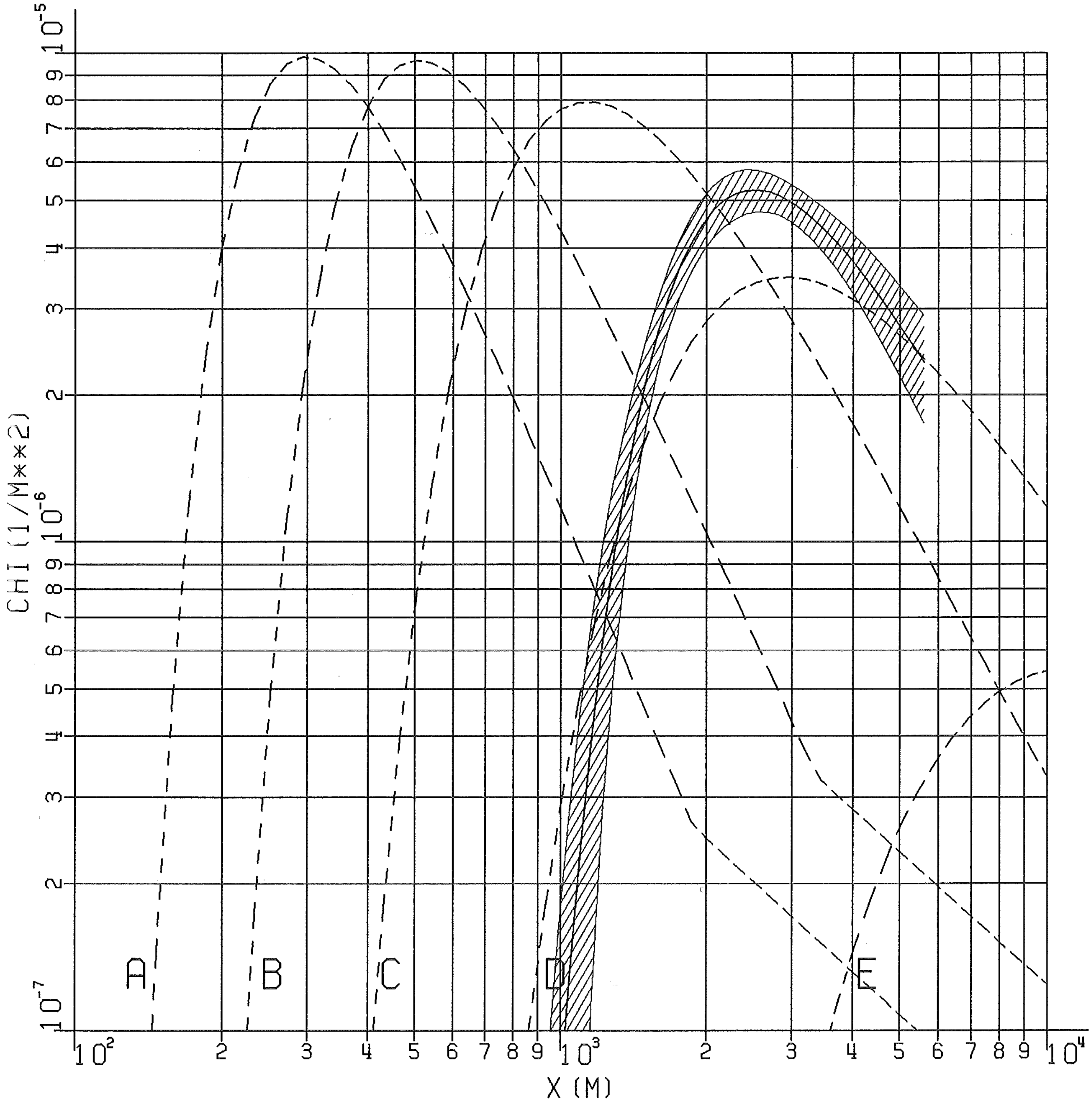

FIG. 7: NORMALIZED DIFFUSION FACTOR
OF EXPERIMENT NO.53, PERIODS 1+2
////////// H=160M, TRACER CF2BR2
- - - - - COMBINED, SMOOTHED, AND CENTERED RESULTS

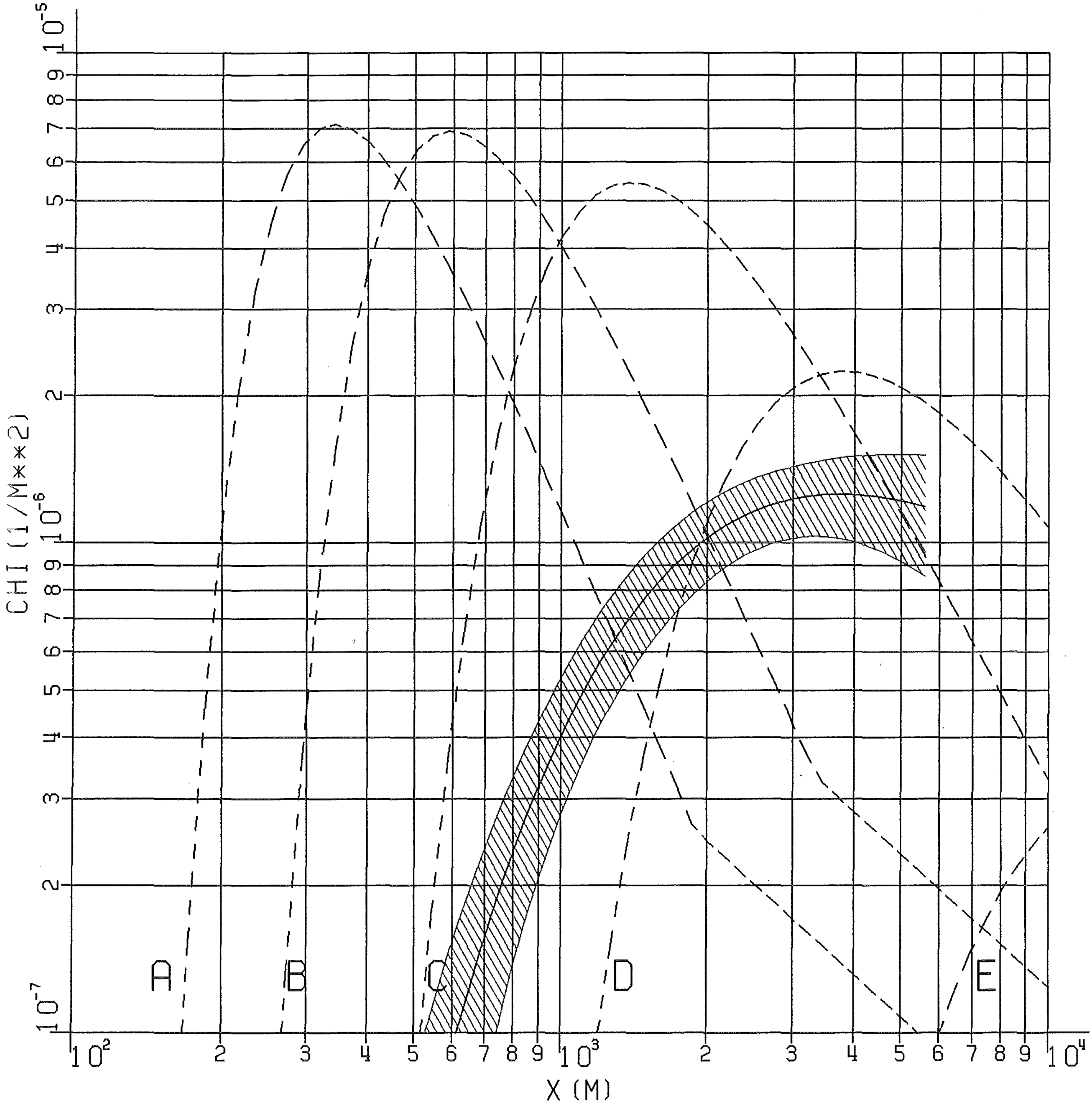

FIG. 8: NORMALIZED DIFFUSION FACTOR
OF EXPERIMENT NO.53, PERIODS 1+2

H=195M, TRACER CFCL3

- - - - - COMBINED, SMOOTHED, AND CENTERED RESULTS

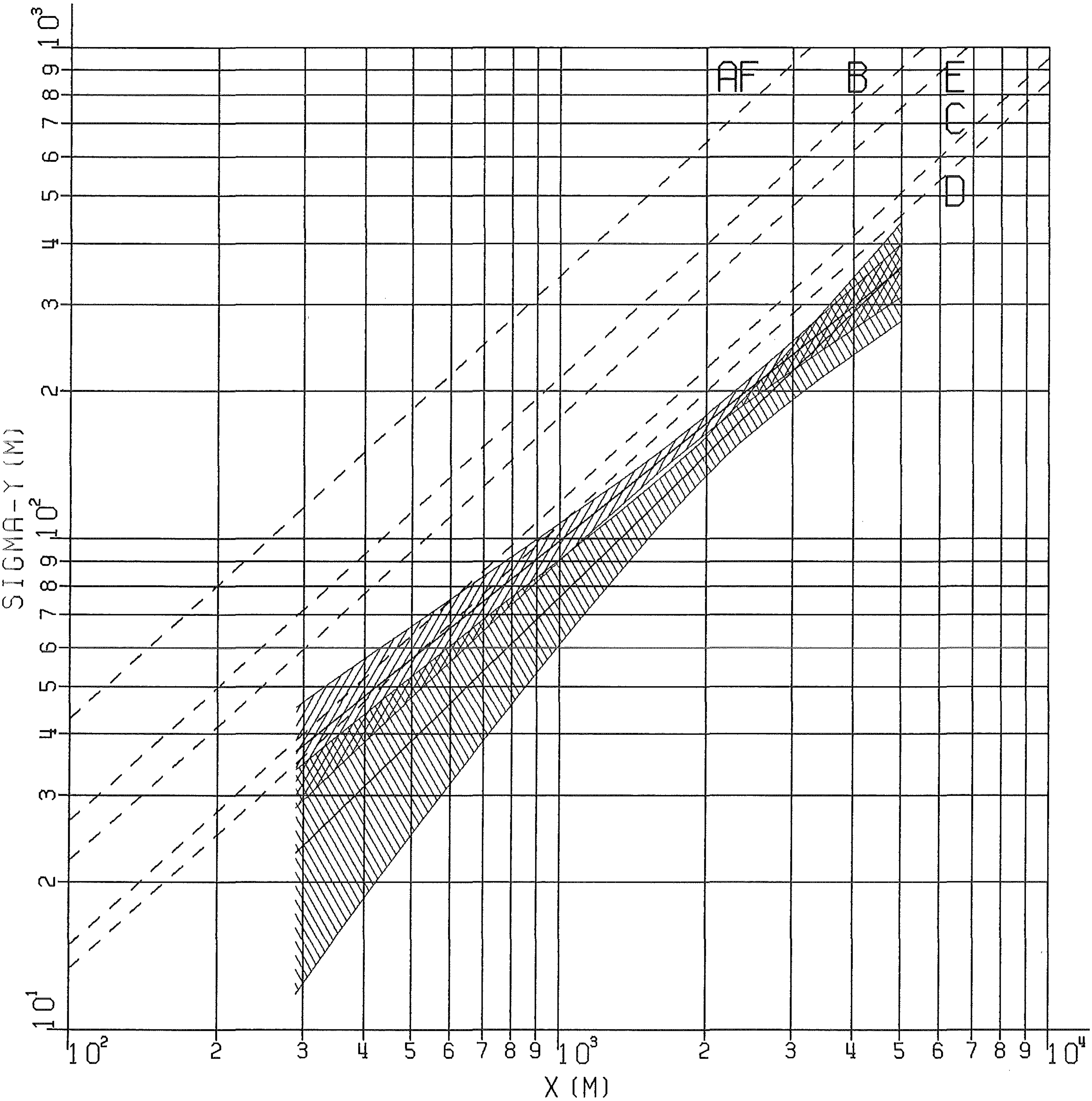

FIG. 9: HORIZONTAL DISPERSION PARAMETER
OF EXPERIMENT NO.55, PERIODS 1+2
H=160M, TRACER CF2BR2
H=195M, TRACER CFCL3
- - - - - COMBINED, SMOOTHED, AND CENTERED RESULTS

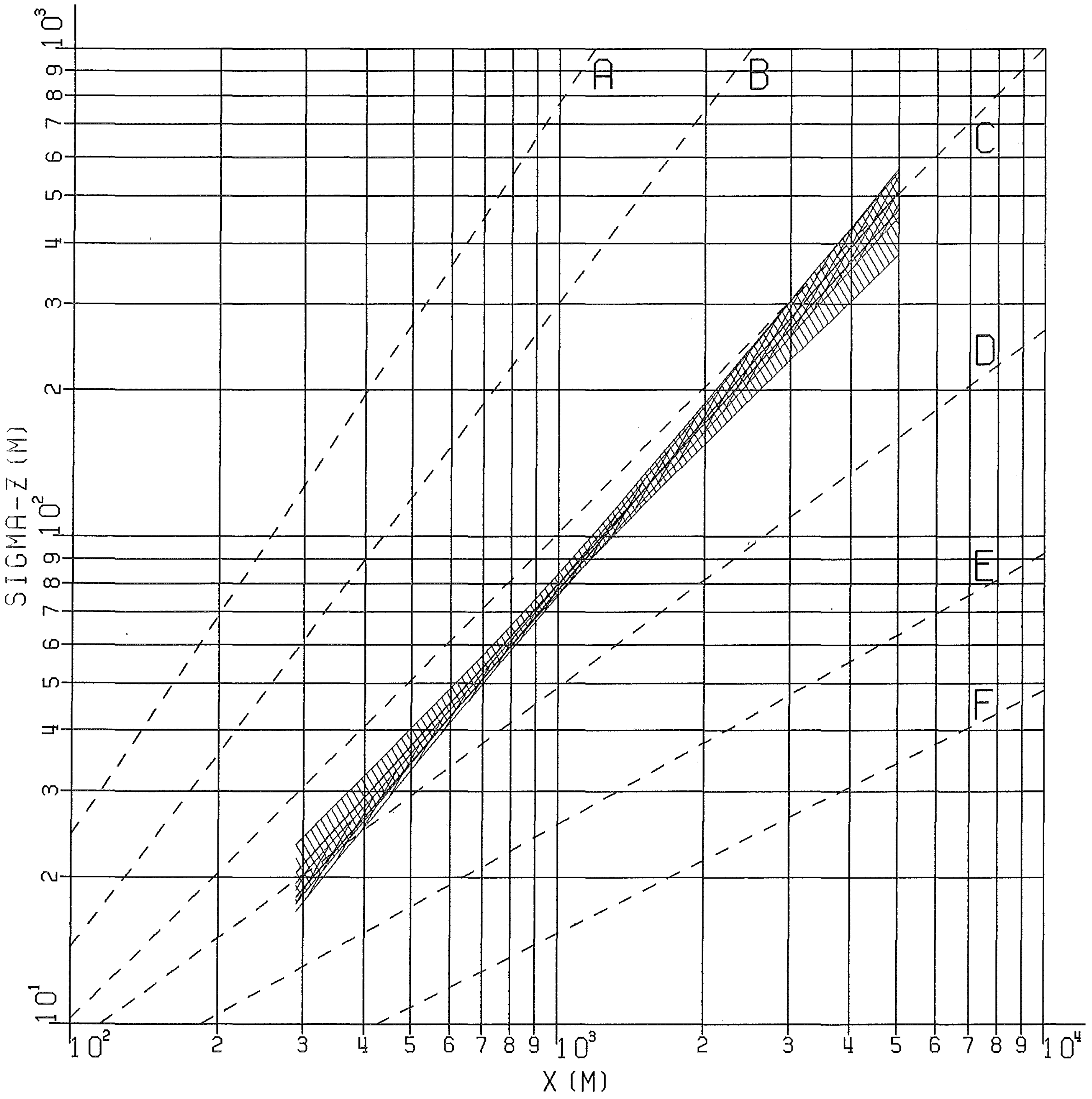

FIG. 10: VERTICAL DISPERSION PARAMETER
OF EXPERIMENT NO.55, PERIODS 1+2

H=160M, TRACER CF2BR2

H=195M, TRACER CFCL3

- - - - - COMBINED, SMOOTHED, AND CENTERED RESULTS

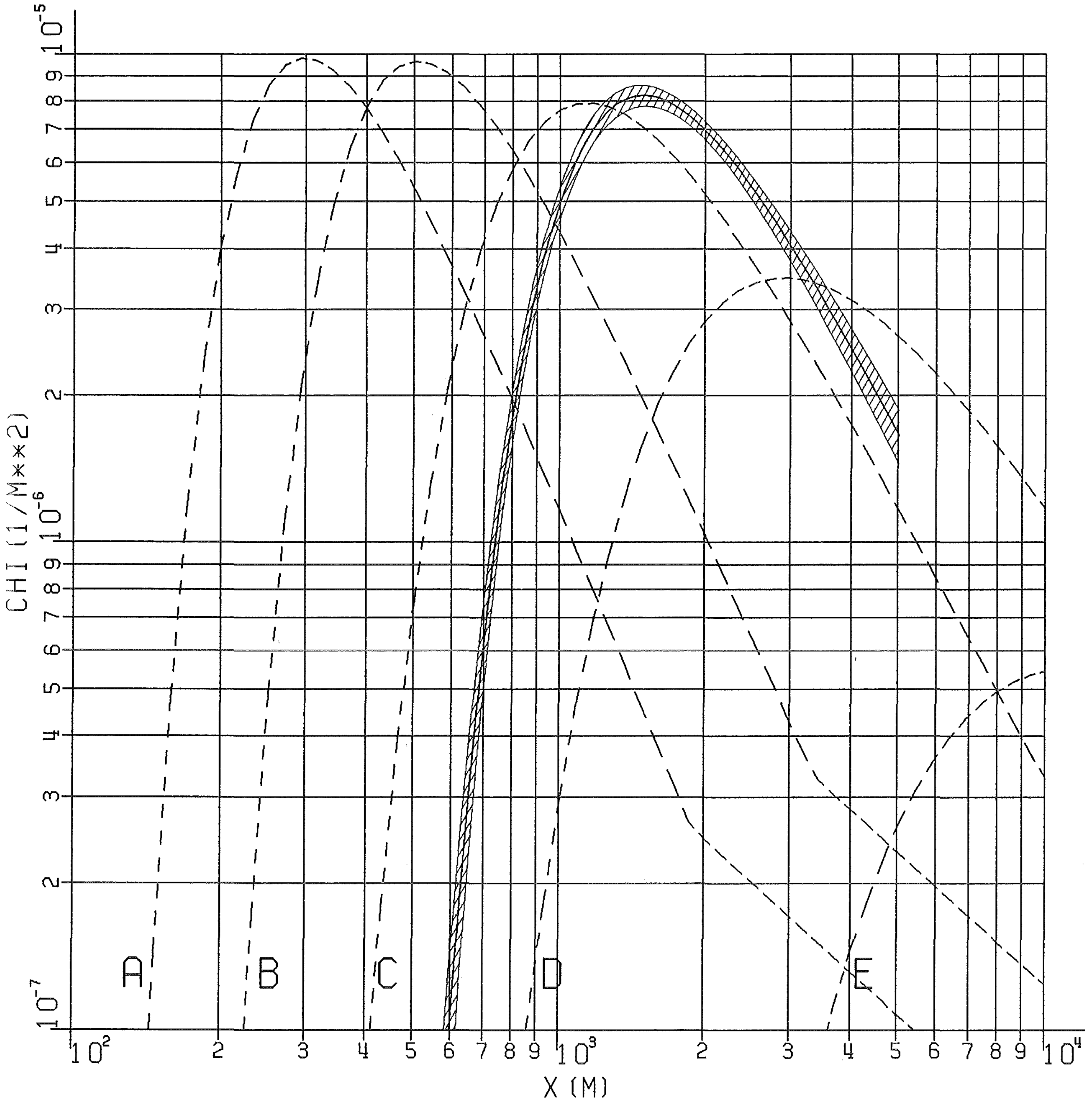

FIG. 11: NORMALIZED DIFFUSION FACTOR
OF EXPERIMENT NO.55, PERIODS 1+2
H=160M, TRACER CF2BR2
- - - - - COMBINED, SMOOTHED, AND CENTERED RESULTS

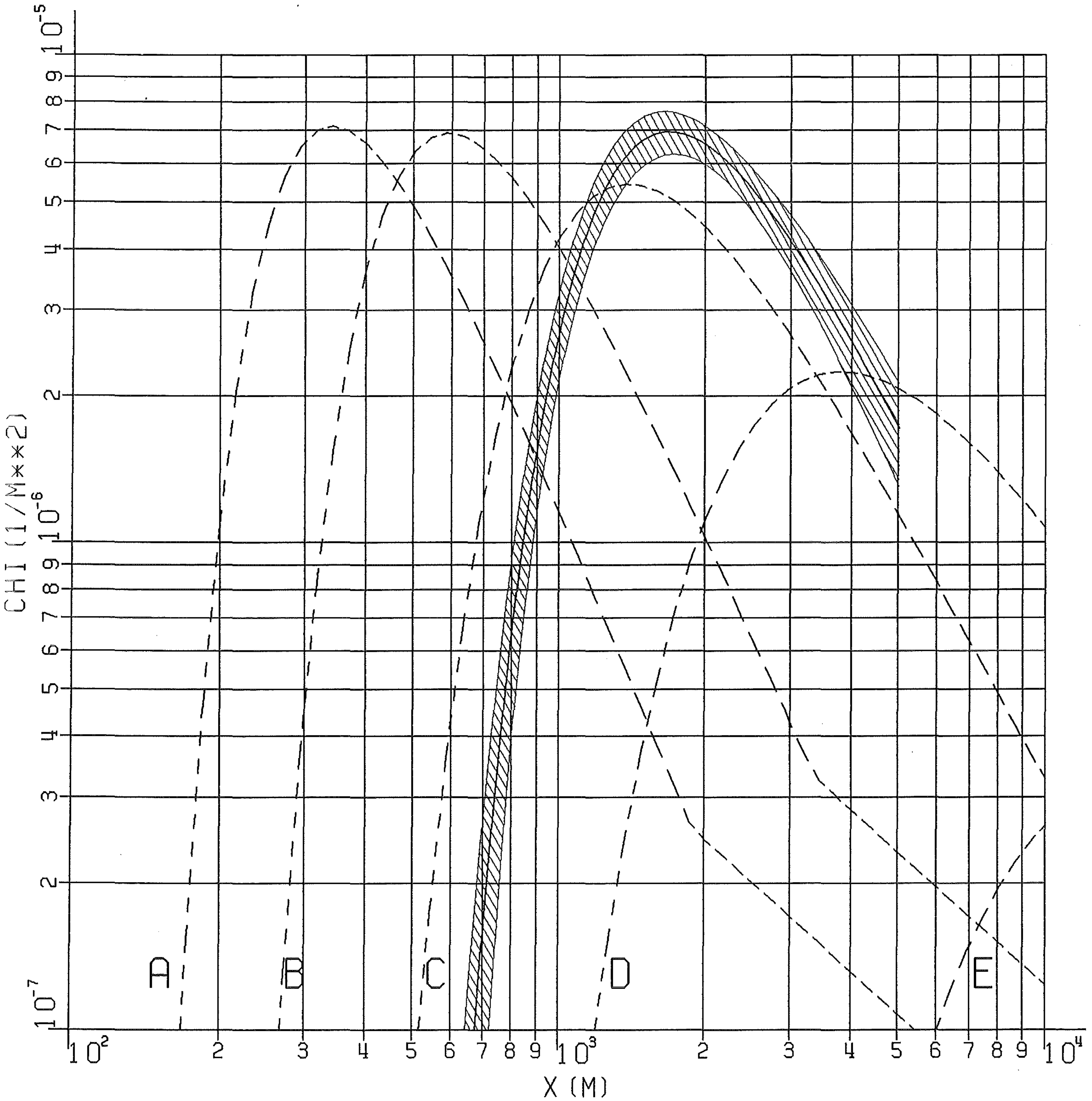

FIG. 12: NORMALIZED DIFFUSION FACTOR
OF EXPERIMENT NO.55, PERIODS 1+2
\\\\\\\\\\\\ H=195M, TRACER CFCL3
- - - - - COMBINED, SMOOTHED, AND CENTERED RESULTS

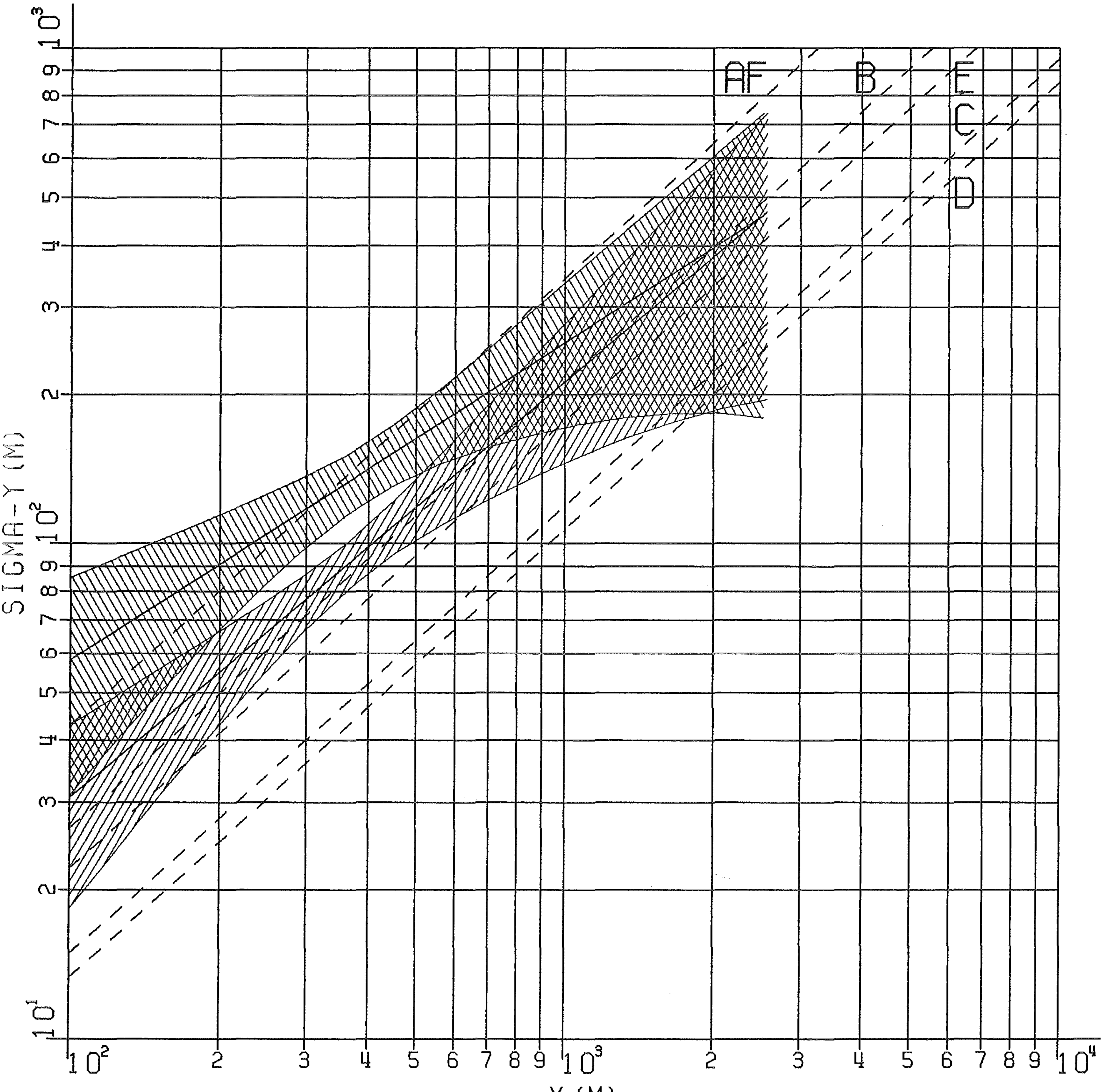

FIG. 13: HORIZONTAL DISPERSION PARAMETER
OF EXPERIMENT NO.57, PERIODS 1+2
H=160M, TRACER CF2BR2
H=195M, TRACER CFCL3
- - - - - COMBINED, SMOOTHED, AND CENTERED RESULTS

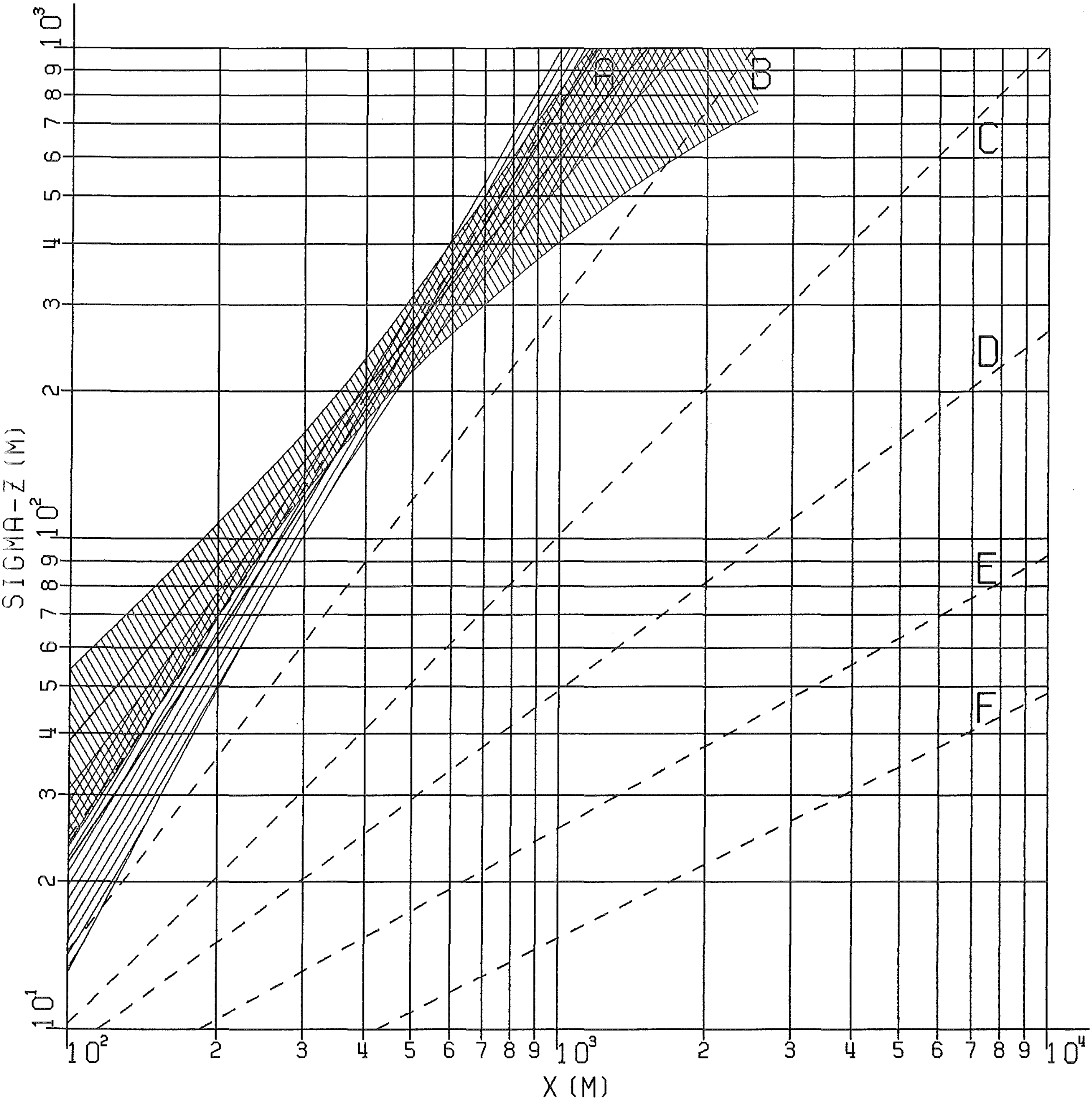

FIG. 14: VERTICAL DISPERSION PARAMETER
OF EXPERIMENT NO.57, PERIODS 1+2
H=160M, TRACER CF2BR2
H=195M, TRACER CFCL3
- - - - - COMBINED, SMOOTHED, AND CENTERED RESULTS

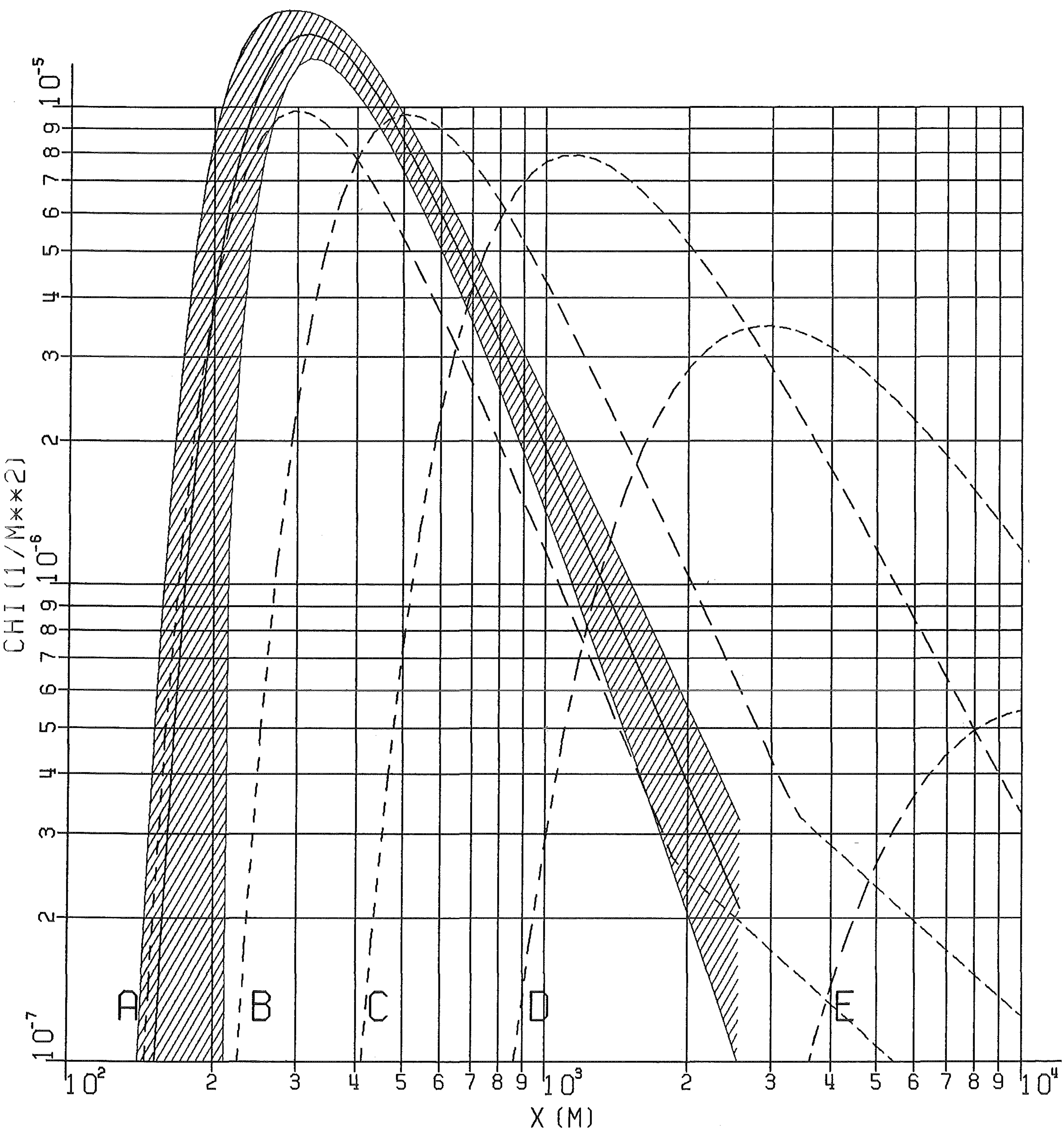

FIG. 15: NORMALIZED DIFFUSION FACTOR
OF EXPERIMENT NO.57, PERIODS 1+2

H=160M, TRACER CF2BR2

- - - - - COMBINED, SMOOTHED, AND CENTERED RESULTS

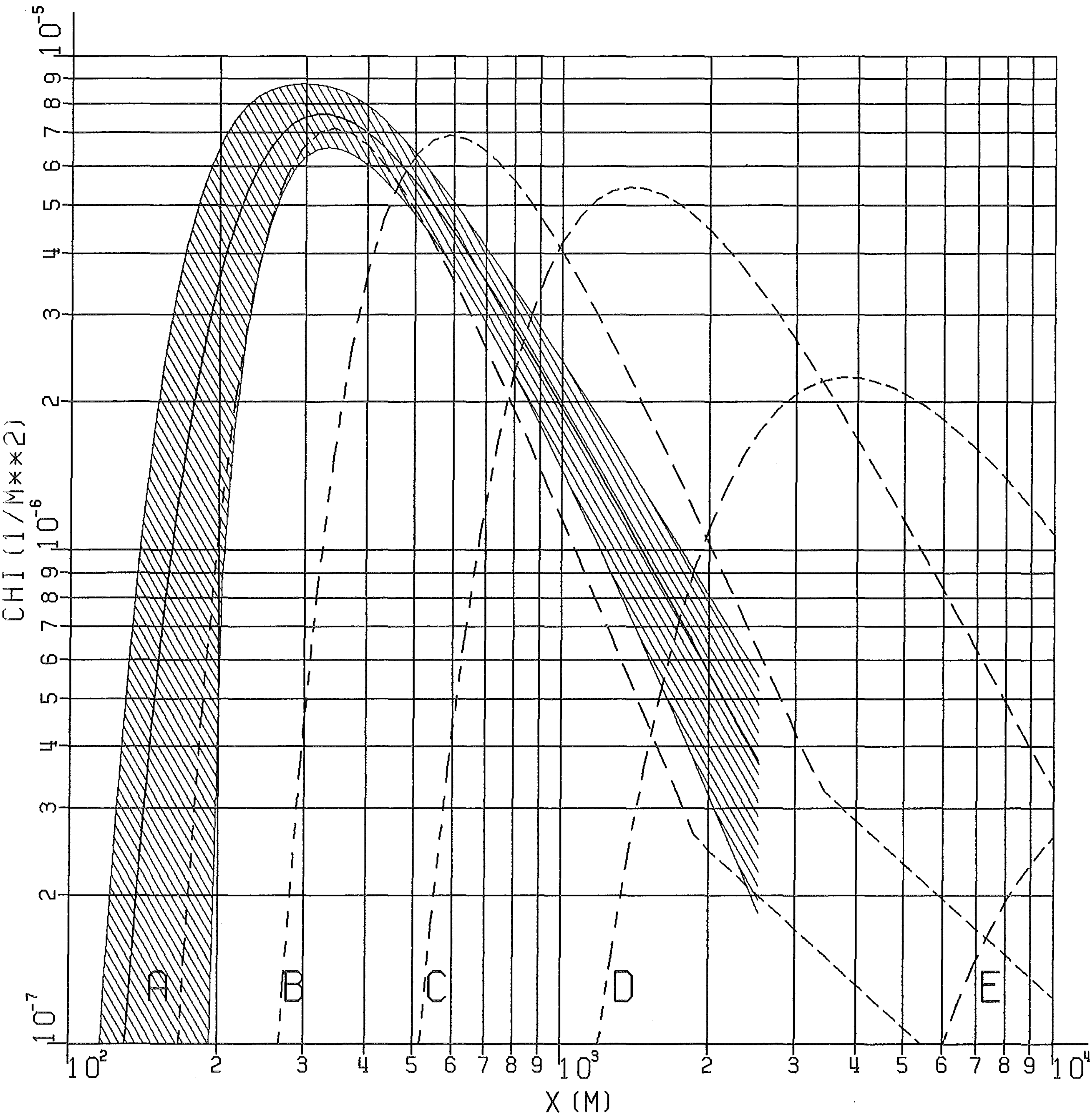

FIG. 16: NORMALIZED DIFFUSION FACTOR
OF EXPERIMENT NO.57, PERIODS 1+2

H=195M, TRACER CFCL3

- - - - - COMBINED, SMOOTHED, AND CENTERED RESULTS

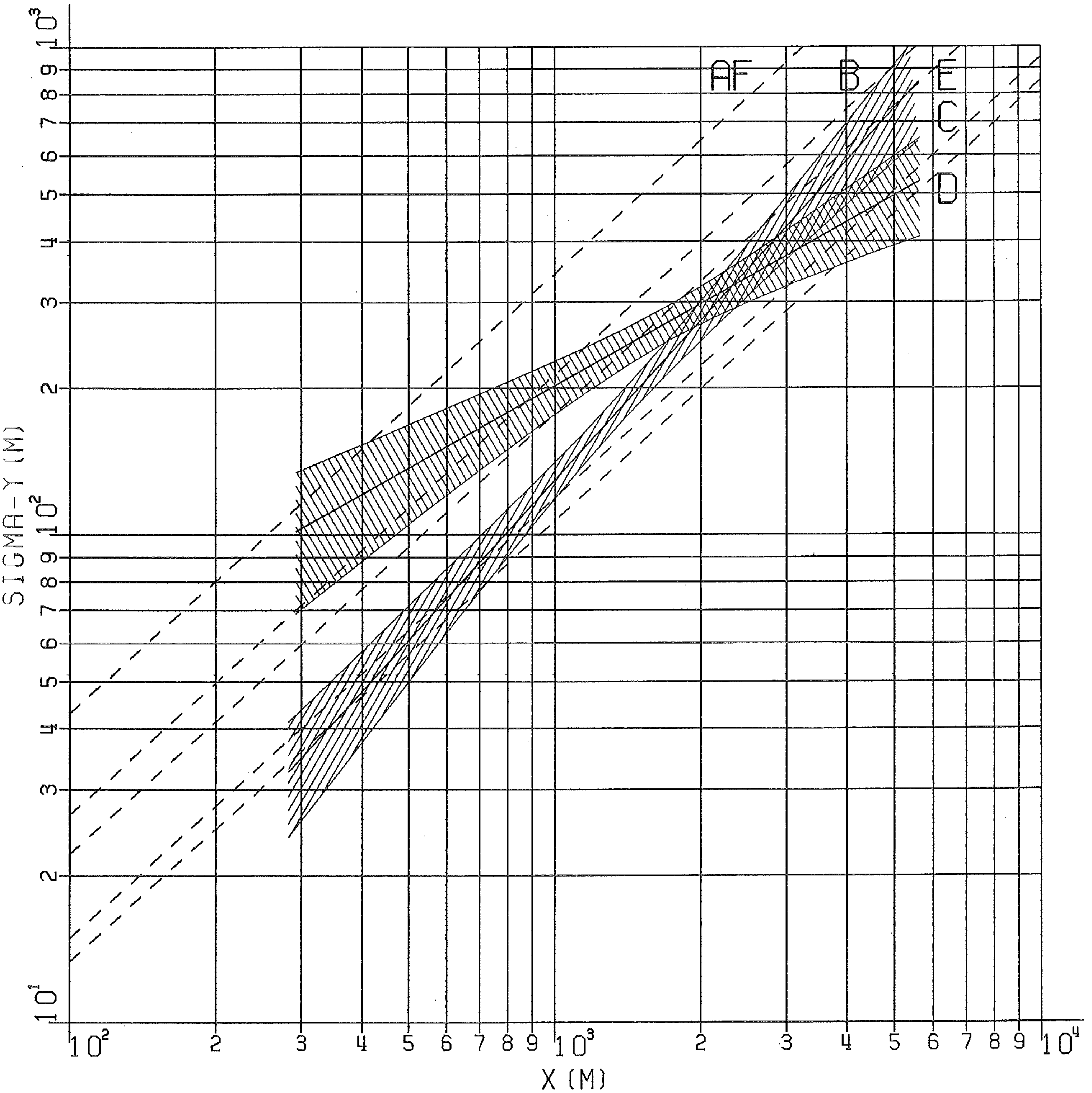

FIG. 17: HORIZONTAL DISPERSION PARAMETER
OF EXPERIMENT NO.58, PERIODS 1+2

H=160M, TRACER CF2BR2

H=195M, TRACER CFCL3

----- COMBINED, SMOOTHED, AND CENTERED RESULTS

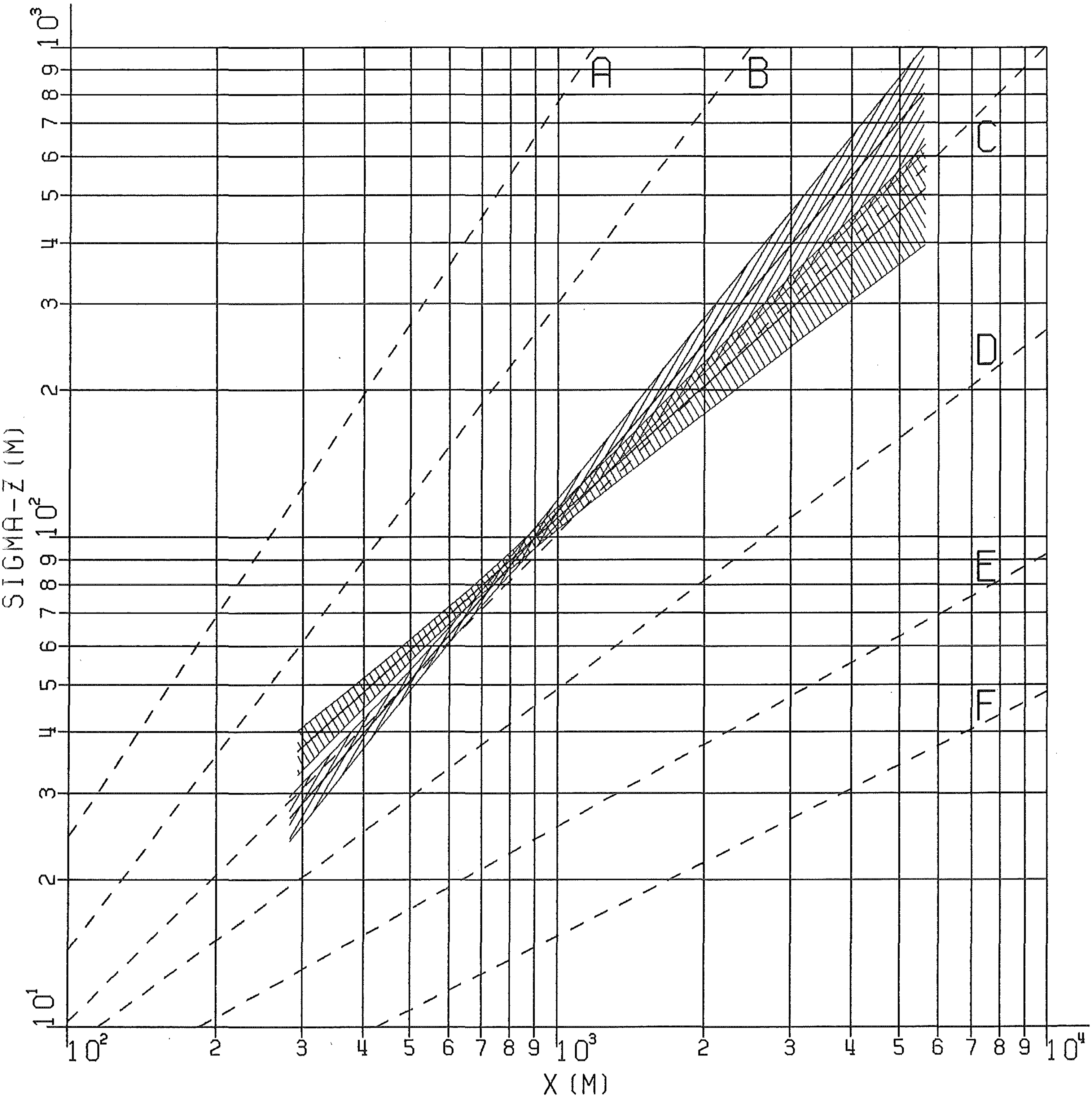

FIG. 18: VERTICAL DISPERSION PARAMETER
OF EXPERIMENT NO.58, PERIODS 1+2
H=160M, TRACER CF2BR2
H=195M, TRACER CFCL3
- - - - - COMBINED, SMOOTHED, AND CENTERED RESULTS

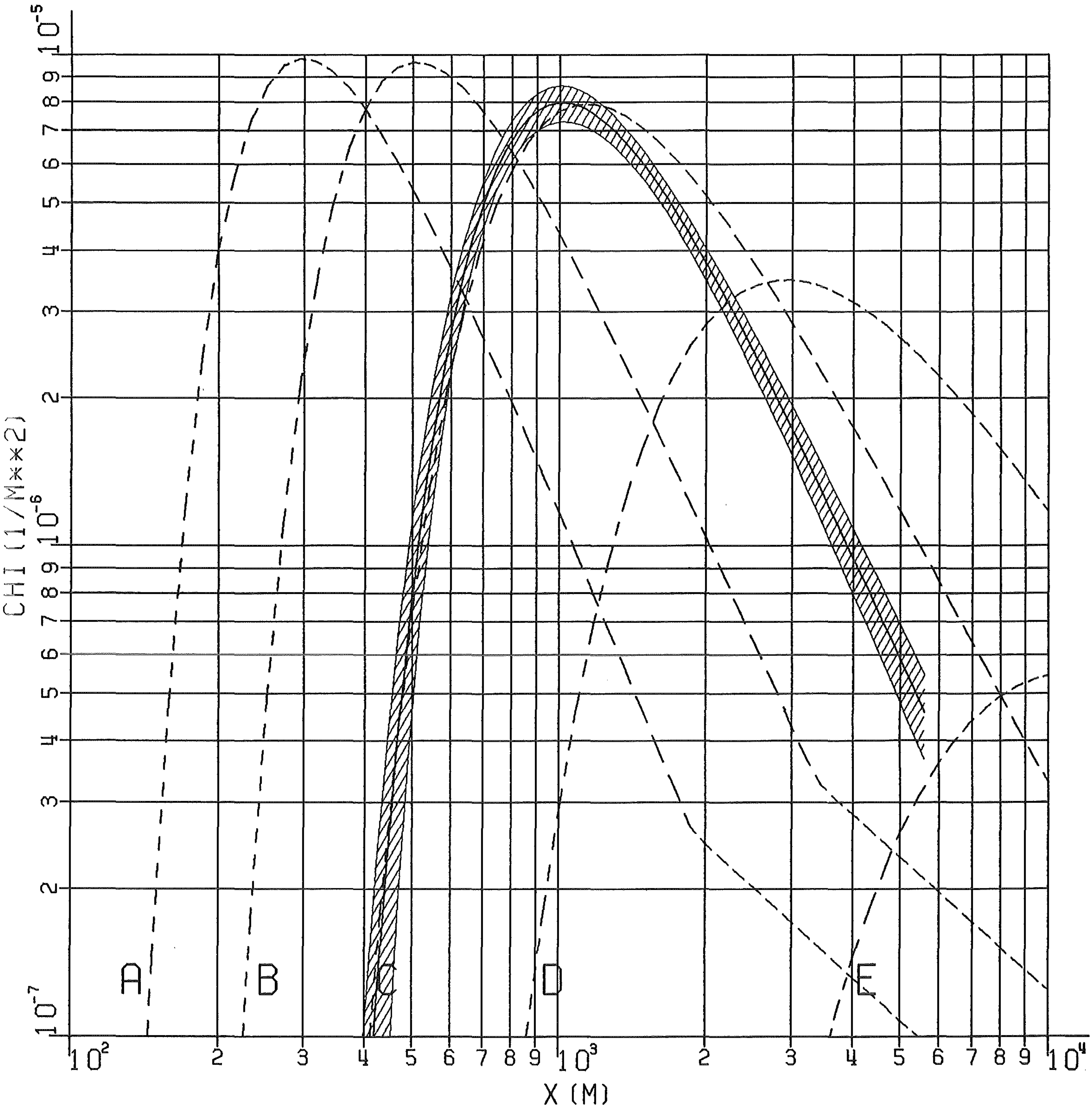

FIG. 19: NORMALIZED DIFFUSION FACTOR
OF EXPERIMENT NO.58, PERIODS 1+2
////////// H=160M, TRACER CF2BR2
- - - - - COMBINED, SMOOTHED, AND CENTERED RESULTS

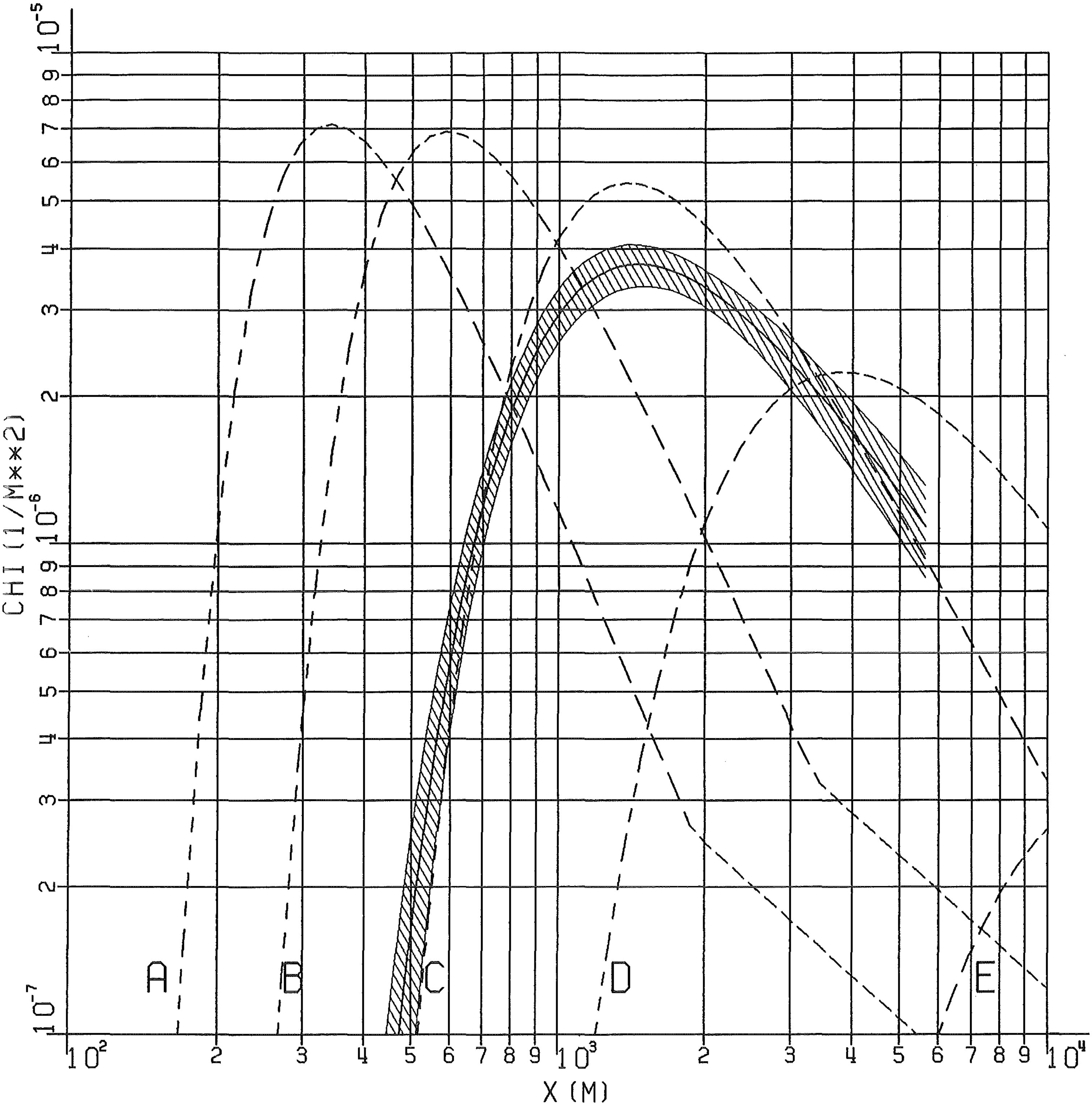

FIG. 20: NORMALIZED DIFFUSION FACTOR
OF EXPERIMENT NO.58, PERIODS 1+2
H=195M, TRACER CFCL3
- - - - - COMBINED, SMOOTHED, AND CENTERED RESULTS

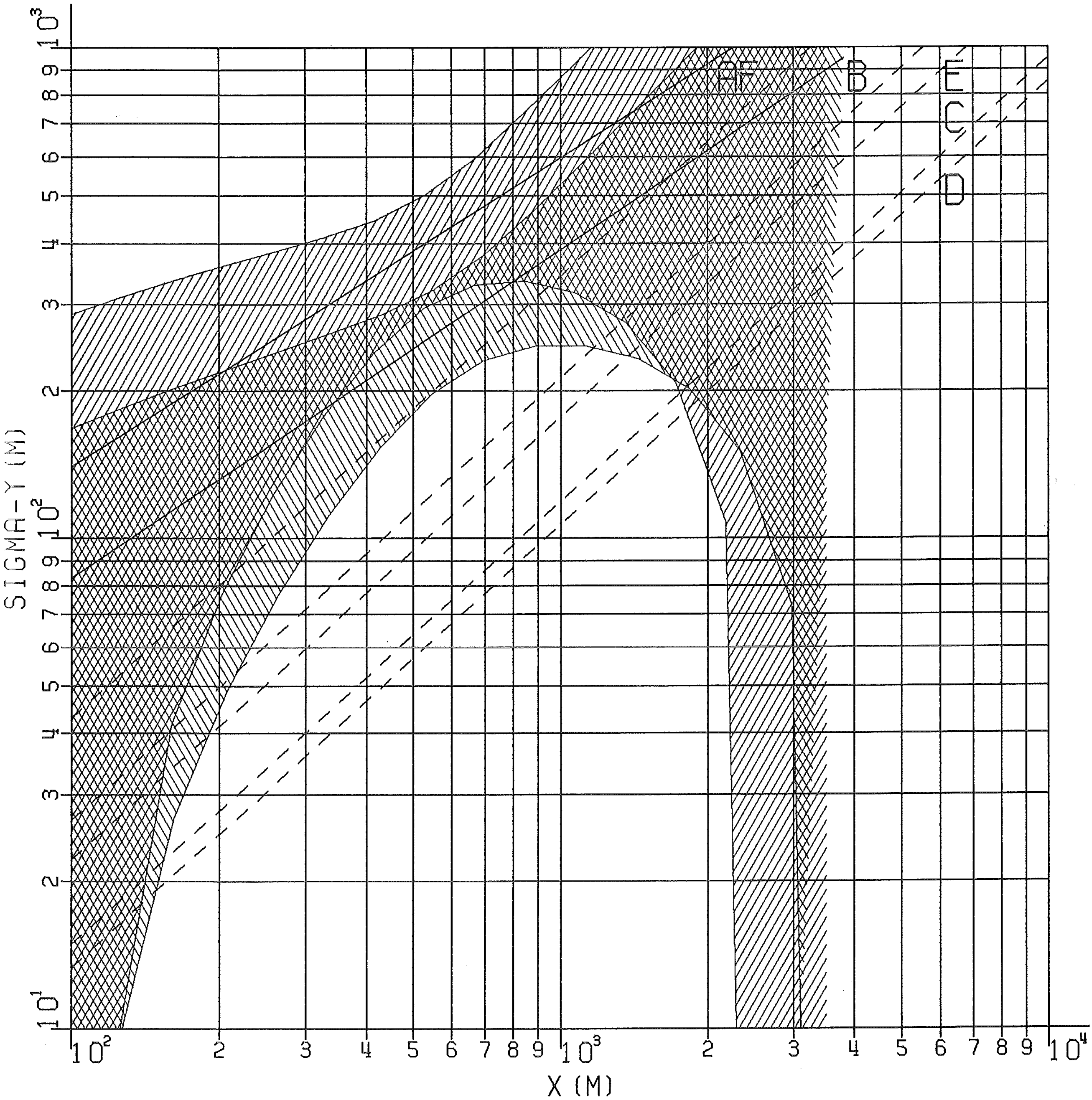

FIG. 21: HORIZONTAL DISPERSION PARAMETER
OF EXPERIMENT NO.60, PERIOD 1

H=160M, TRACER CF2BR2

H=195M, TRACER CFCL3

– – – – – COMBINED, SMOOTHED, AND CENTERED RESULTS

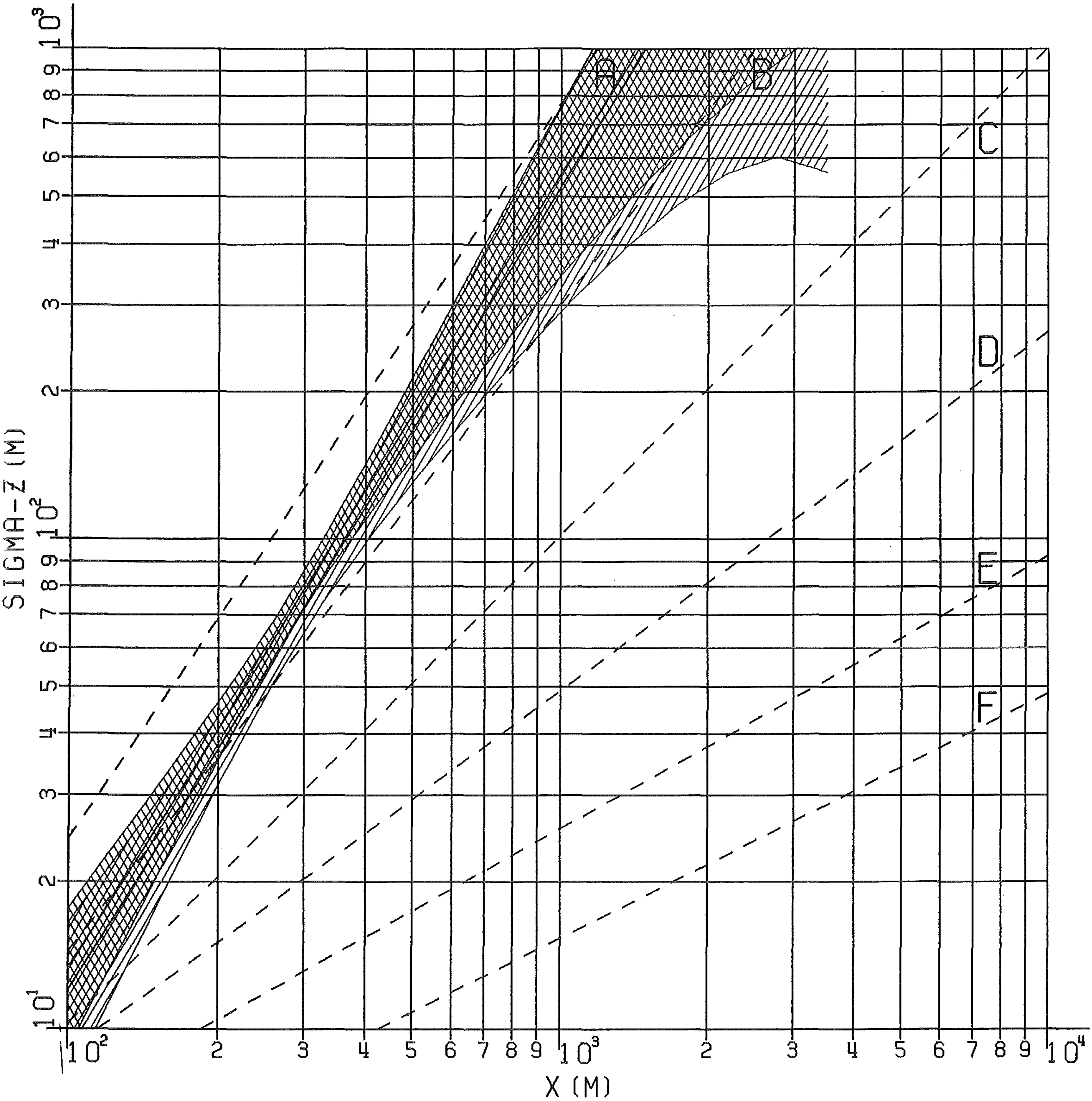

FIG. 22: VERTICAL DISPERSION PARAMETER
OF EXPERIMENT NO.60, PERIOD 1
H=160M, TRACER CF2BR2
H=195M, TRACER CFCL3
COMBINED, SMOOTHED, AND CENTERED RESULTS

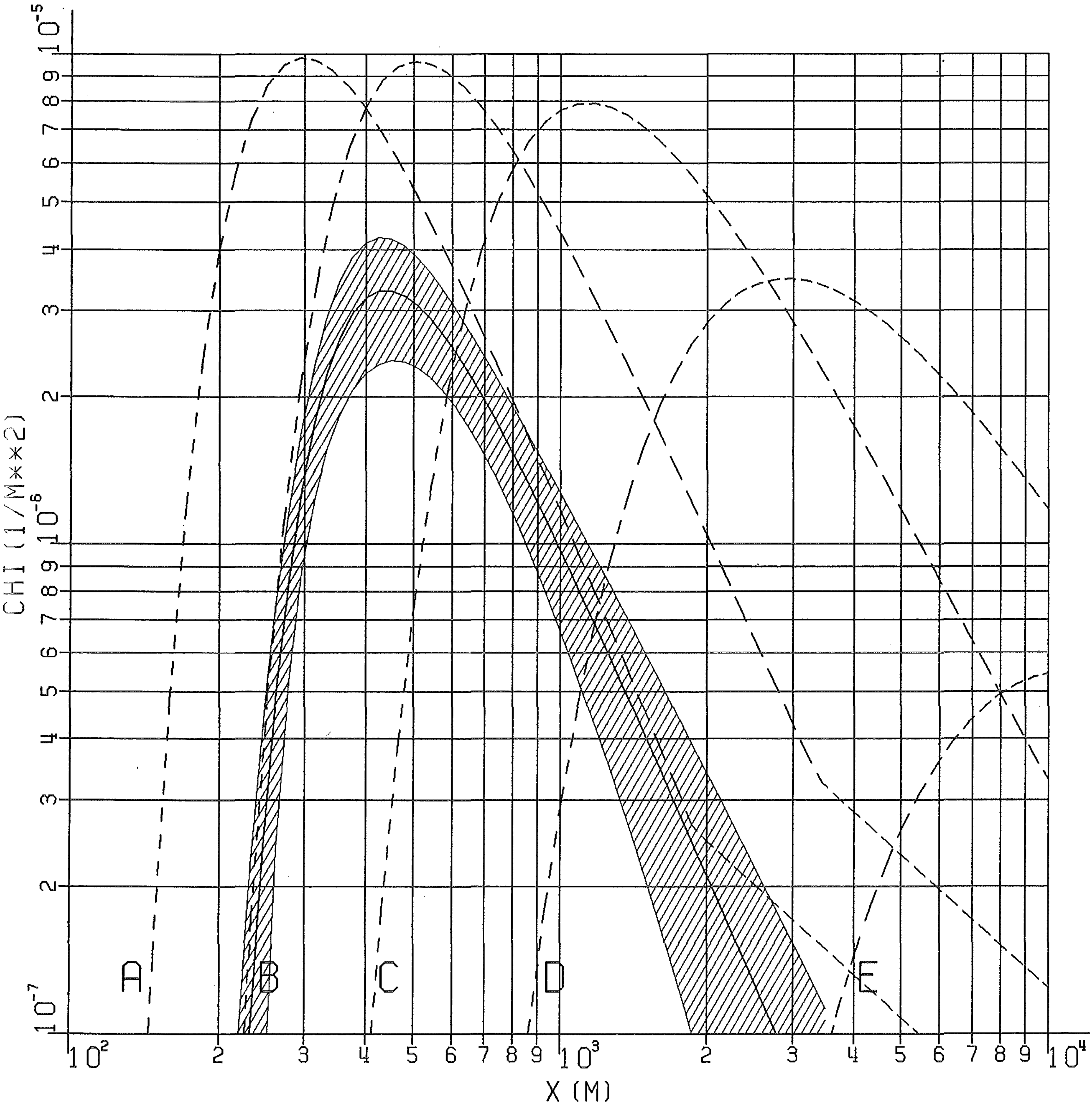

FIG. 23: NORMALIZED DIFFUSION FACTOR
OF EXPERIMENT NO.60, PERIOD 1
H=160M, TRACER CF2BR2
- - - - - COMBINED, SMOOTHED, AND CENTERED RESULTS

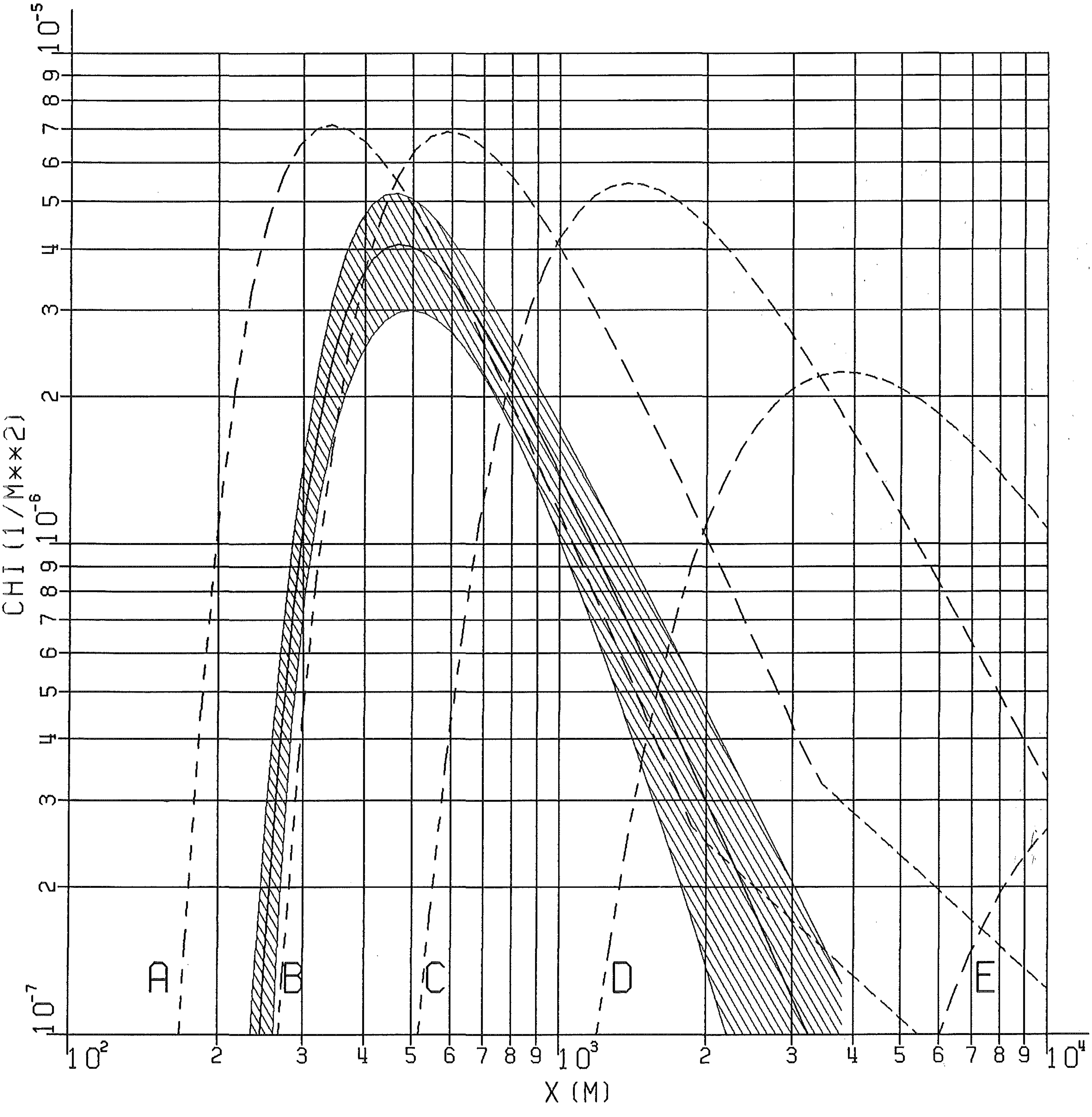

FIG. 24: NORMALIZED DIFFUSION FACTOR
OF EXPERIMENT NO.60, PERIOD 1
H=195M, TRACER CFCL3
- - - - - COMBINED, SMOOTHED, AND CENTERED RESULTS

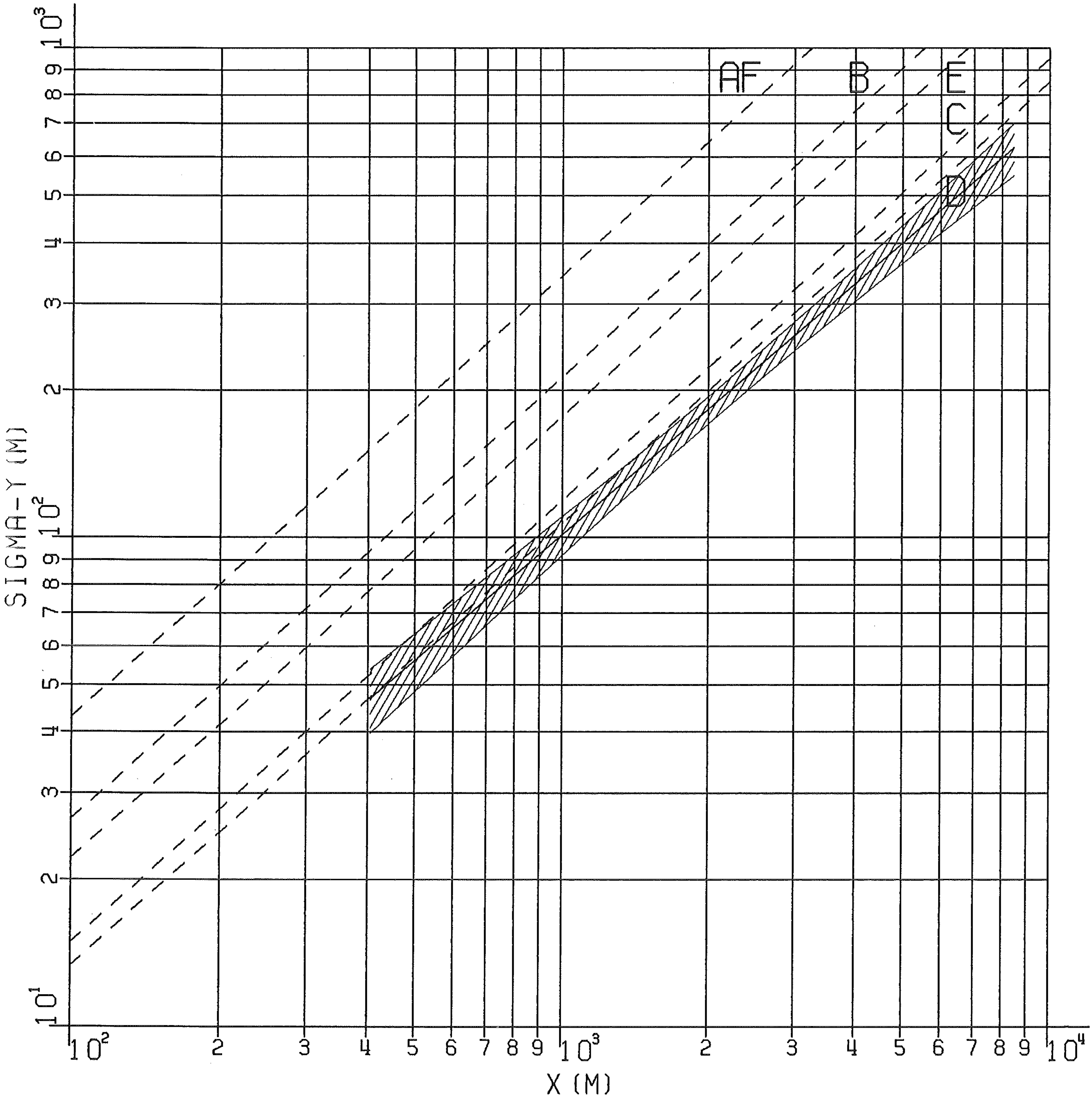

FIG. 25: HORIZONTAL DISPERSION PARAMETER
OF EXPERIMENT NO.61, PERIODS 1+2
////////////// H=160M, TRACER CF2BR2

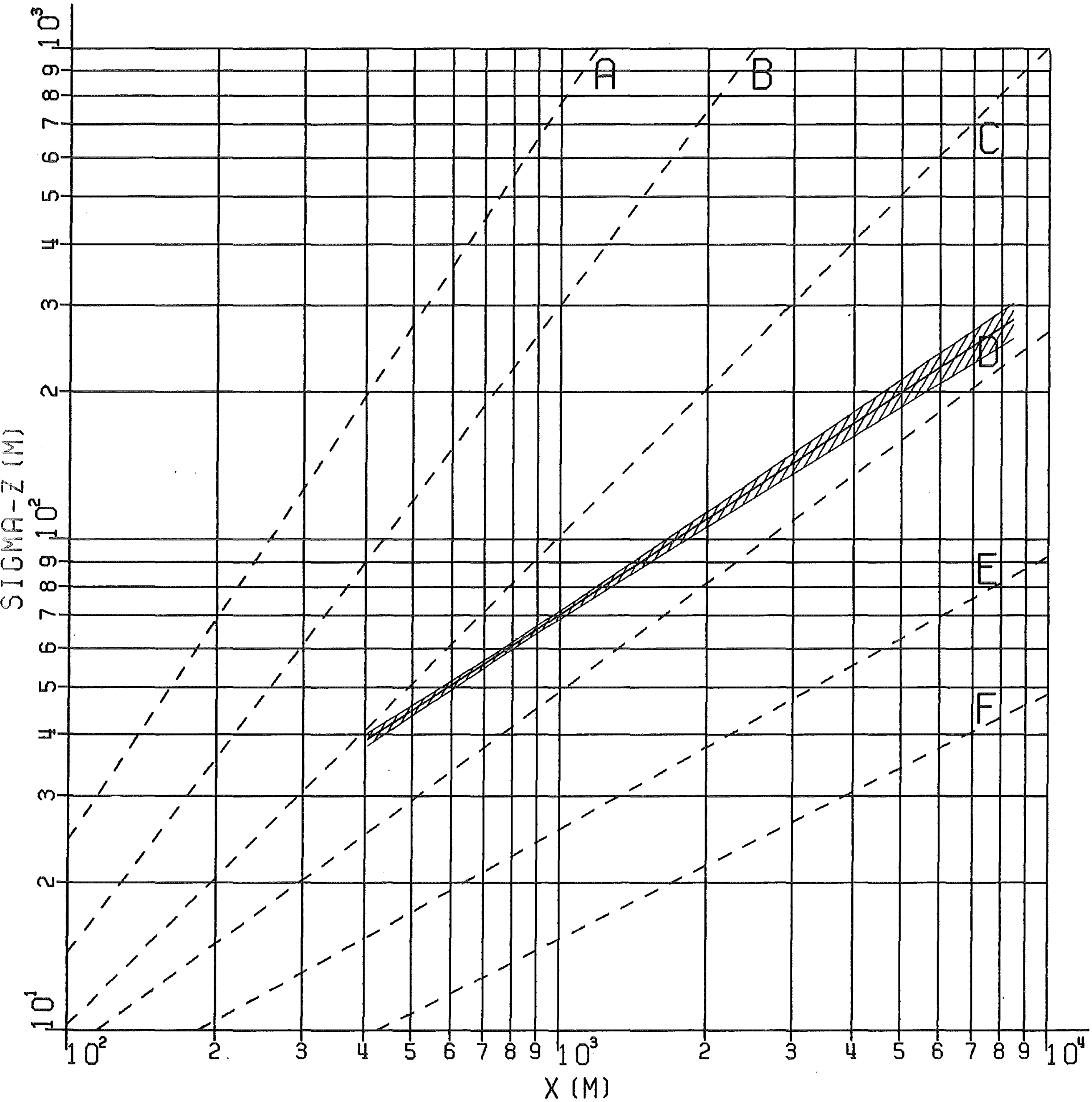

FIG. 26: VERTICAL DISPERSION PARAMETER
OF EXPERIMENT NO.61, PERIODS 1+2
H=160M, TRACER CF2BR2

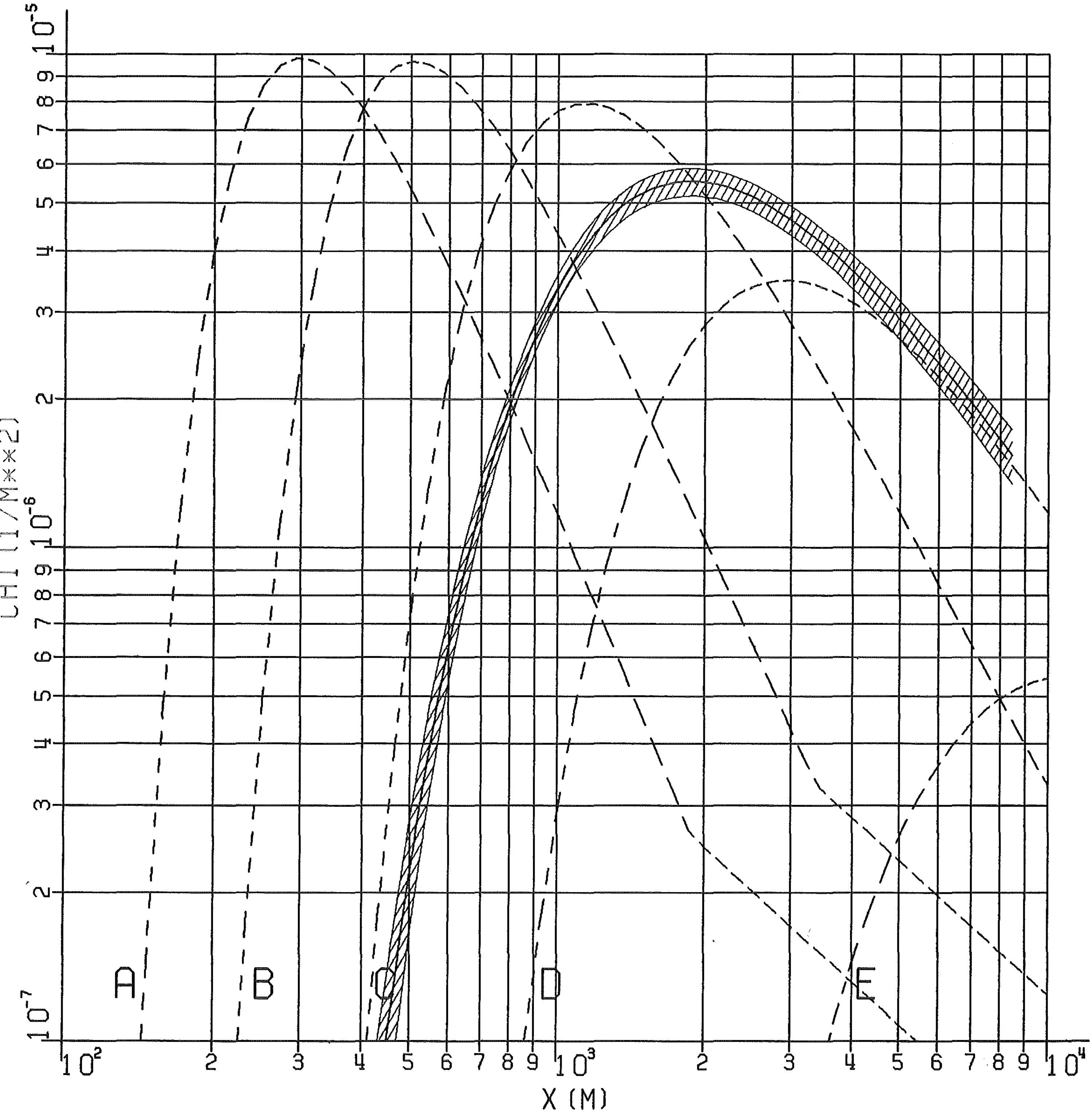

FIG. 27: NORMALIZED DIFFUSION FACTOR
OF EXPERIMENT NO.61, PERIODS 1+2

////////////// H=160M, TRACER CF2BR2

- - - - - COMBINED, SMOOTHED, AND CENTERED RESULTS

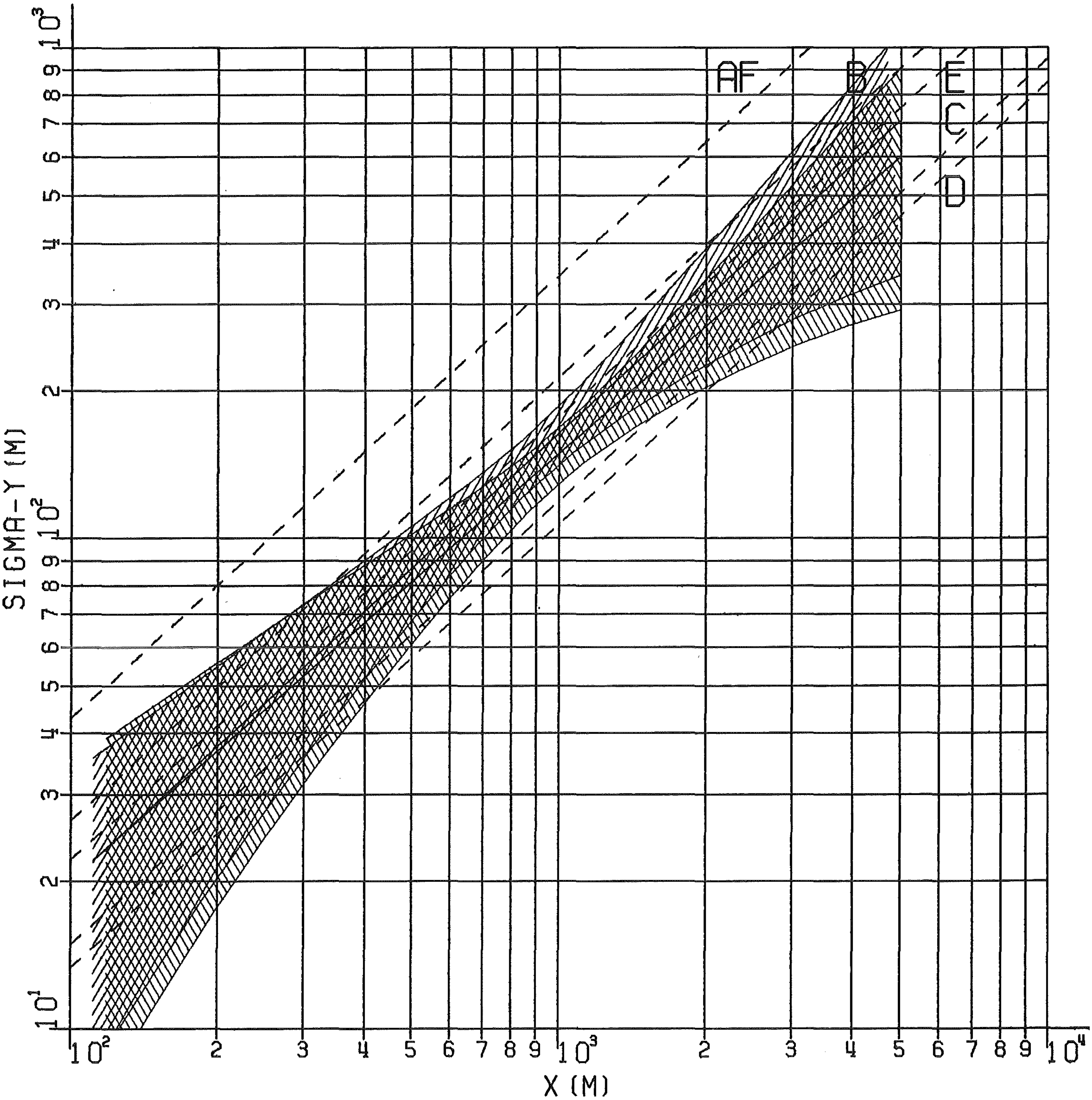

FIG. 28: HORIZONTAL DISPERSION PARAMETER
OF EXPERIMENT NO.62, PERIODS 1+2

H=160M, TRACER CF2BR2

H=195M, TRACER CFCL3

----- COMBINED, SMOOTHED, AND CENTERED RESULTS

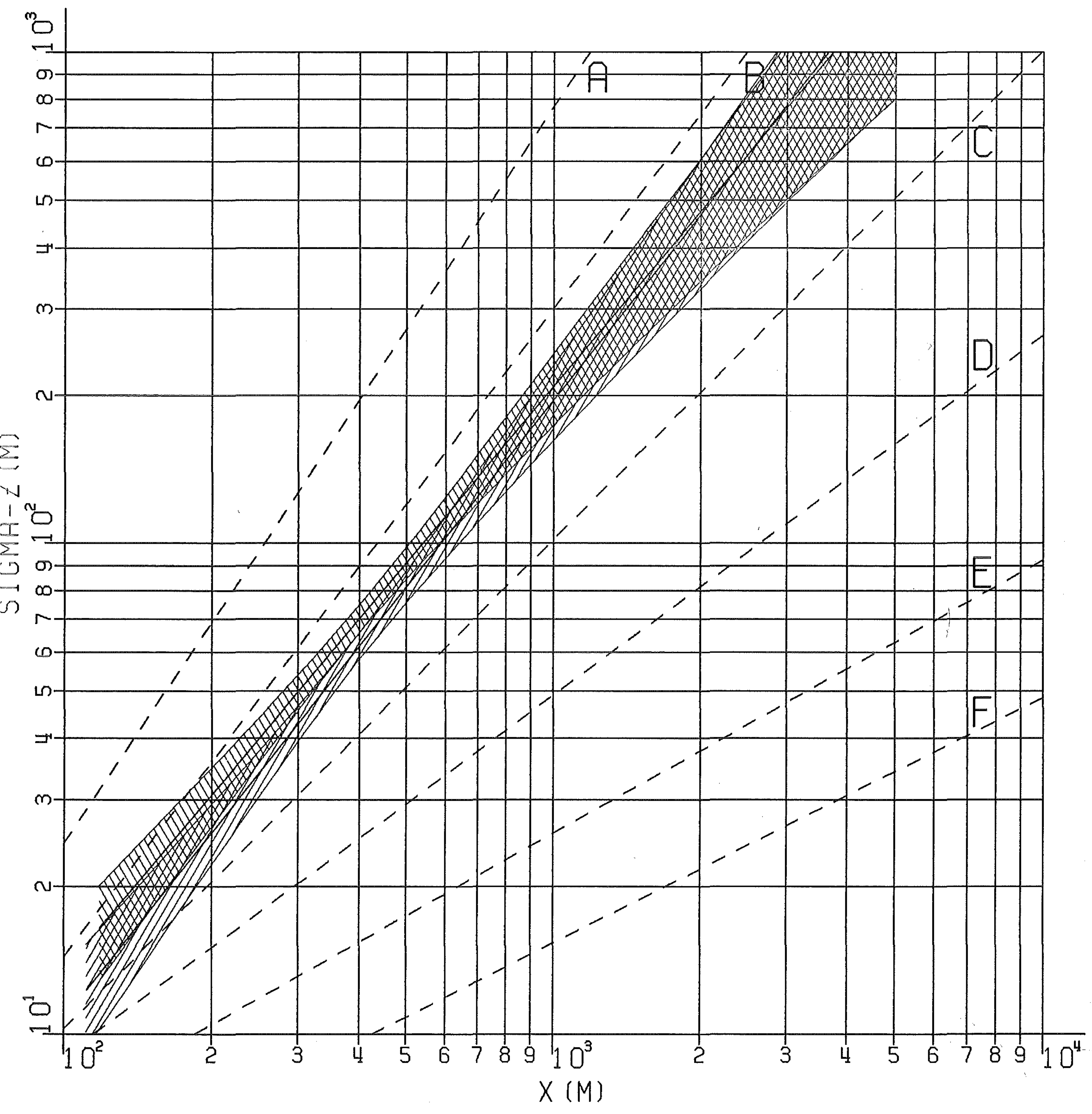

FIG. 29: VERTICAL DISPERSION PARAMETER
OF EXPERIMENT NO.62, PERIODS 1+2

H=160M, TRACER CF2BR2

H=195M, TRACER CFCL3

– – – – – COMBINED, SMOOTHED, AND CENTERED RESULTS

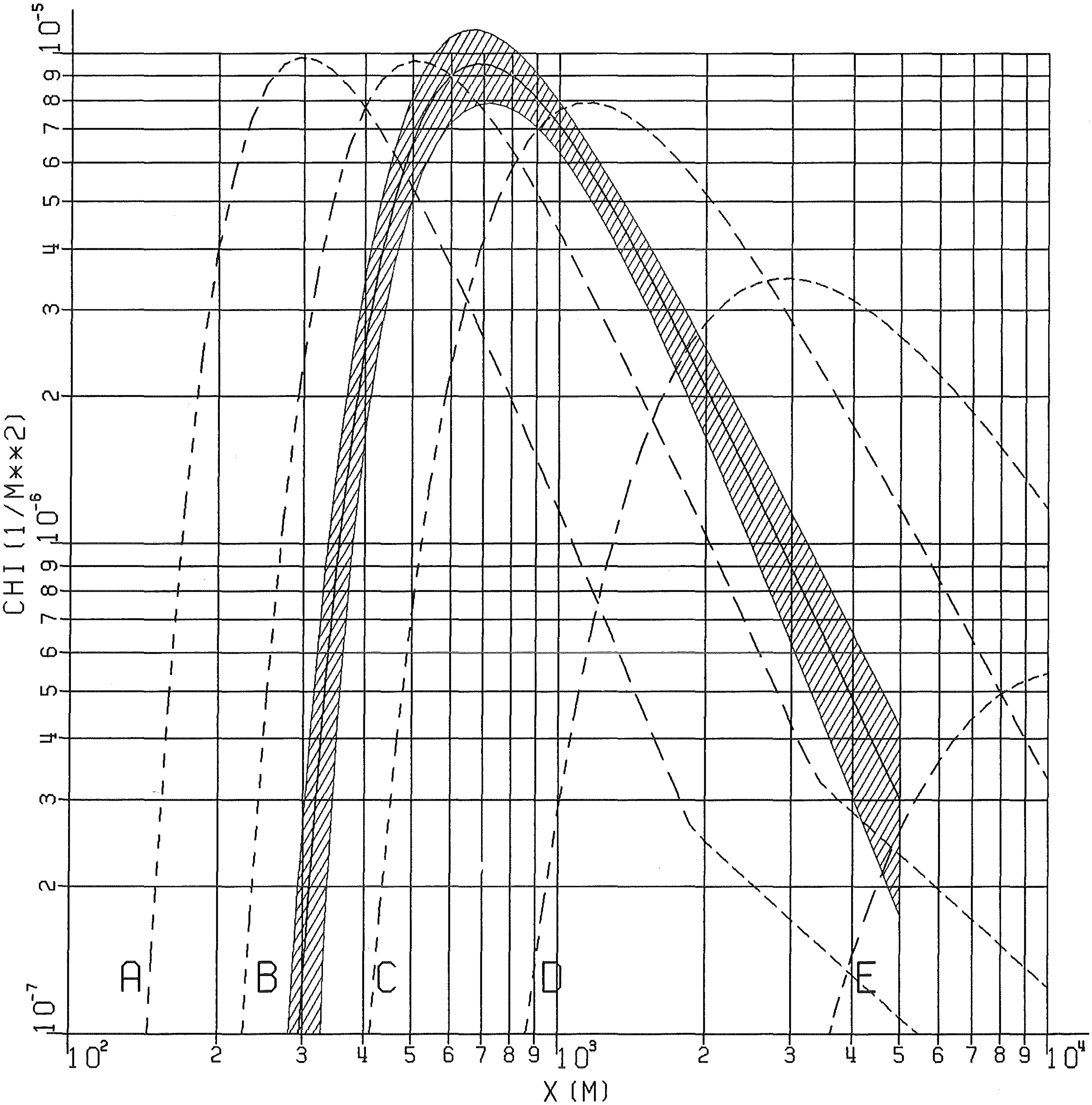

FIG. 30: NORMALIZED DIFFUSION FACTOR
OF EXPERIMENT NO.62, PERIODS 1+2
H=160M, TRACER CF2BR2
----- COMBINED, SMOOTHED, AND CENTERED RESULTS

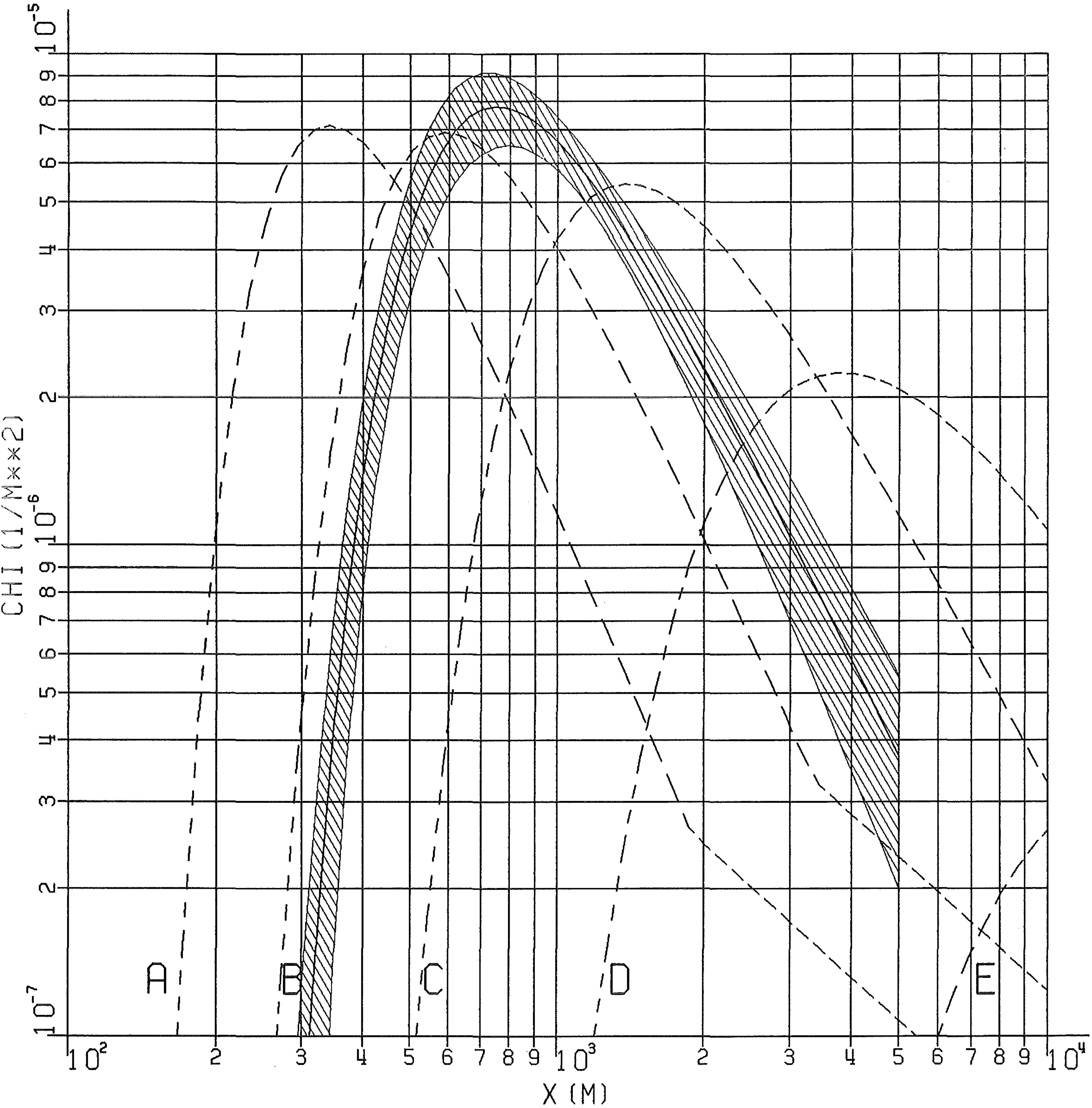

FIG. 31: NORMALIZED DIFFUSION FACTOR
OF EXPERIMENT NO.62, PERIODS 1+2
H=195M, TRACER CFCL3
- - - - - COMBINED, SMOOTHED, AND CENTERED RESULTS

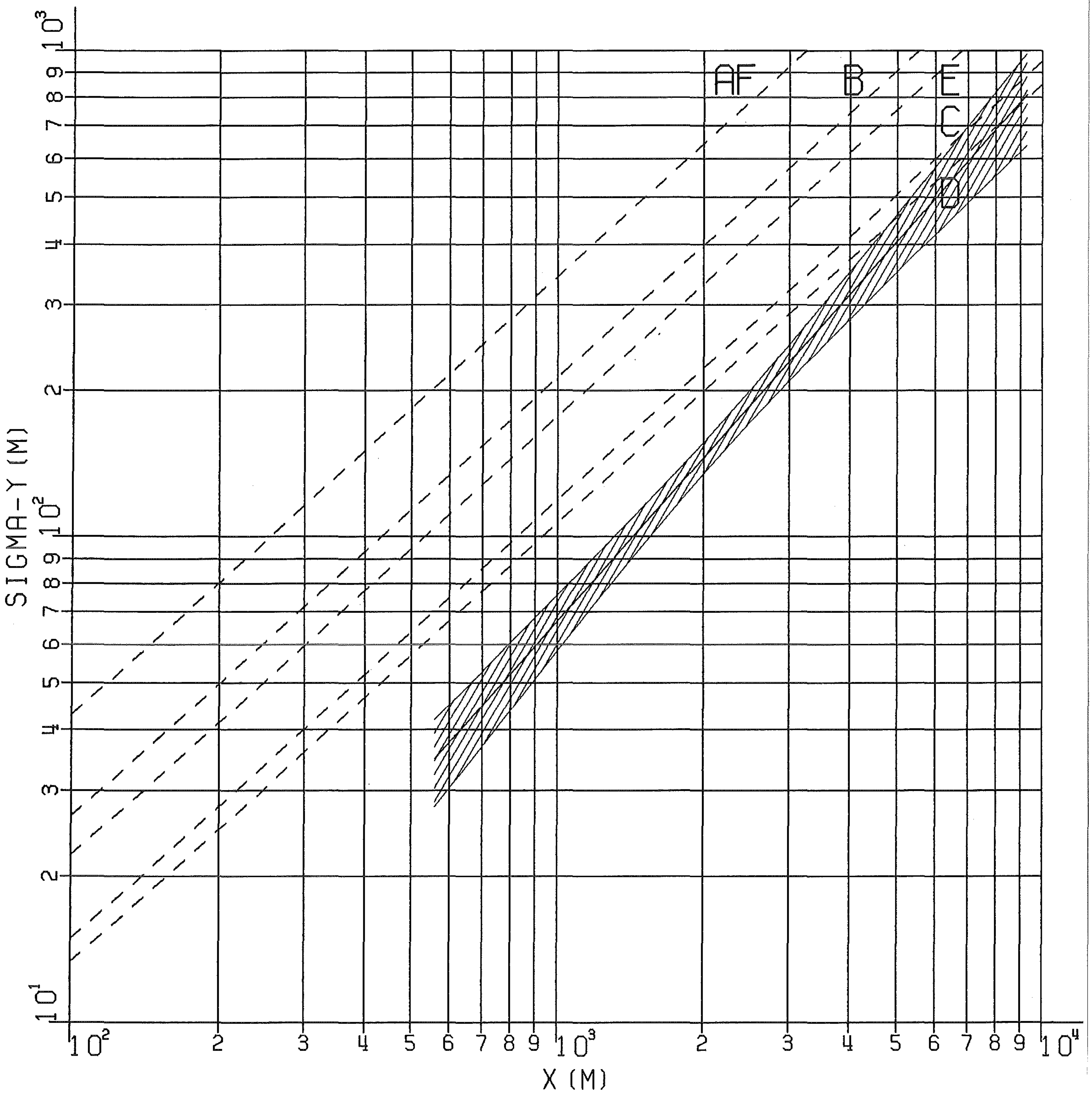

FIG. 32: HORIZONTAL DISPERSION PARAMETER
OF EXPERIMENT NO.63, PERIODS 1+2
H=160M, TRACER CF2BR2

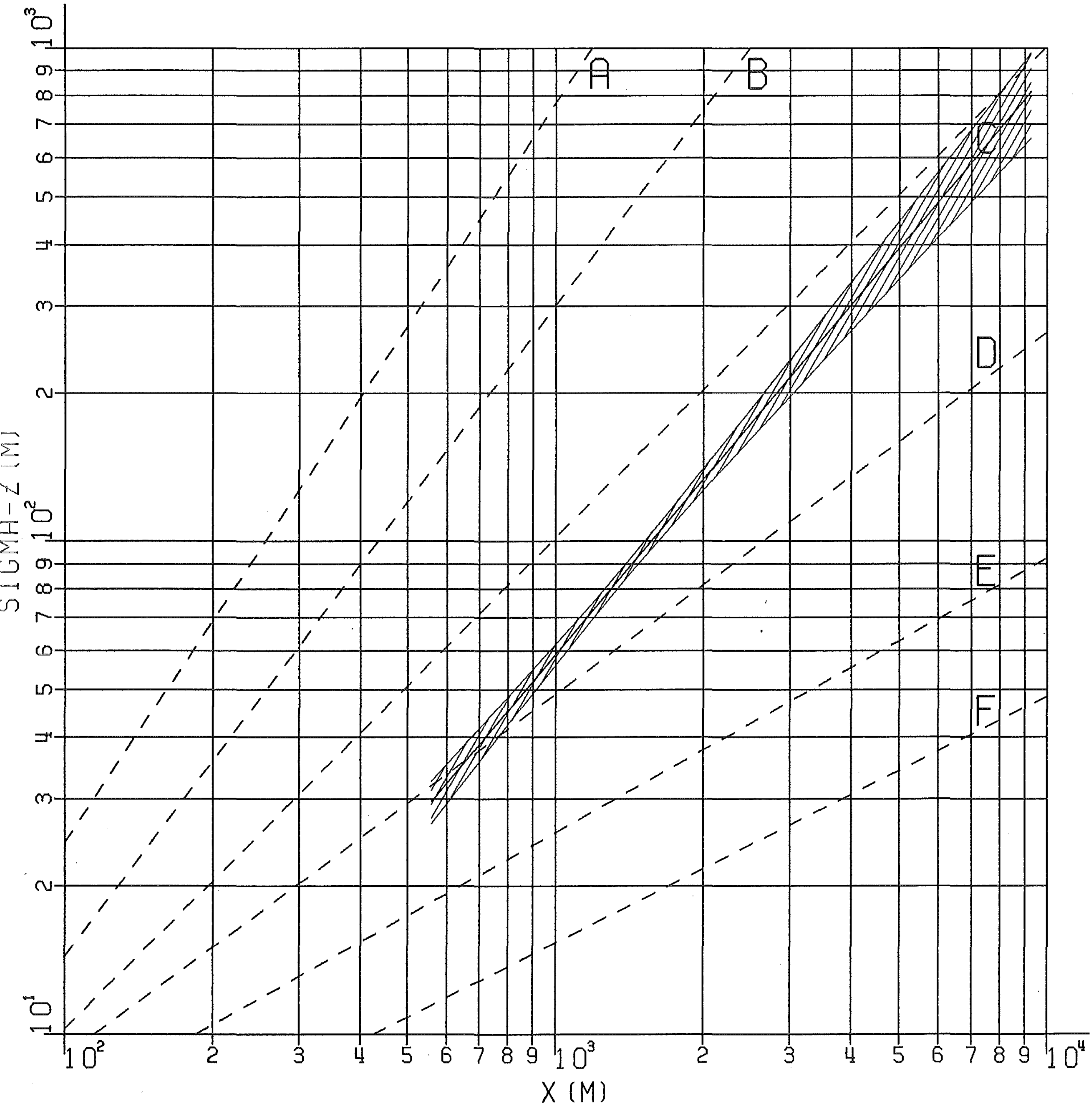

FIG. 33: VERTICAL DISPERSION PARAMETER
OF EXPERIMENT NO.63, PERIODS 1+2
H=160M, TRACER CF2BR2

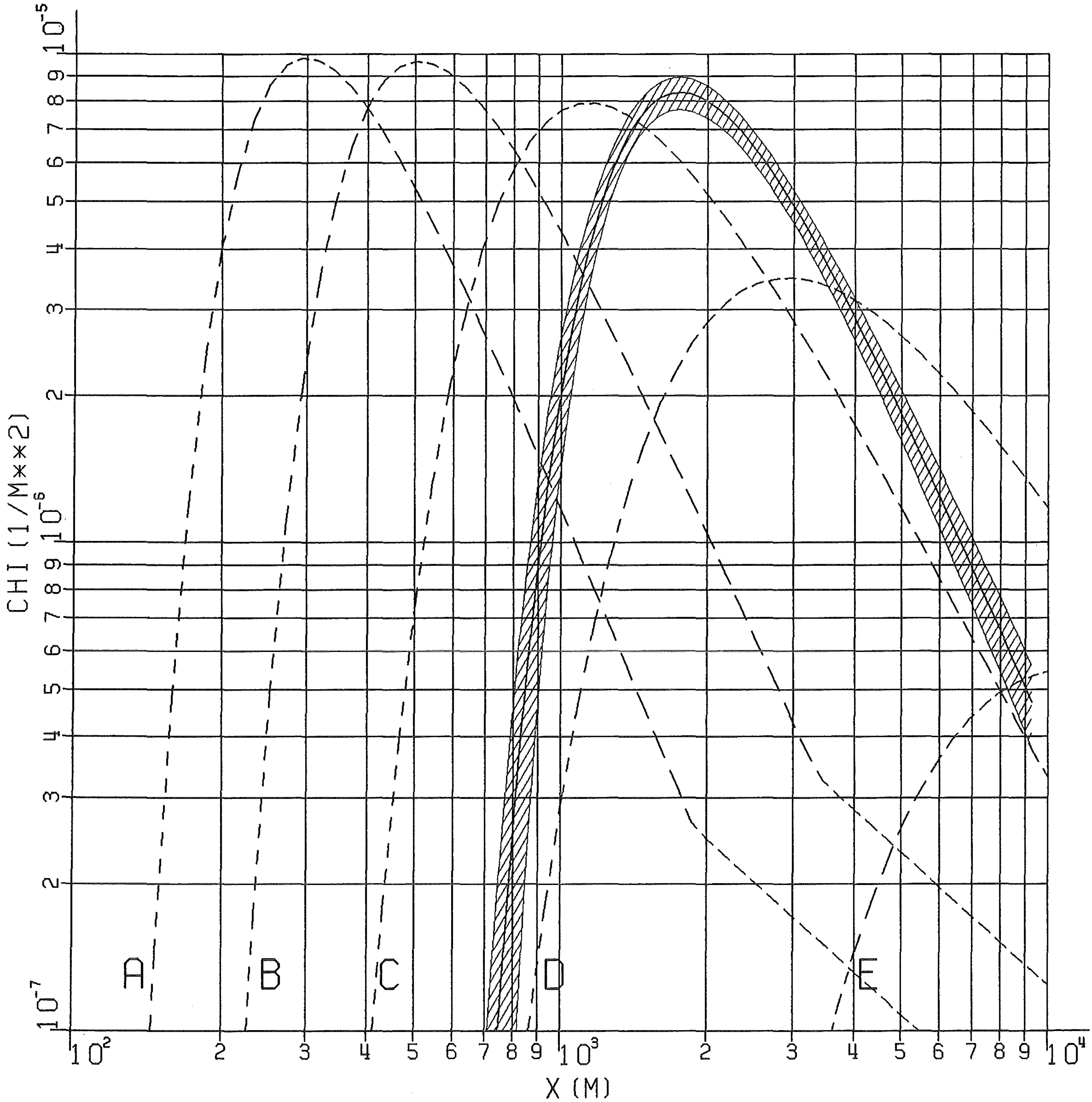

FIG. 34: NORMALIZED DIFFUSION FACTOR
OF EXPERIMENT NO.63, PERIODS 1+2
////////////// H=160M, TRACER CF2BR2
- - - - - COMBINED, SMOOTHED, AND CENTERED RESULTS

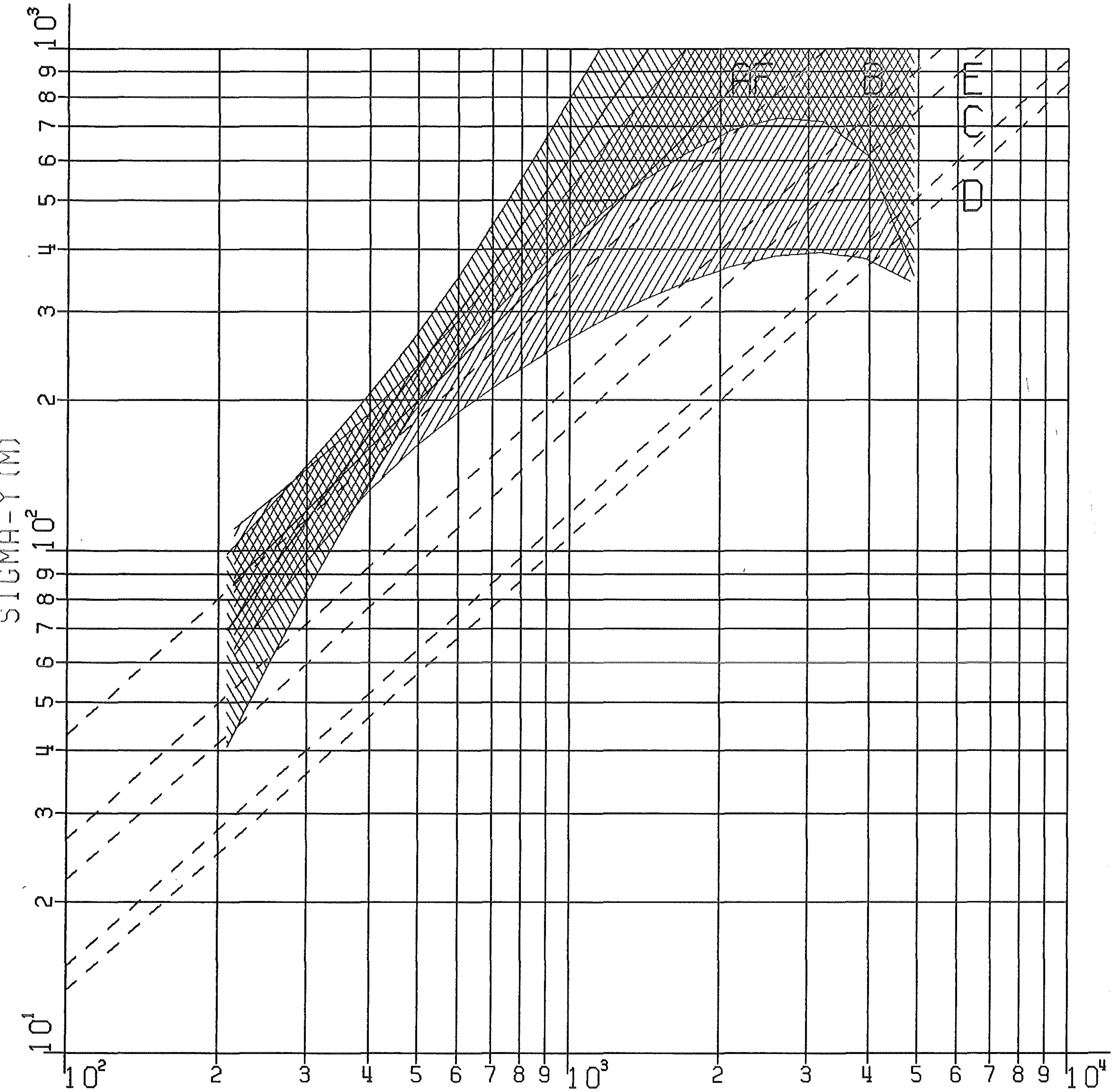

FIG. 35: HORIZONTAL DISPERSION PARAMETER
OF EXPERIMENT NO.64, PERIODS 1+2
H=160M, TRACER CF2BR2
H=195M, TRACER CFCL3
- - - - - COMBINED, SMOOTHED, AND CENTERED RESULTS

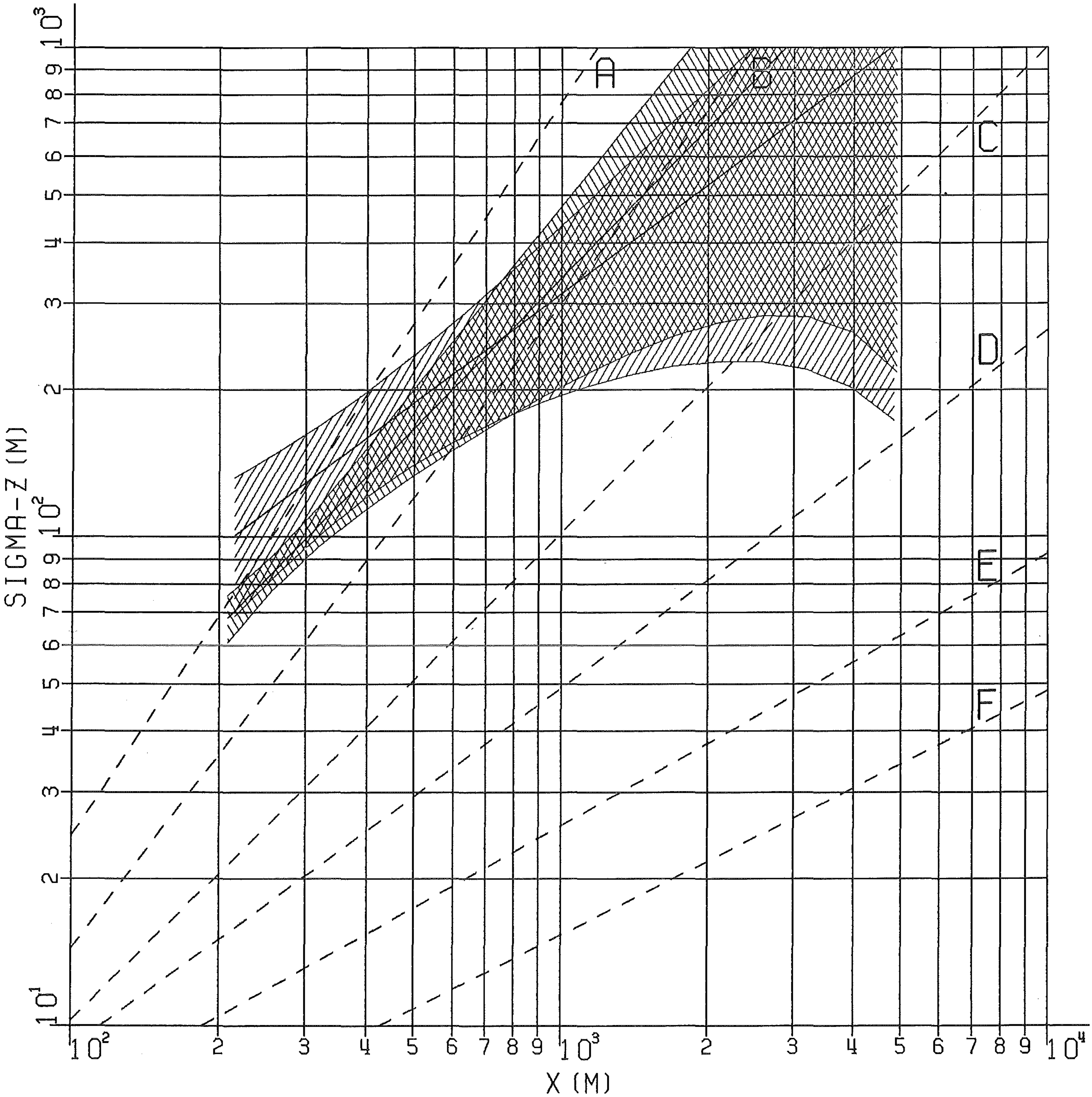

FIG. 36: VERTICAL DISPERSION PARAMETER
OF EXPERIMENT NO.64, PERIODS 1+2
H=160M, TRACER CF2BR2
H=195M, TRACER CFCL3
- - - - - COMBINED, SMOOTHED, AND CENTERED RESULTS

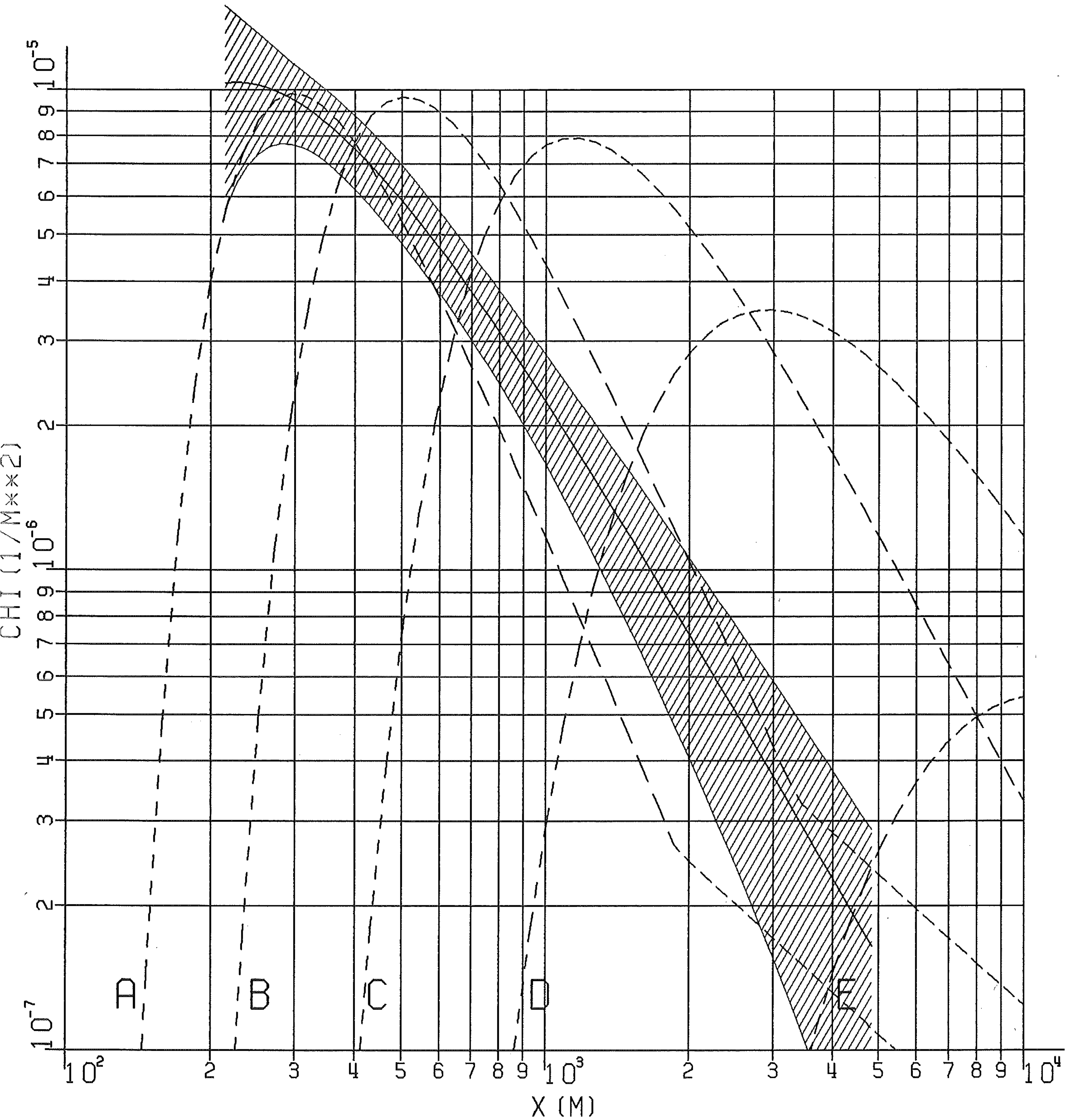

FIG. 37: NORMALIZED DIFFUSION FACTOR
OF EXPERIMENT NO.64, PERIODS 1+2
////////////// H=160M, TRACER CF2BR2
- - - - - COMBINED, SMOOTHED, AND CENTERED RESULTS

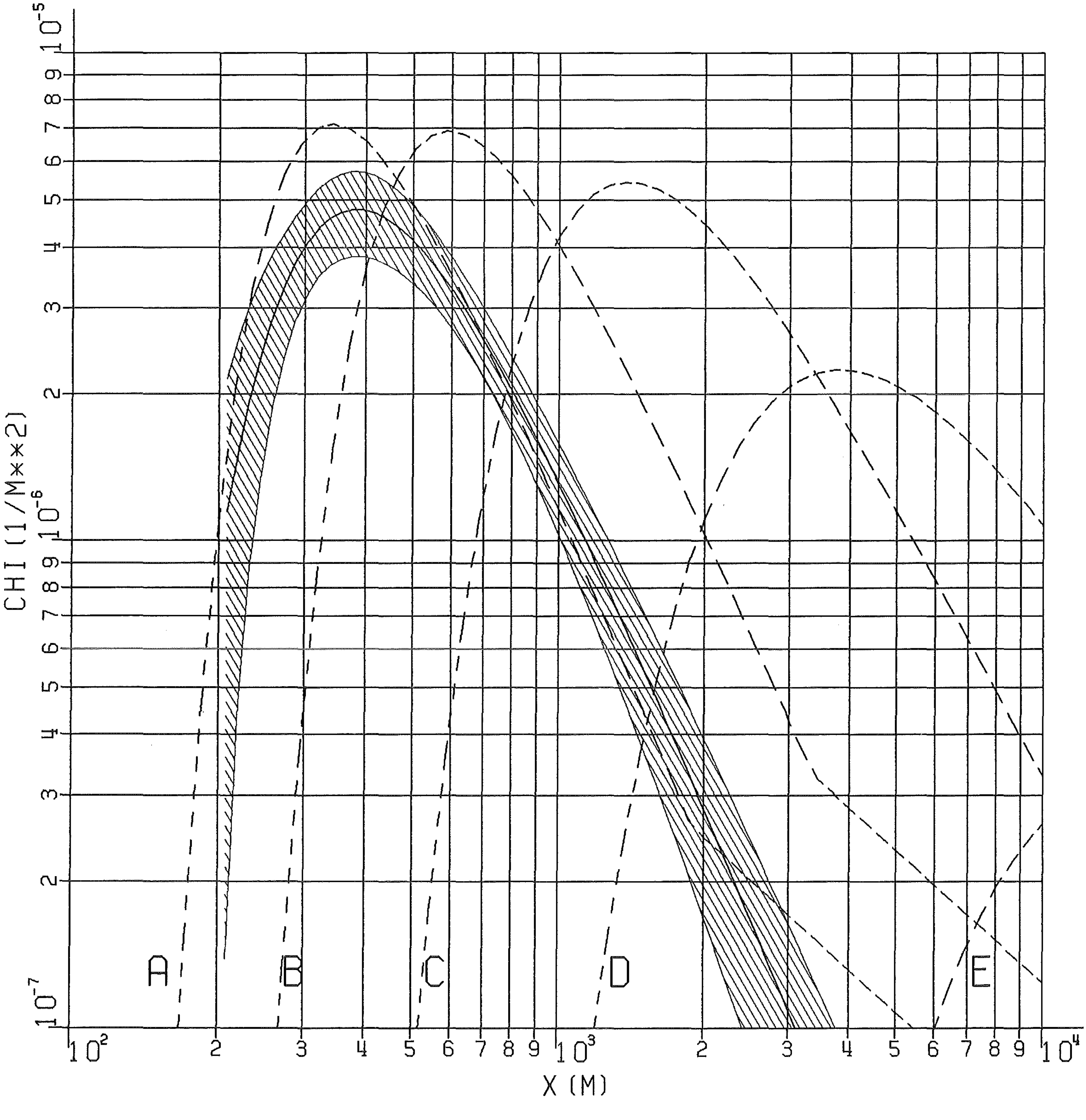

FIG. 38: NORMALIZED DIFFUSION FACTOR
OF EXPERIMENT NO.64, PERIODS 1+2
H=195M, TRACER CFCL3
- - - - - COMBINED, SMOOTHED, AND CENTERED RESULTS

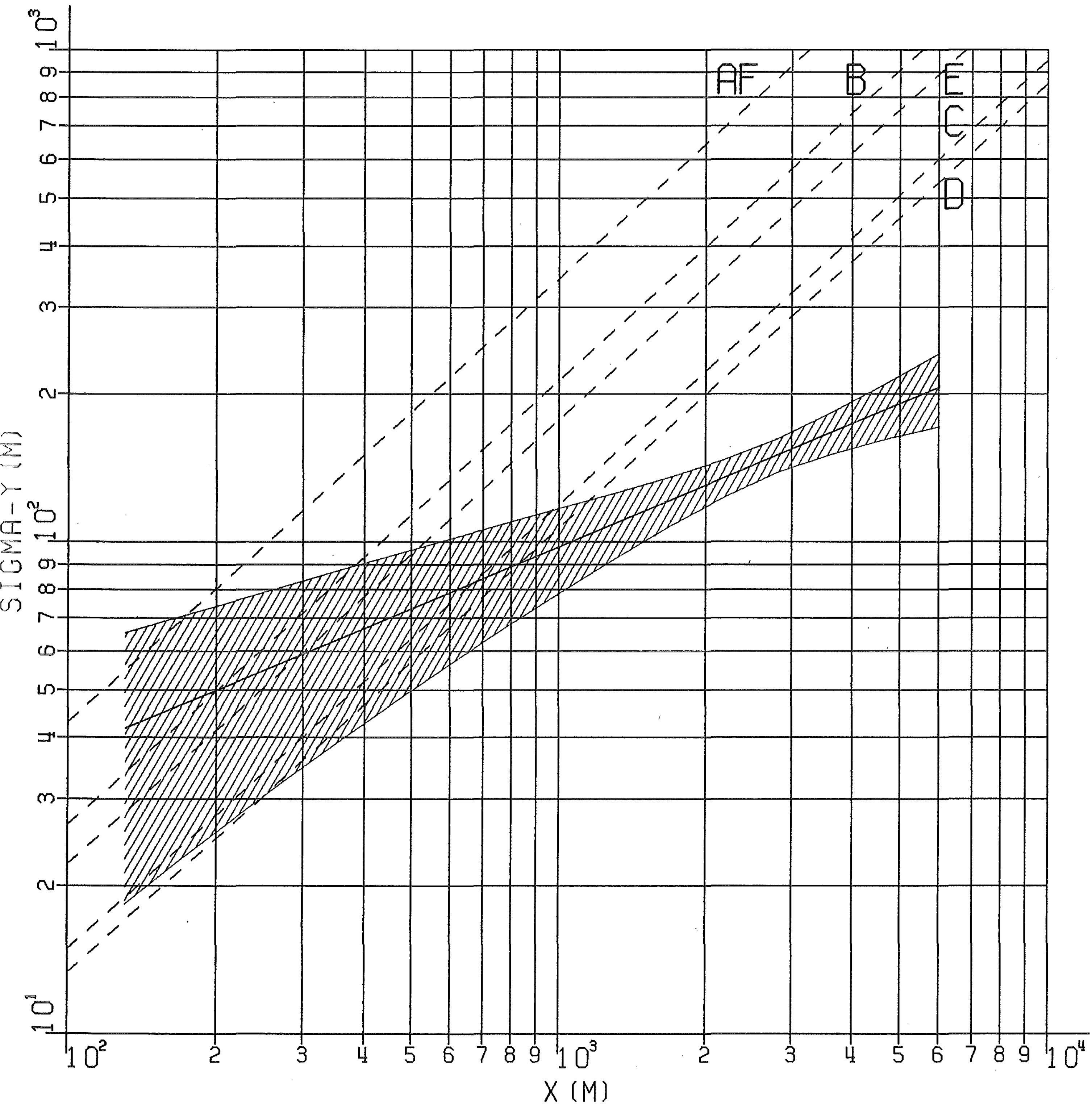

FIG. 39: HORIZONTAL DISPERSION PARAMETER
OF EXPERIMENT NO.65, PERIODS 1+2
H=160M, TRACER CF2BR2

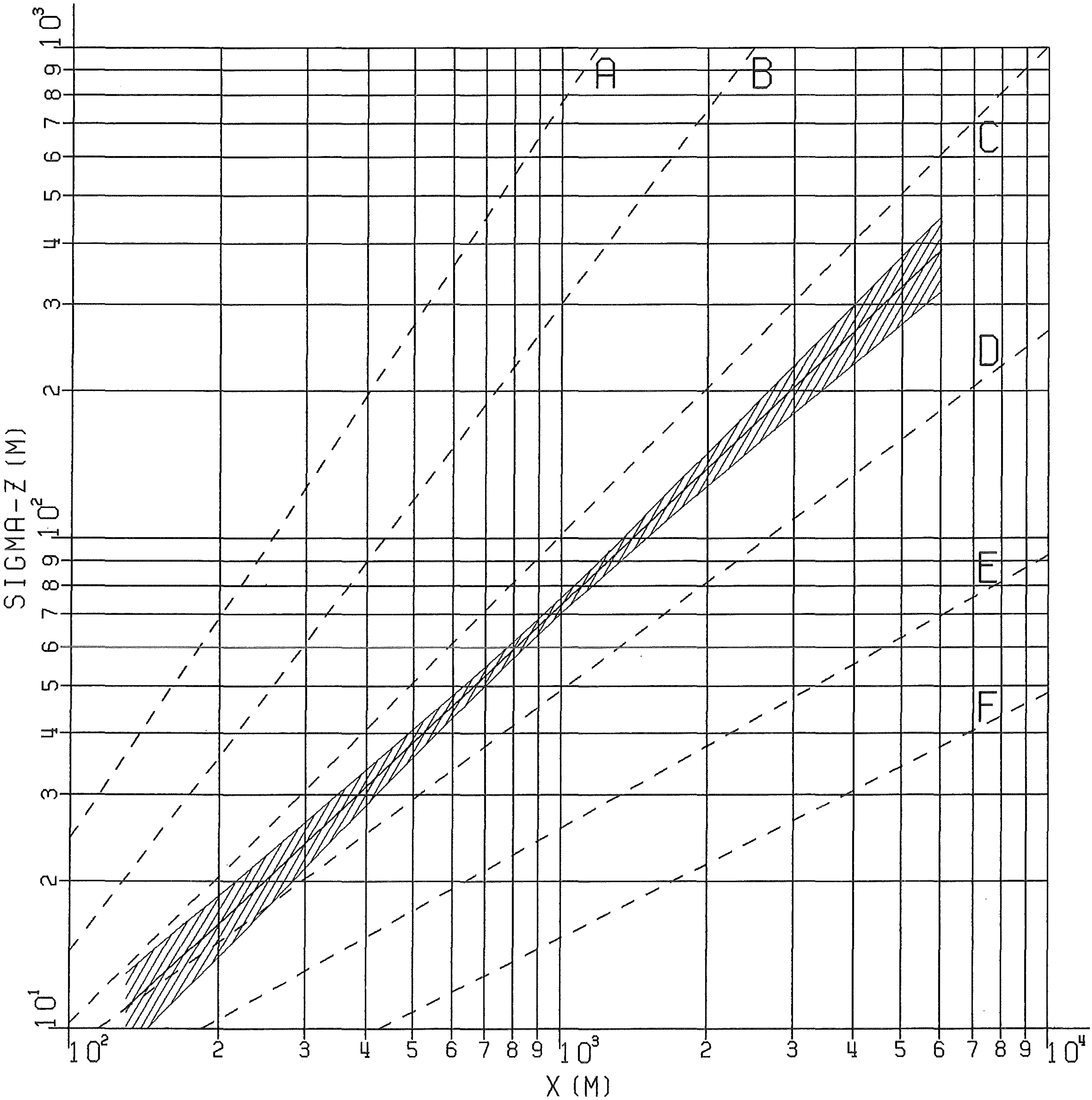

FIG. 40: VERTICAL DISPERSION PARAMETER
OF EXPERIMENT NO.65, PERIODS 1+2
H=160M, TRACER CF2BR2

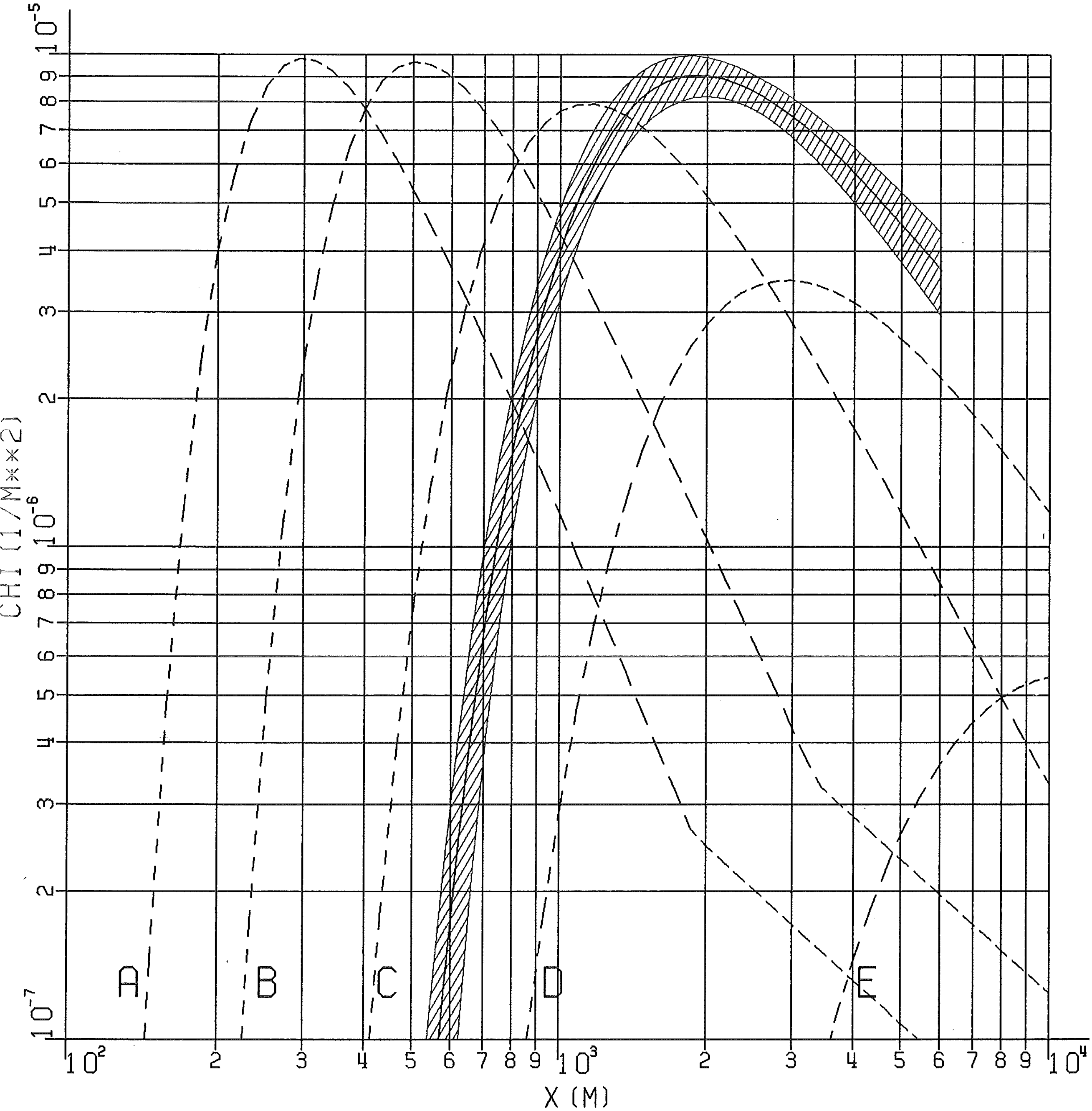

FIG. 41: NØRMALIZED DIFFUSIØN FACTØR
ØF EXPERIMENT NØ.65, PERIØDS 1+2
////////////// H=160M, TRACER CF2BR2
- - - - - CØMBINED, SMØØTHED, AND CENTERED RESULTS

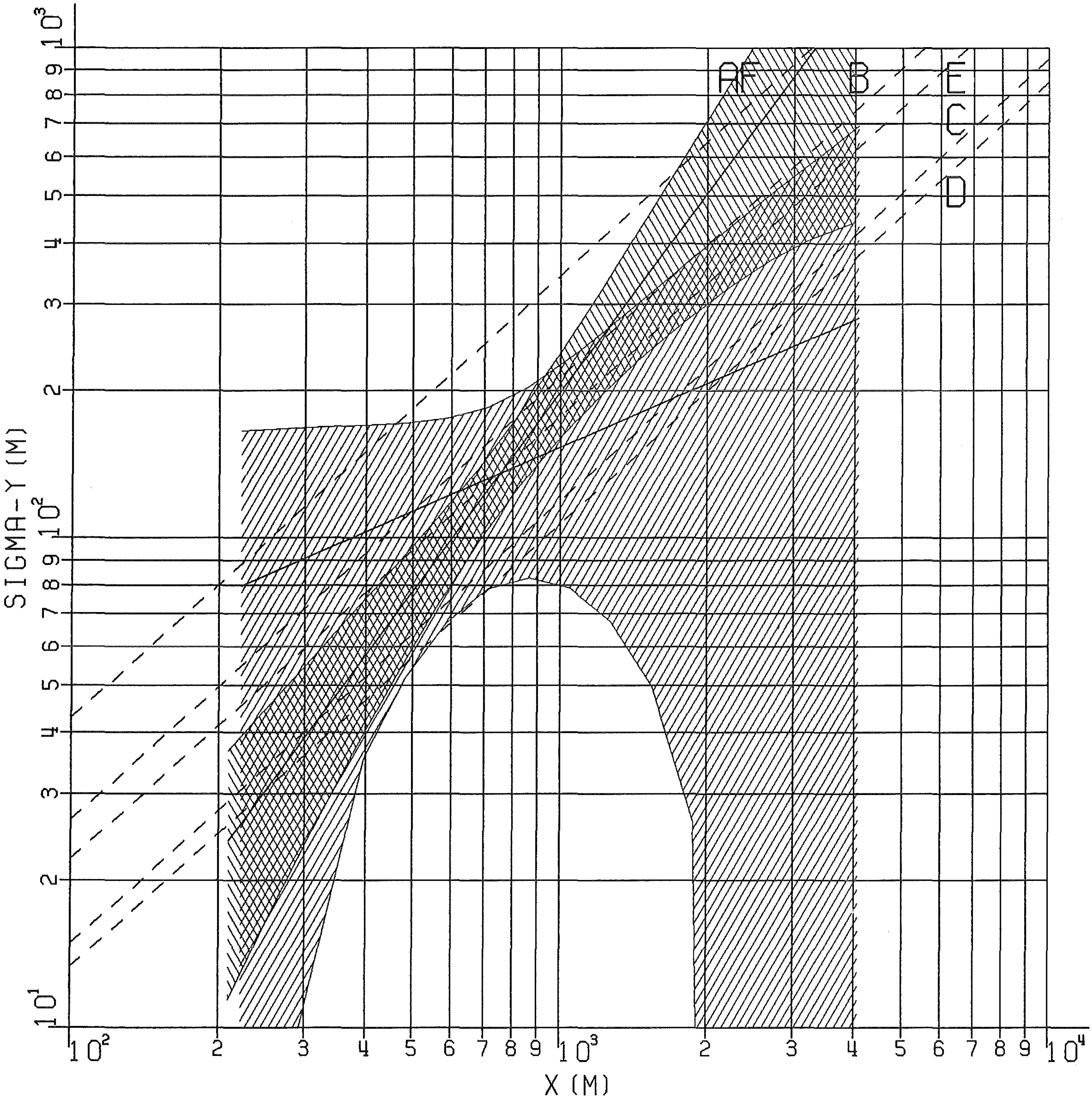

FIG. 42: HORIZONTAL DISPERSION PARAMETER
OF EXPERIMENT NO.66, PERIOD 2
H=160M, TRACER CF2BR2
H=195M, TRACER CFCL3
- - - - - COMBINED, SMOOTHED, AND CENTERED RESULTS

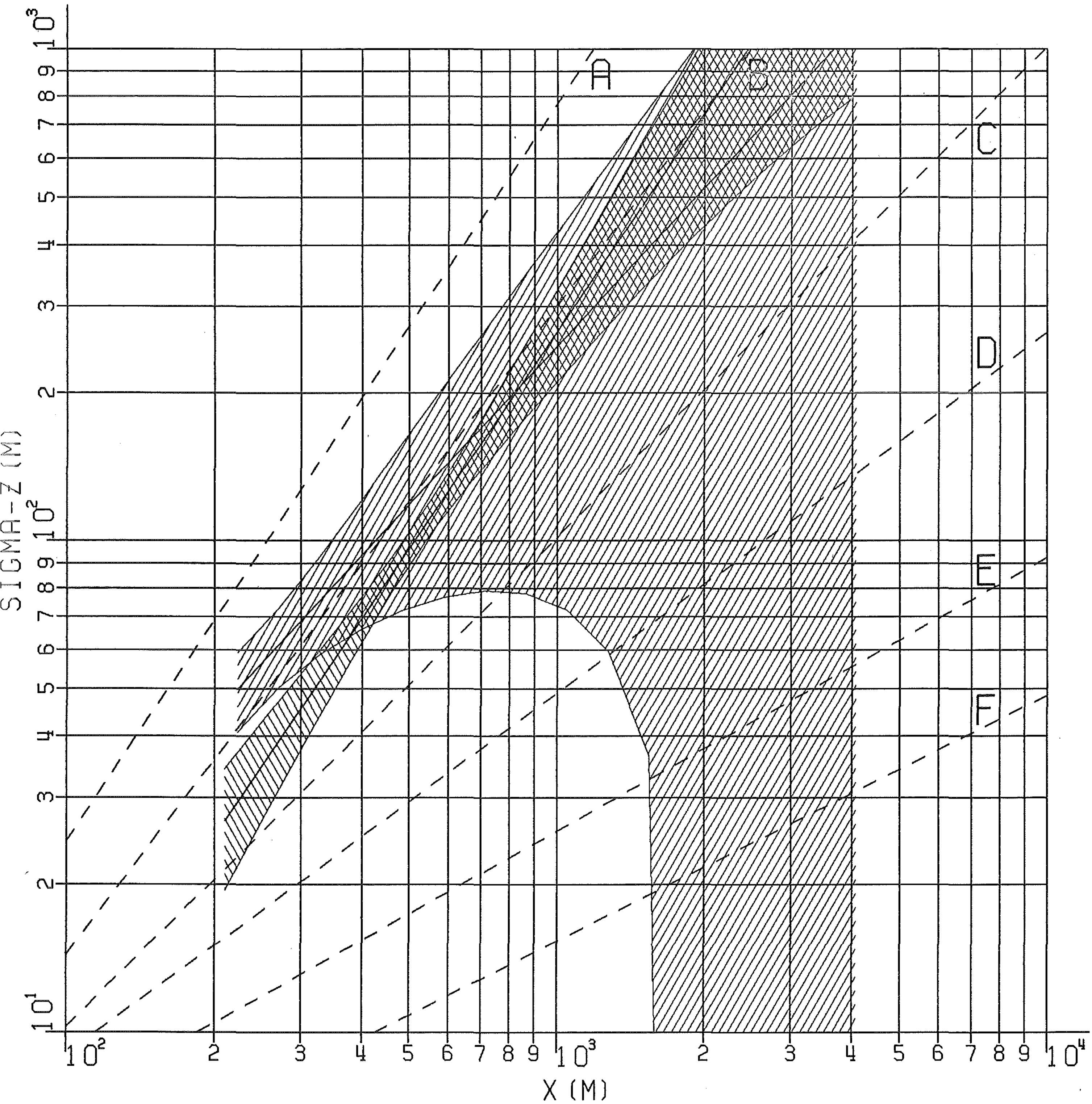

FIG. 43: VERTICAL DISPERSION PARAMETER
OF EXPERIMENT NO.66, PERIOD 2
H=160M, TRACER CF2BR2
H=195M, TRACER CFCL3
- - - - - COMBINED, SMOOTHED, AND CENTERED RESULTS

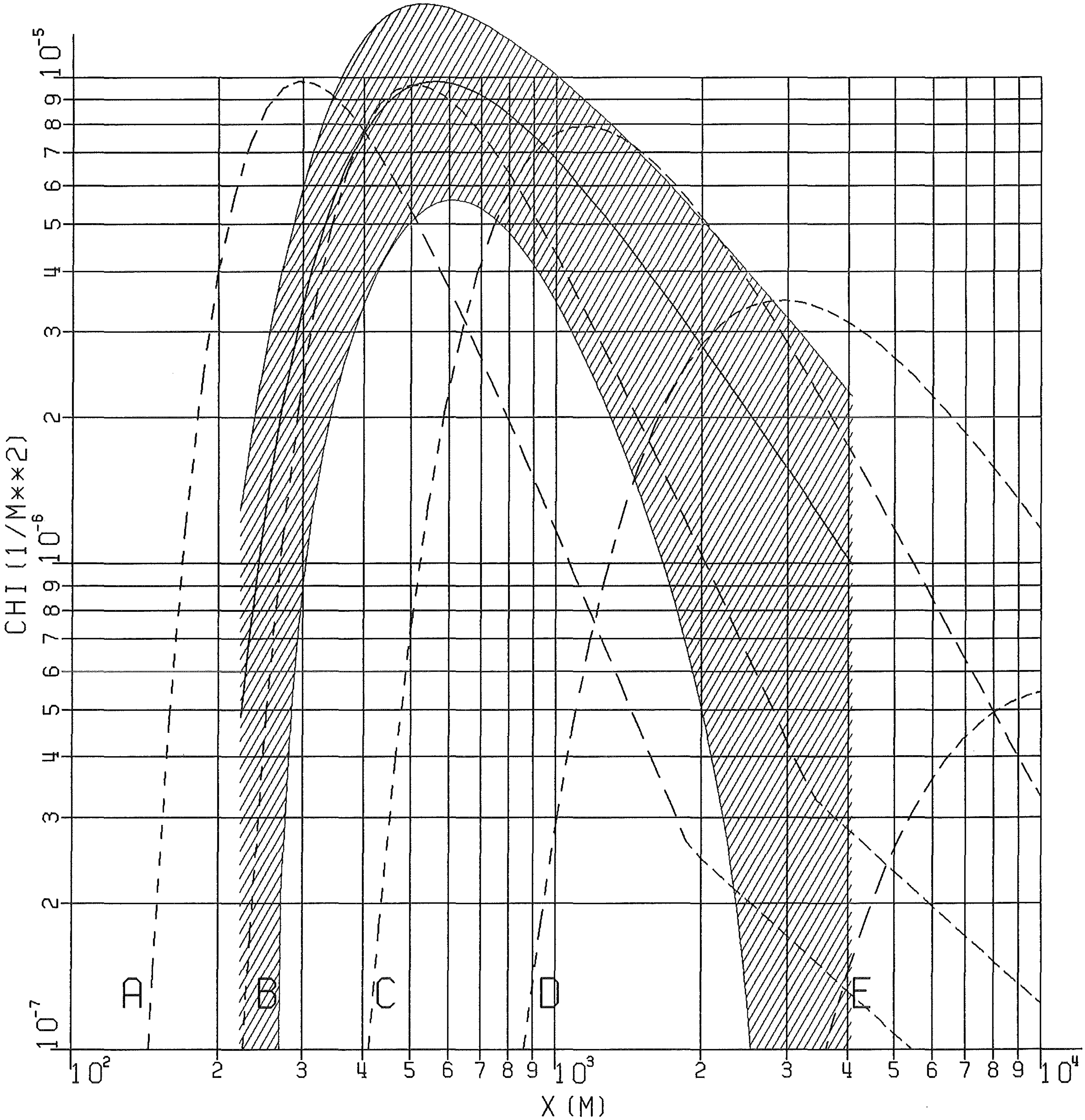

FIG. 44: NORMALIZED DIFFUSION FACTOR
OF EXPERIMENT NO.66, PERIOD 2
////////////// H=160M, TRACER CF2BR2
- - - - - COMBINED, SMOOTHED, AND CENTERED RESULTS

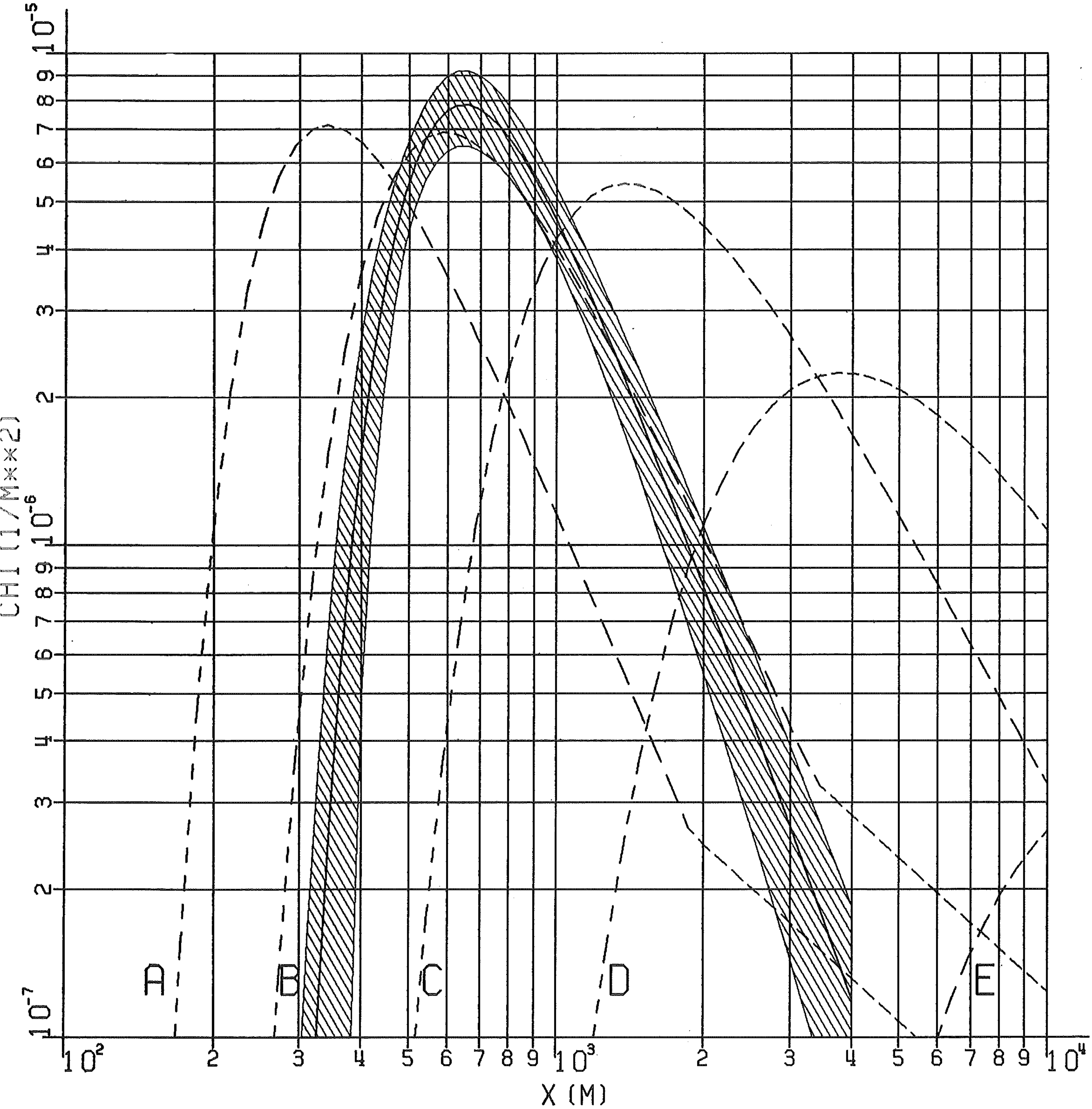

FIG. 45: NORMALIZED DIFFUSION FACTOR
OF EXPERIMENT NO.66, PERIOD 2
H=195M, TRACER CFCL3
COMBINED, SMOOTHED, AND CENTERED RESULTS

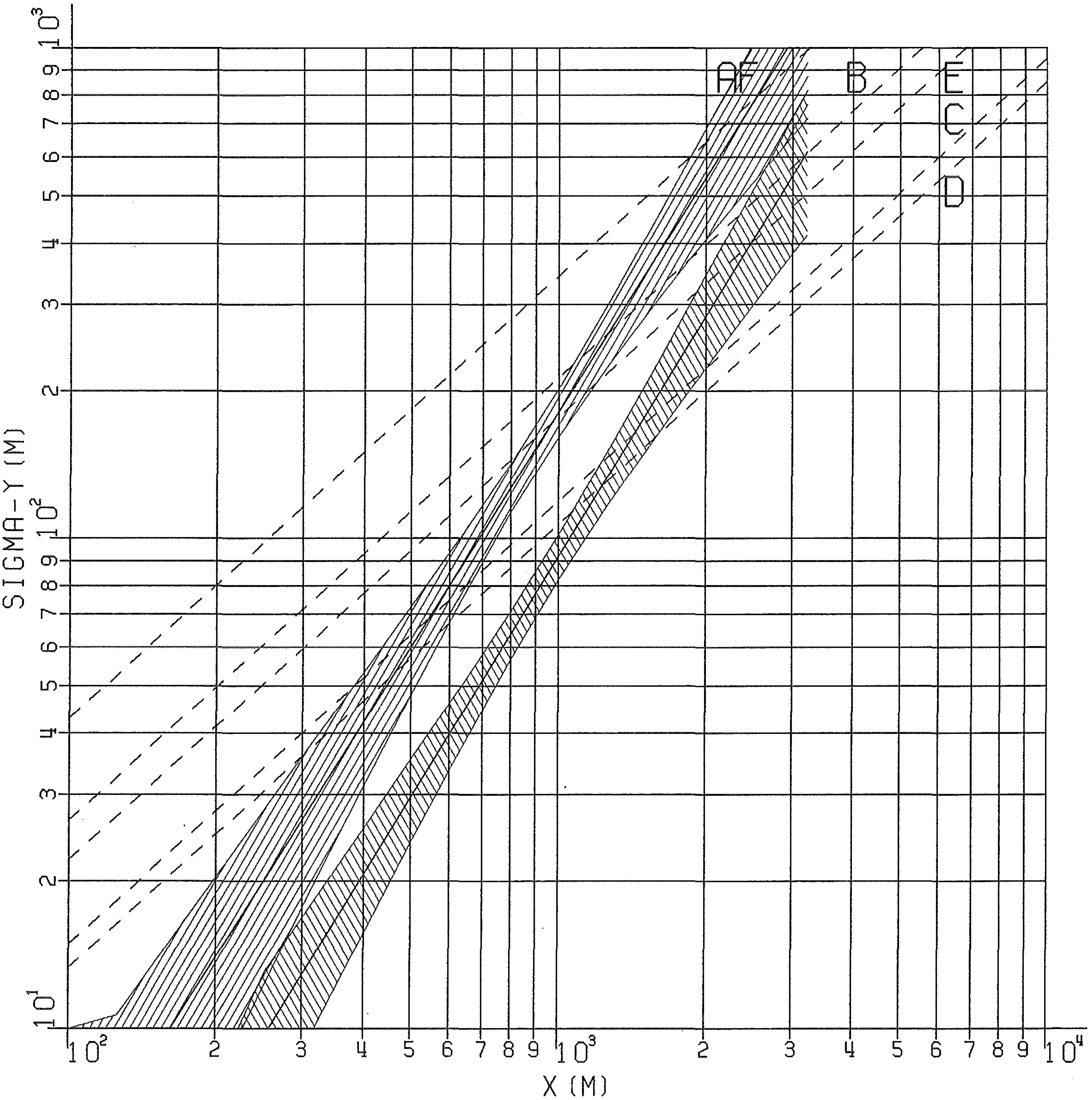

FIG. 46: HORIZONTAL DISPERSION PARAMETER
OF EXPERIMENT NO. 67, PERIOD 1

////////////// H=160M, TRACER CF2BR2

\\\\\\\\\\\\\\ H=195M, TRACER CFCL3

- - - - - COMBINED, SMOOTHED, AND CENTERED RESULTS

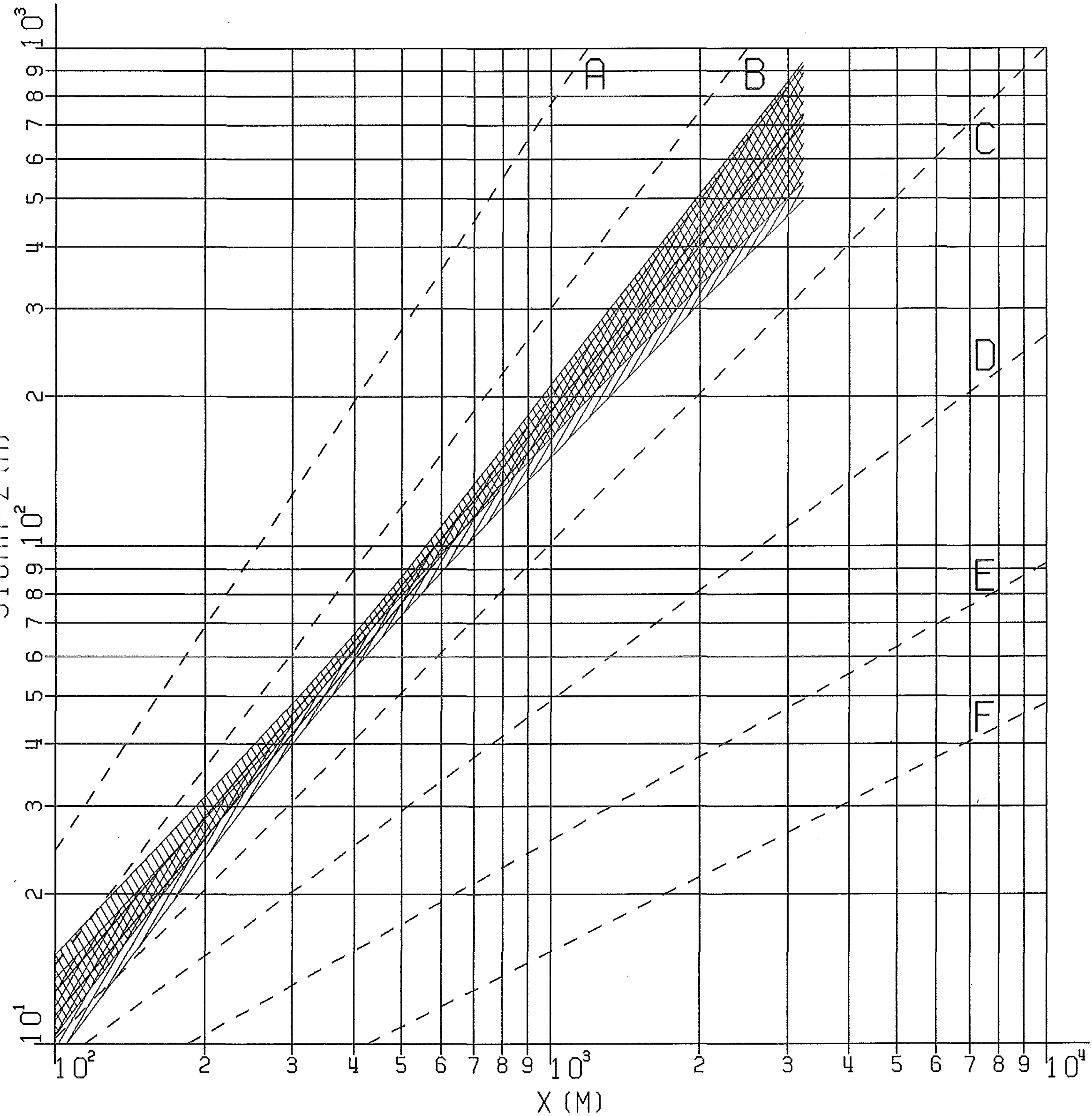

FIG. 47: VERTICAL DISPERSION PARAMETER
OF EXPERIMENT NO.67, PERIOD 1
H=160M, TRACER CF2BR2
H=195M, TRACER CFCL3
- - - - - COMBINED, SMOOTHED, AND CENTERED RESULTS

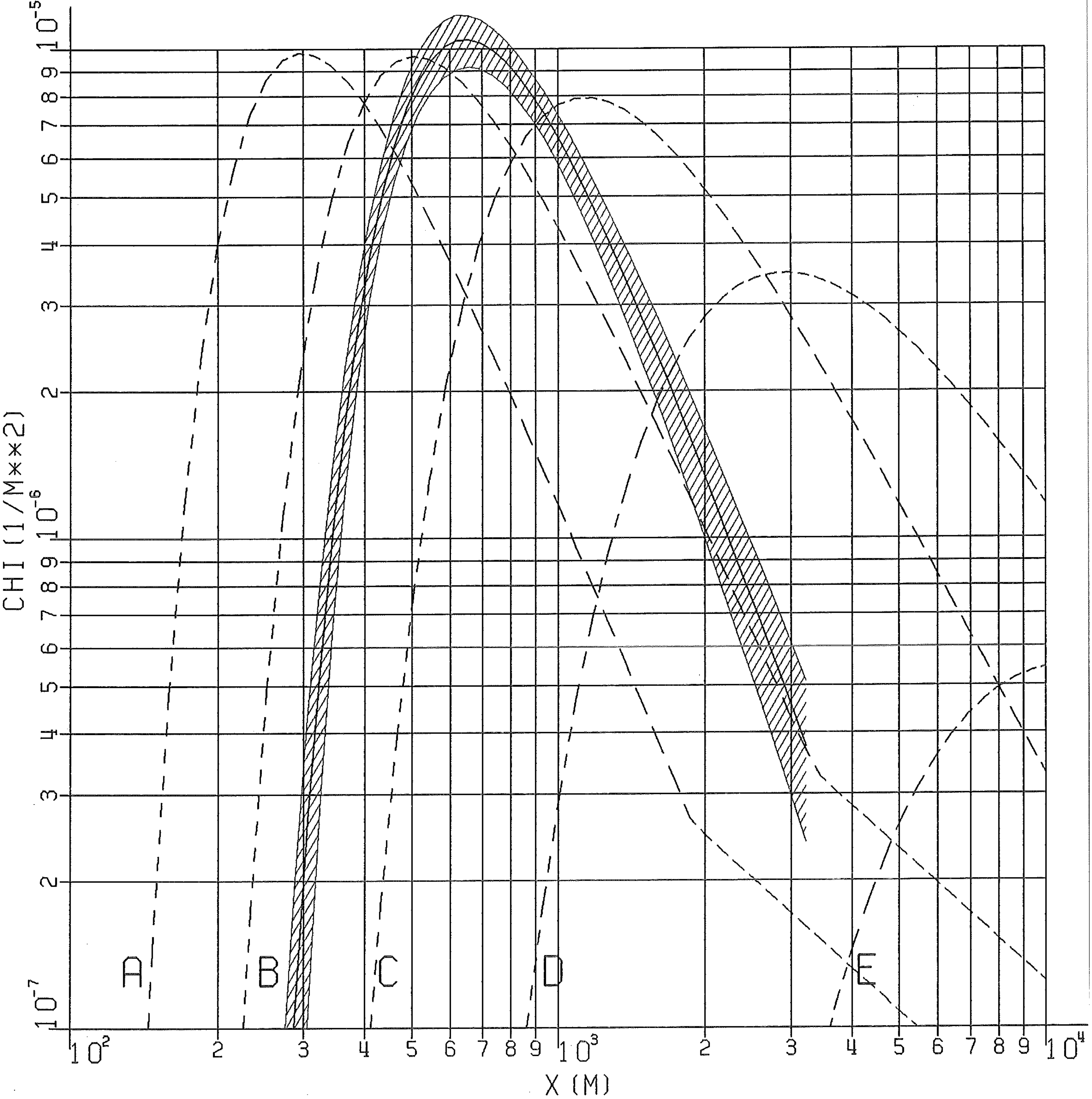

FIG. 48: NORMALIZED DIFFUSION FACTOR
OF EXPERIMENT NO.67, PERIOD 1
////////////// H=160M, TRACER CF2BR2
- - - - - COMBINED, SMOOTHED, AND CENTERED RESULTS

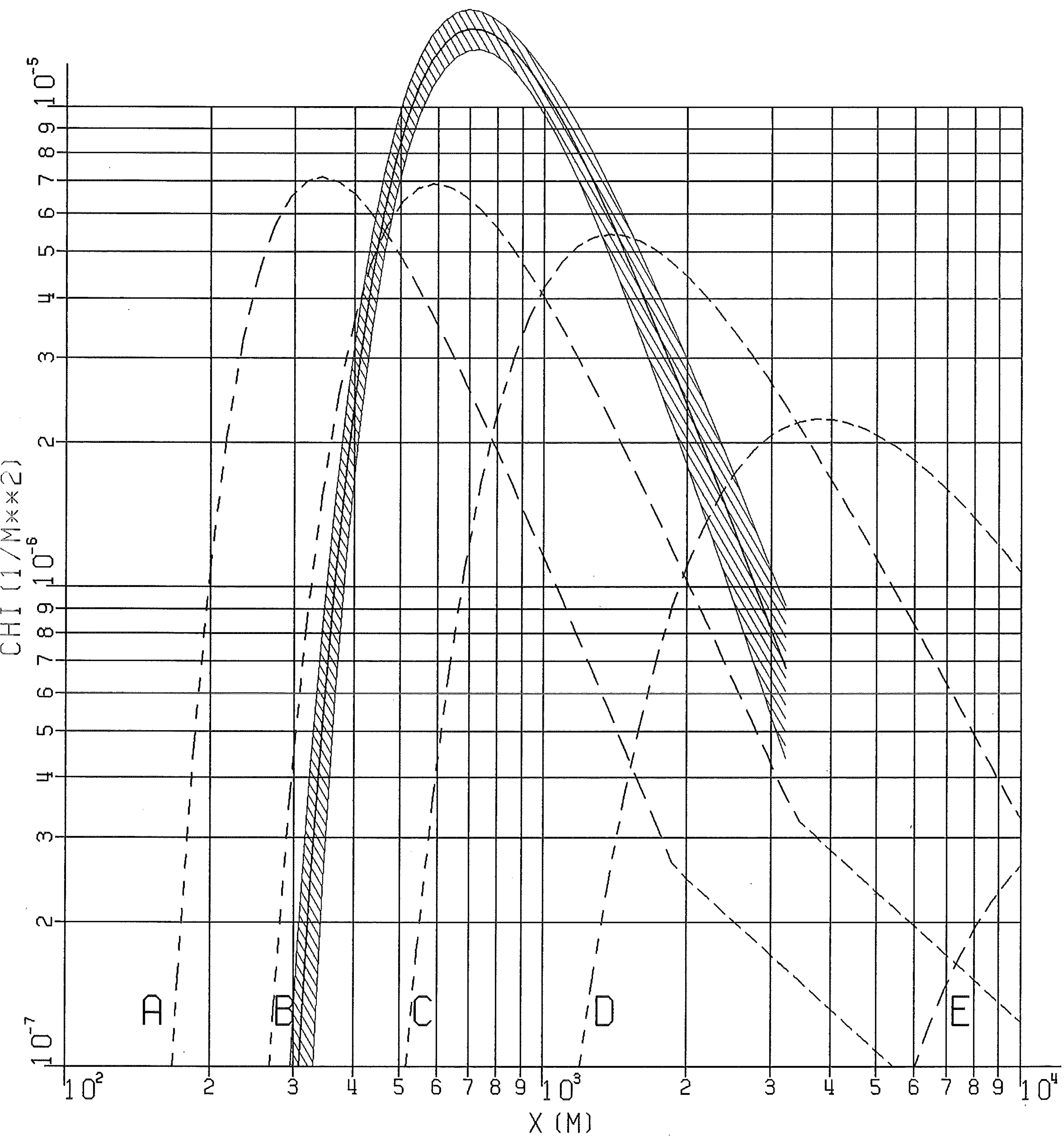

FIG. 49: NØRMALIZED DIFFUSIØN FACTØR
ØF EXPERIMENT NØ.67, PERIØD 1
H=195M, TRACER CFCL3
– – – – – COMBINED, SMØØTHED, AND CENTERED RESULTS

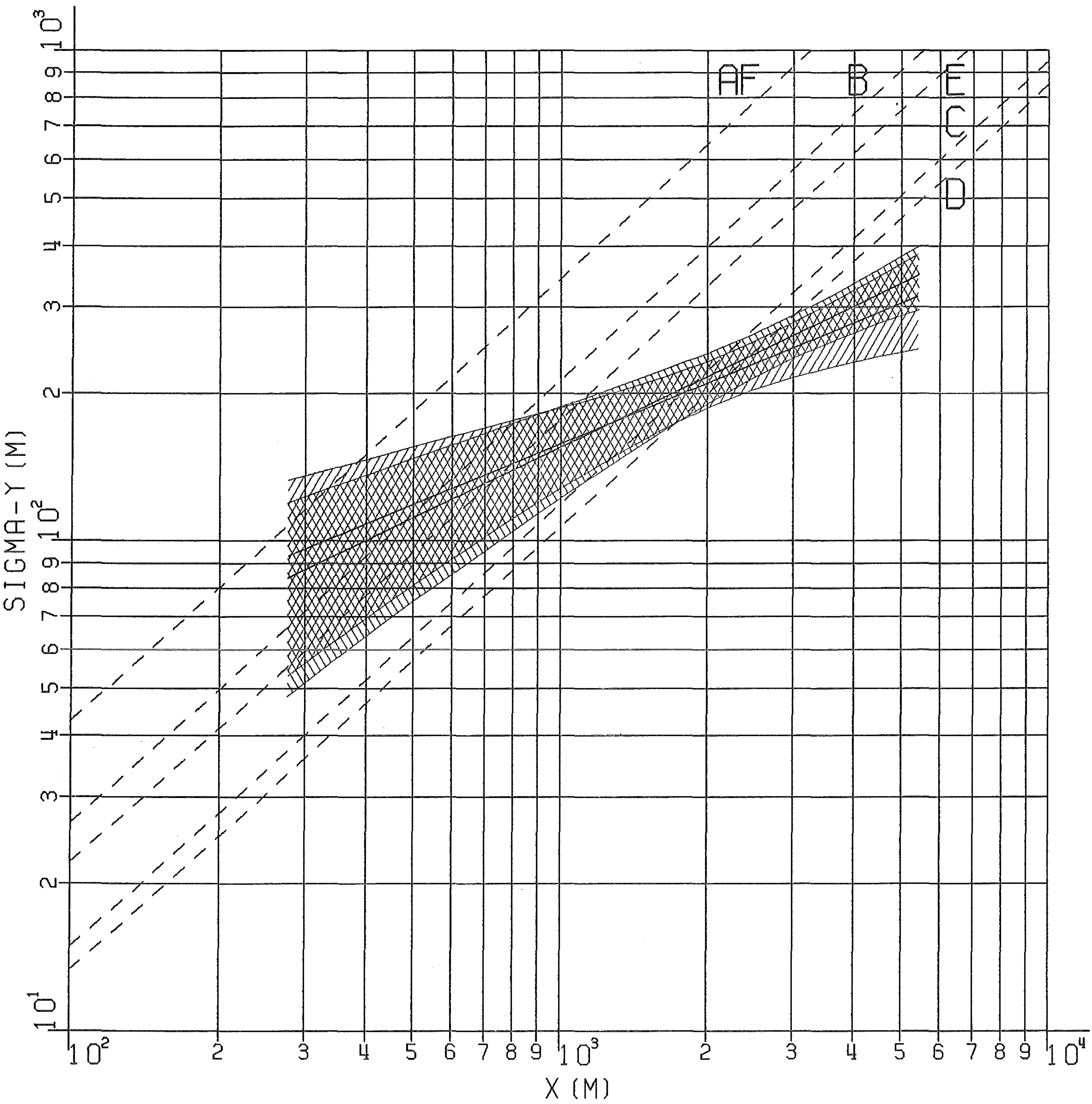

FIG. 50: HORIZONTAL DISPERSION PARAMETER
OF EXPERIMENT NO.68, PERIODS 1+2

H=160M, TRACER CF2BR2

H=195M, TRACER CFCL3

- - - - - COMBINED, SMOOTHED, AND CENTERED RESULTS

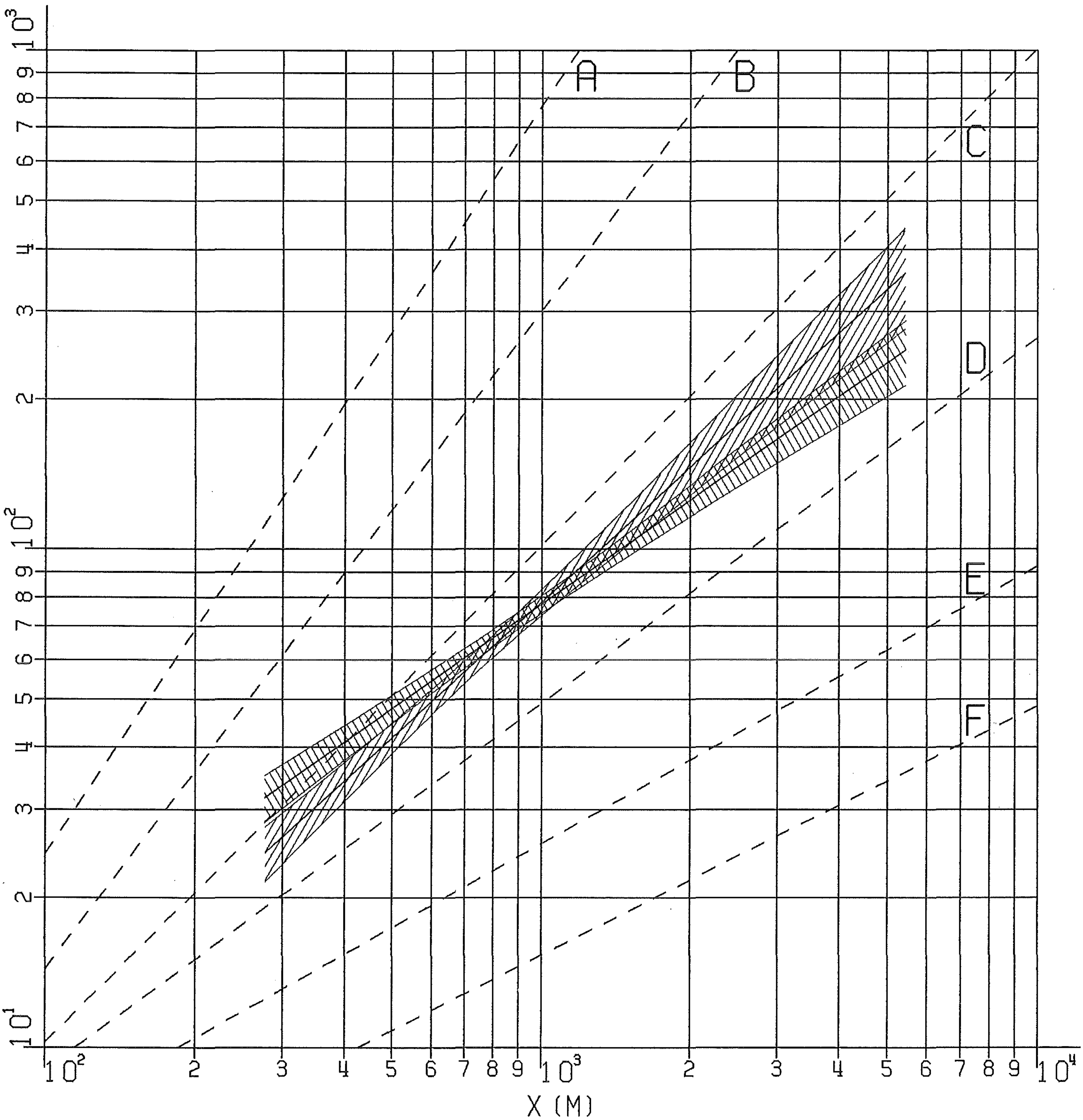

FIG. 51: VERTICAL DISPERSION PARAMETER
OF EXPERIMENT NO.68, PERIODS 1+2
/////////////// H=160M, TRACER CF2BR2
\\\\\\\\\\\\\\\ H=195M, TRACER CFCL3
- - - - - COMBINED, SMOOTHED, AND CENTERED RESULTS

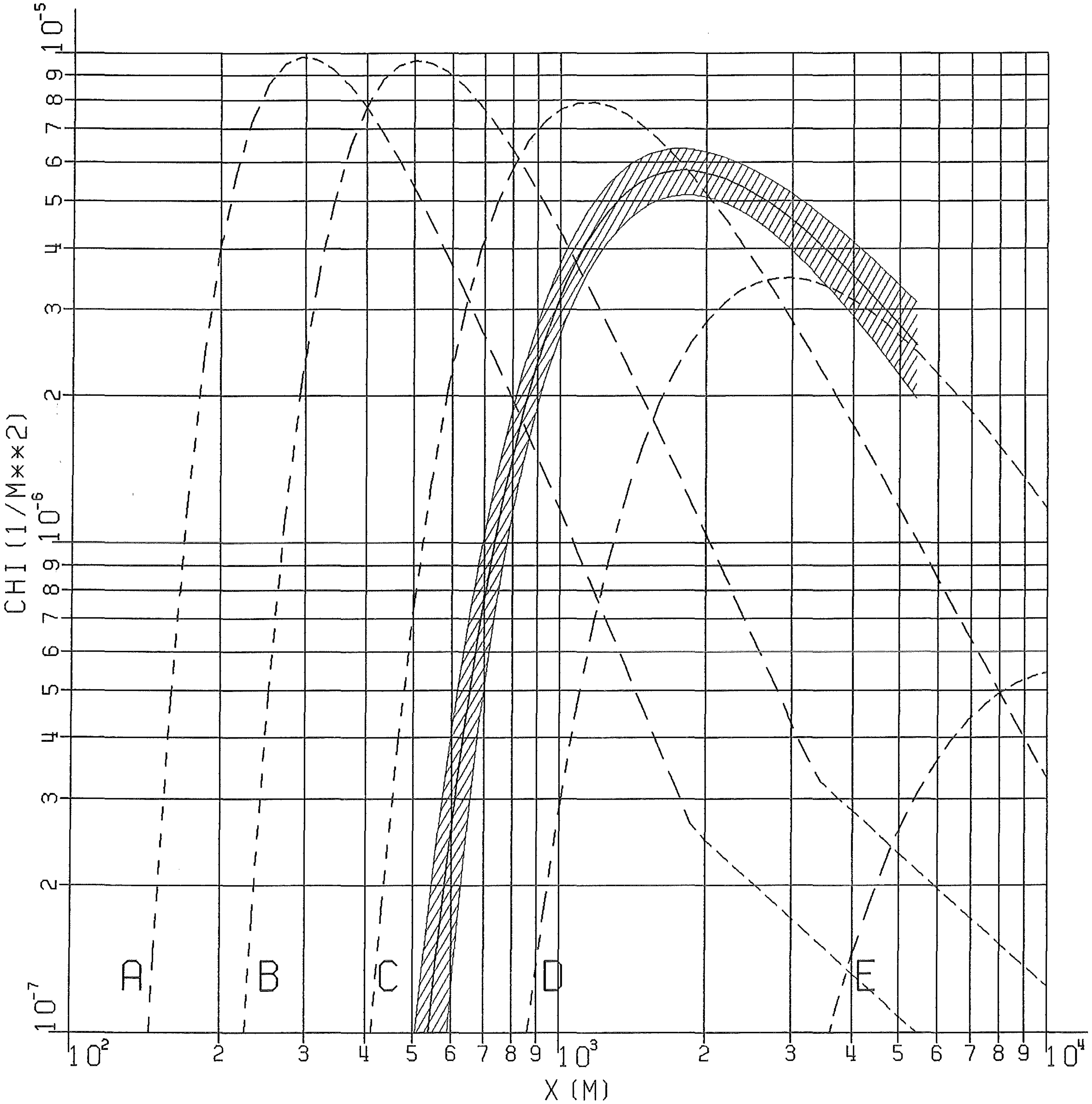

FIG. 52: NORMALIZED DIFFUSION FACTOR
OF EXPERIMENT NO.68, PERIODS 1+2

////////// H=160M, TRACER CF2BR2

- - - - - COMBINED, SMOOTHED, AND CENTERED RESULTS

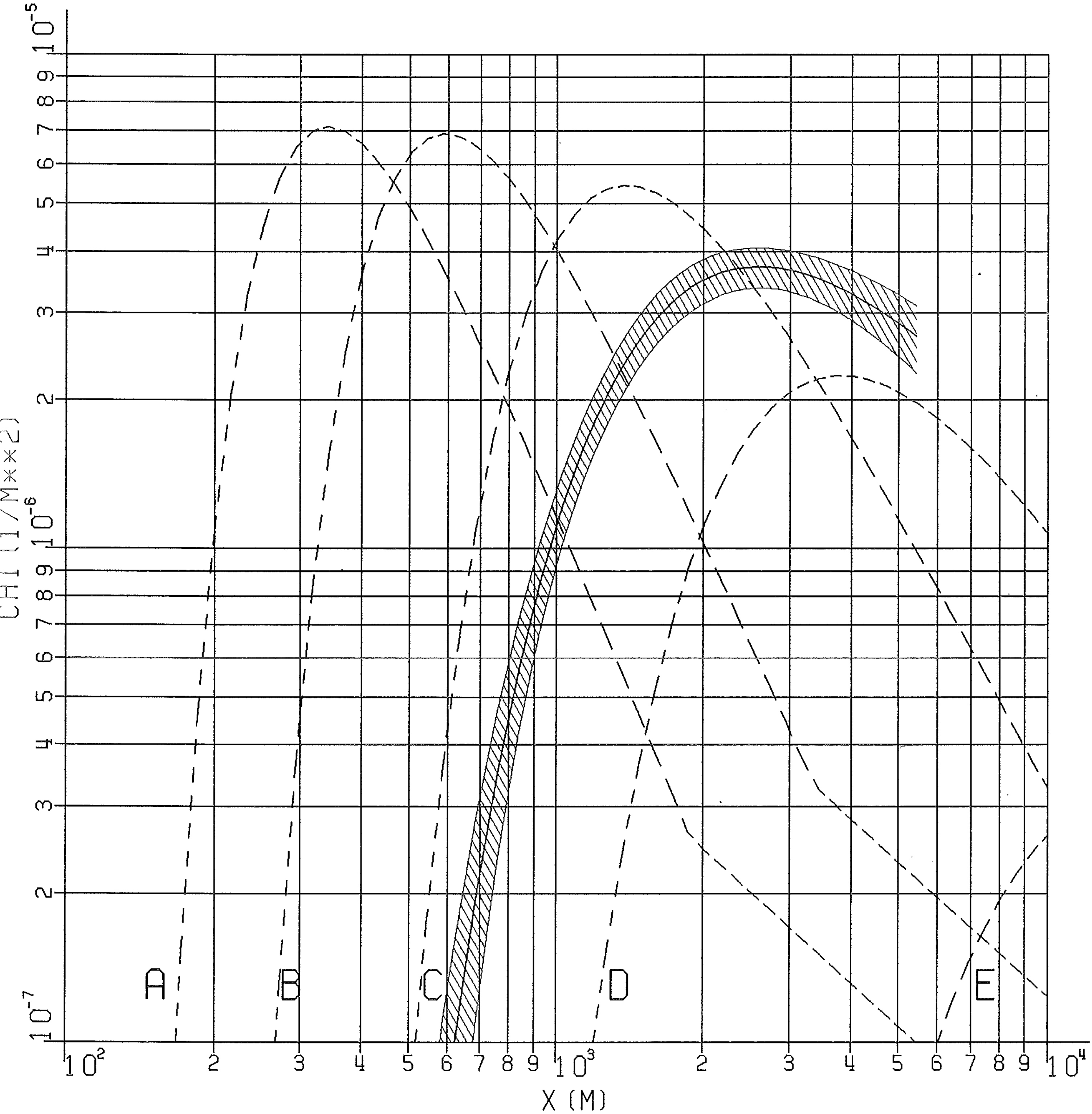

FIG. 53: NORMALIZED DIFFUSION FACTOR
OF EXPERIMENT NO.68, PERIODS 1+2
H=195M, TRACER CFCL3
- - - - - COMBINED, SMOOTHED, AND CENTERED RESULTS

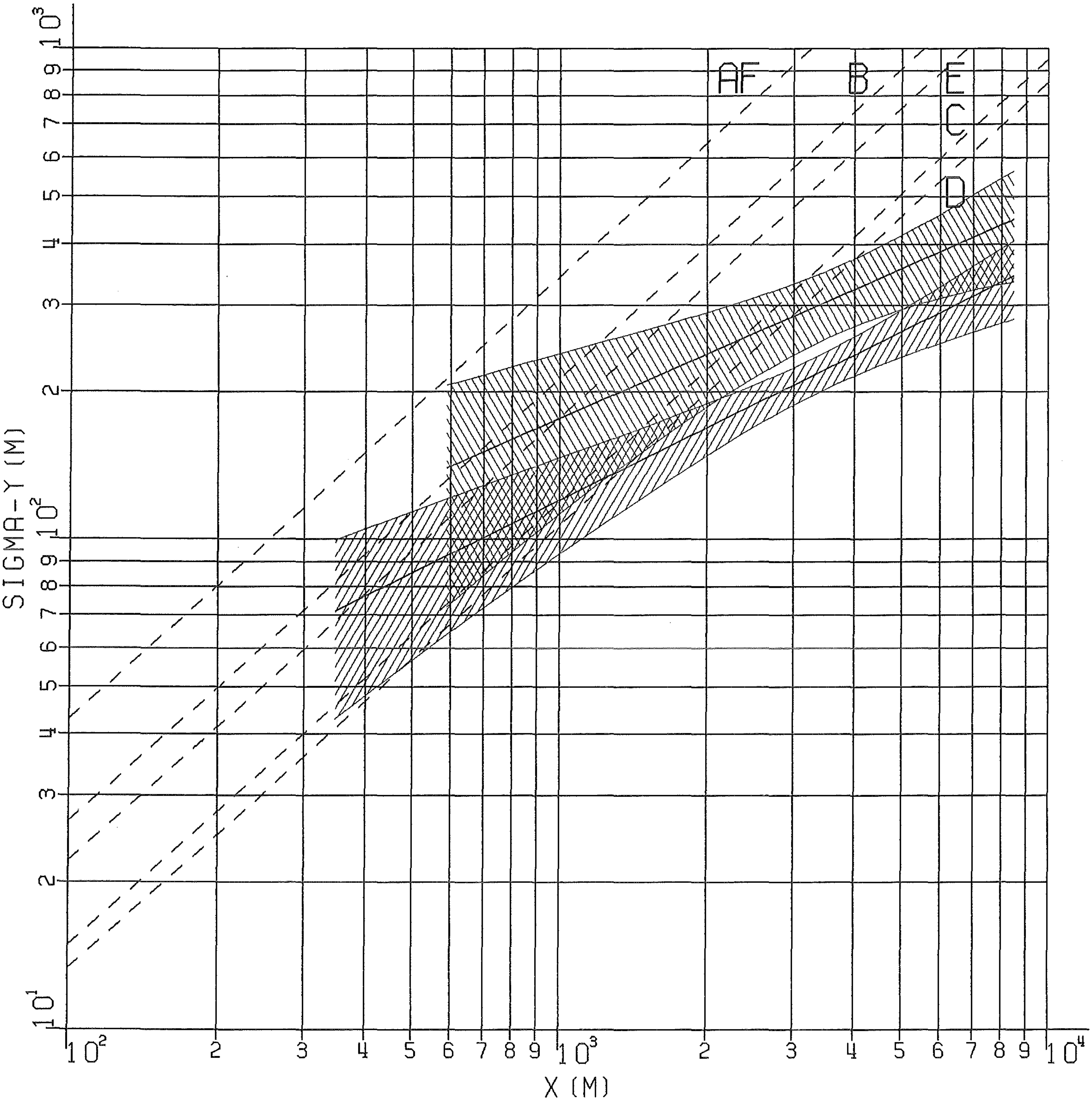

FIG. 54: HORIZONTAL DISPERSION PARAMETER
OF EXPERIMENT NO.69, PERIODS 1+2
H=160M, TRACER CF2BR2
H=195M, TRACER CFCL3
- - - - - COMBINED, SMOOTHED, AND CENTERED RESULTS

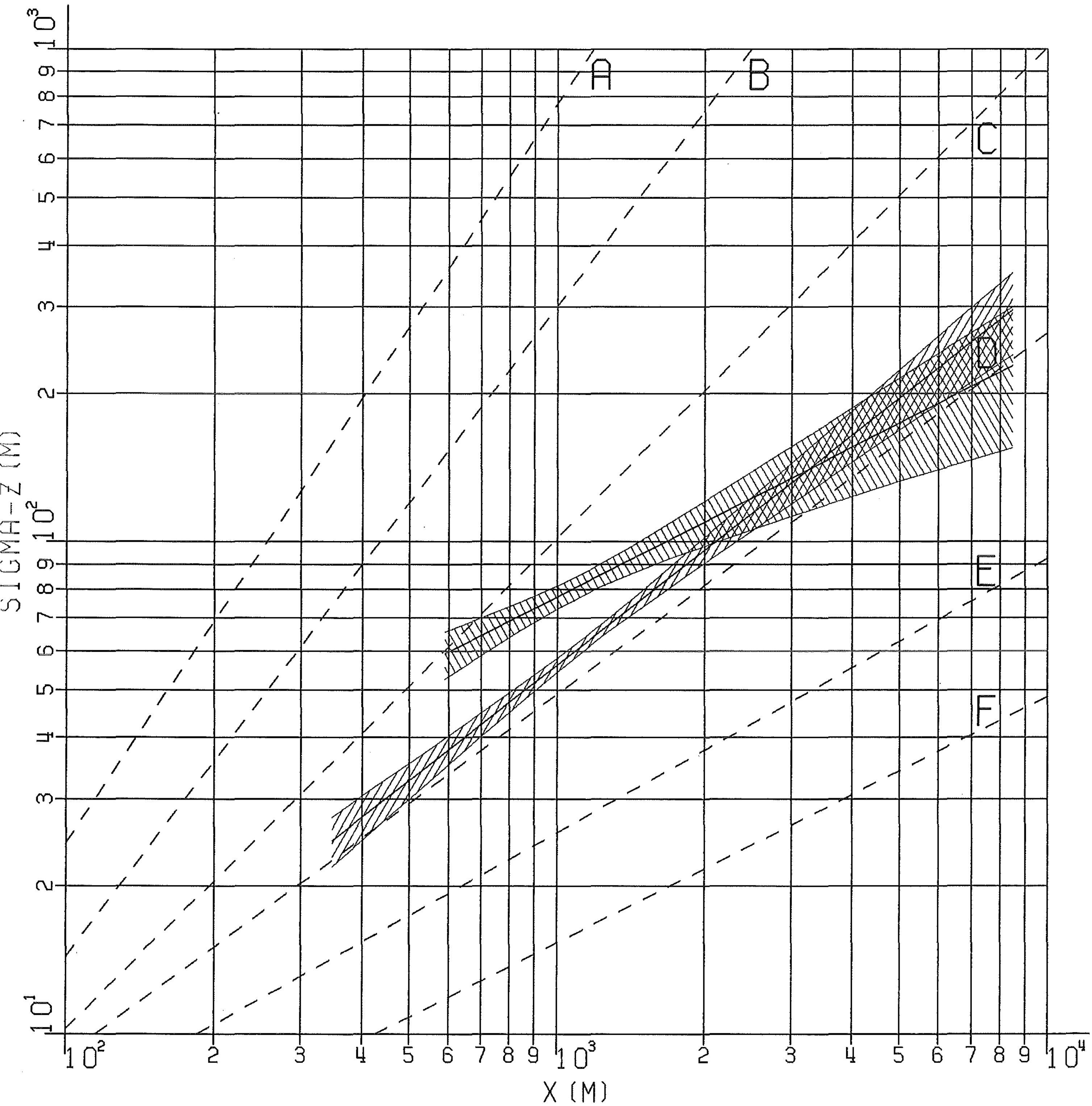

FIG. 55: VERTICAL DISPERSION PARAMETER
OF EXPERIMENT NO.69, PERIODS 1+2
////////////// H=160M, TRACER CF2BR2
\\\\\\\\\\\\\\ H=195M, TRACER CFCL3
- - - - - COMBINED, SMOOTHED, AND CENTERED RESULTS

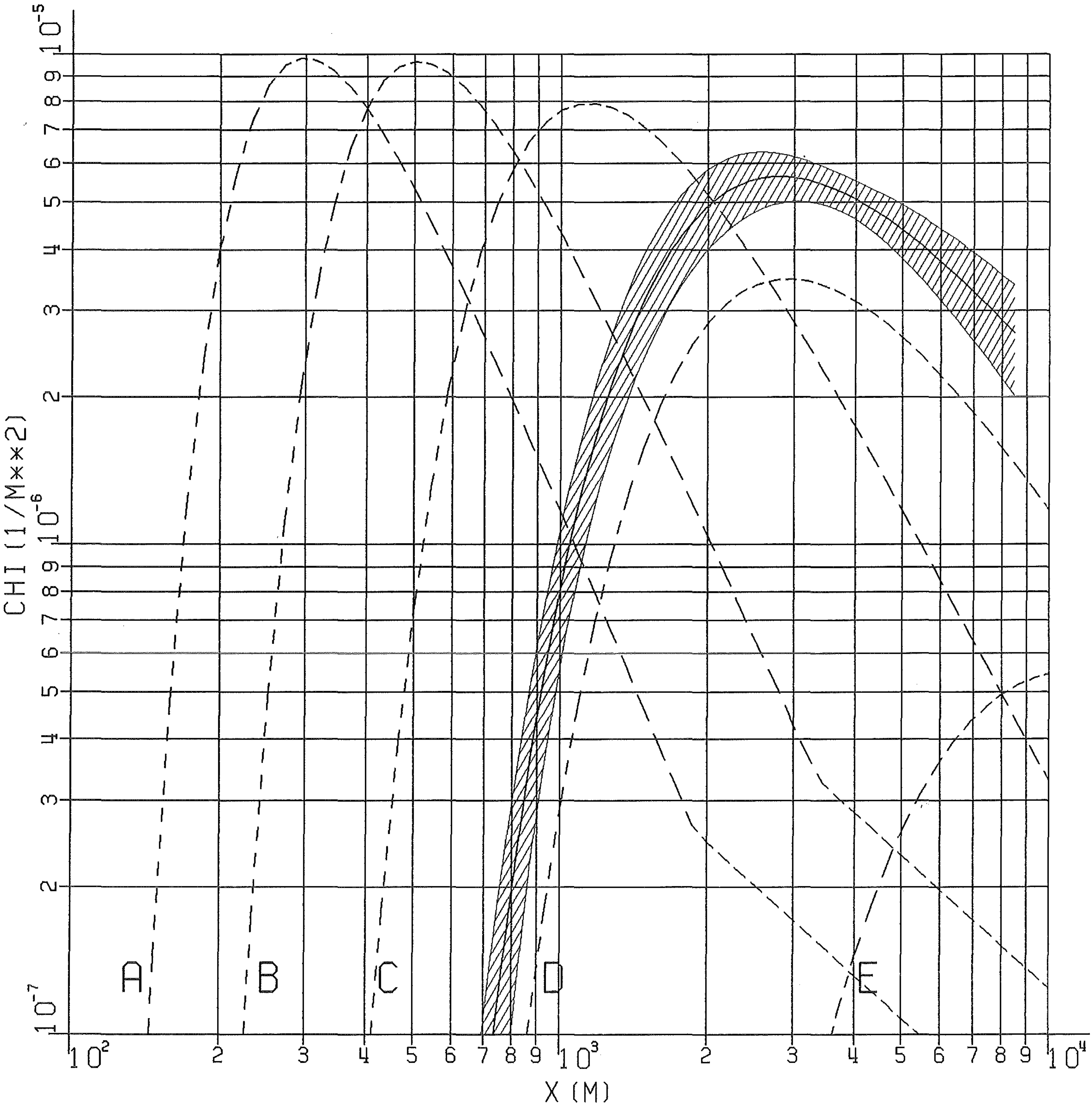

FIG. 56: NORMALIZED DIFFUSION FACTOR
OF EXPERIMENT NO.69, PERIODS 1+2
H=160M, TRACER CF2BR2
COMBINED, SMOOTHED, AND CENTERED RESULTS

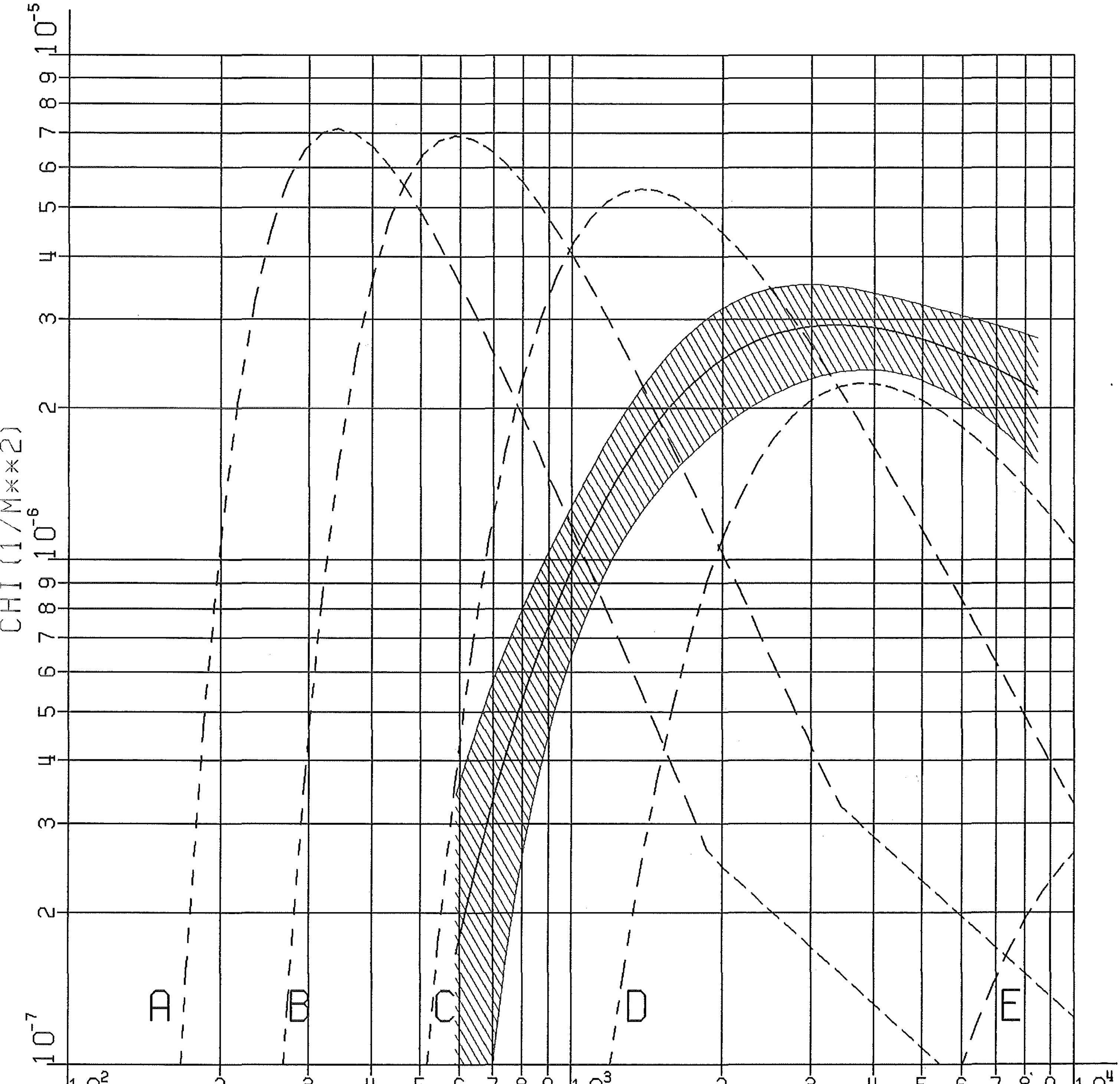

FIG. 57: NØRMALIZED DIFFUSIØN FACTØR
ØF EXPERIMENT NØ.69, PERIØDS 1+2
H=195M, TRACER CFCL3
- - - - - CØMBINED, SMØØTHED, AND CENTERED RESULTS

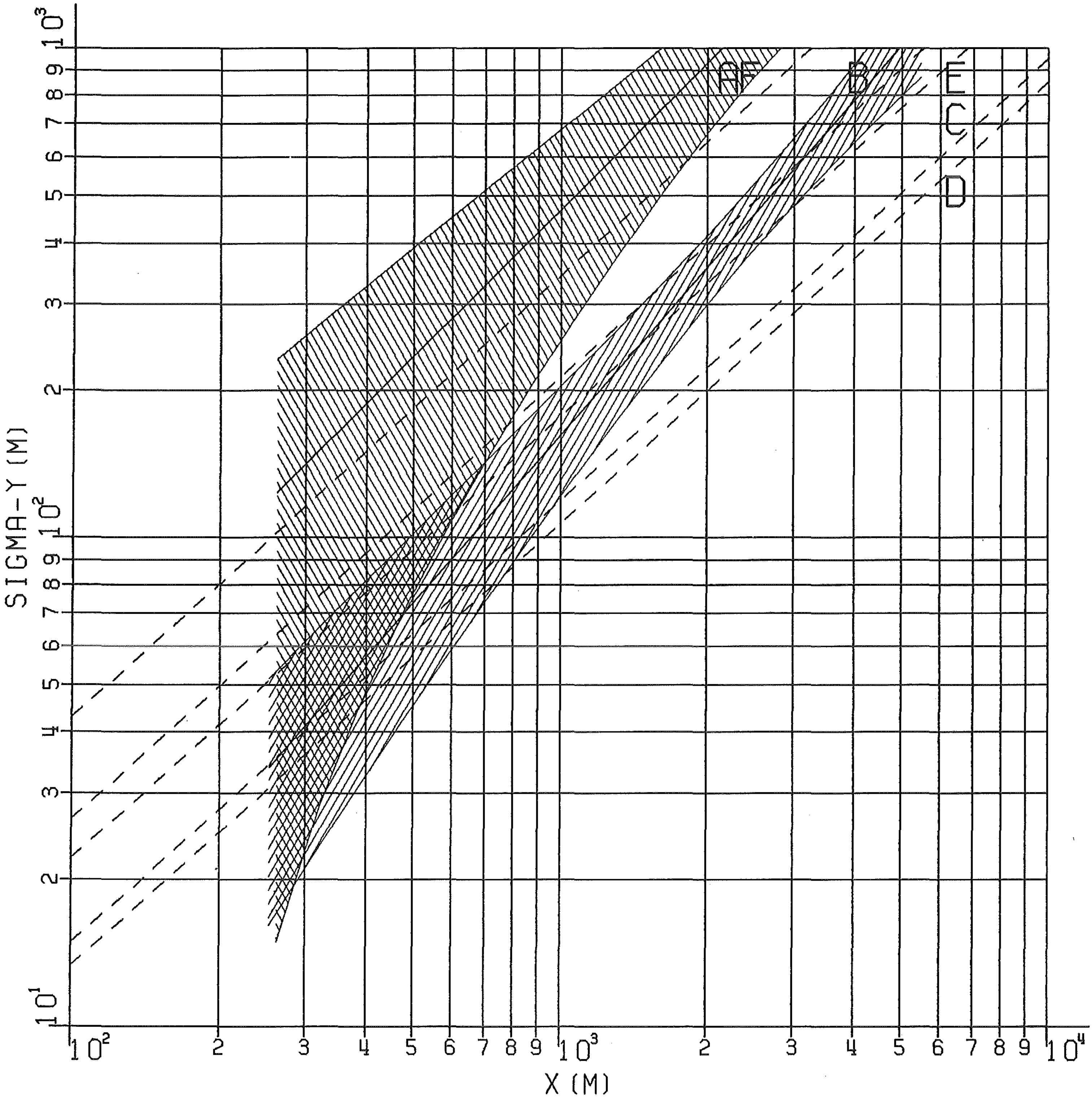

FIG. 58: HORIZONTAL DISPERSION PARAMETER
OF EXPERIMENT NO.70, PERIODS 1+2

H=160M, TRACER CFCL3

H=195M, TRACER CF2BR2

– – – – – COMBINED, SMOOTHED, AND CENTERED RESULTS

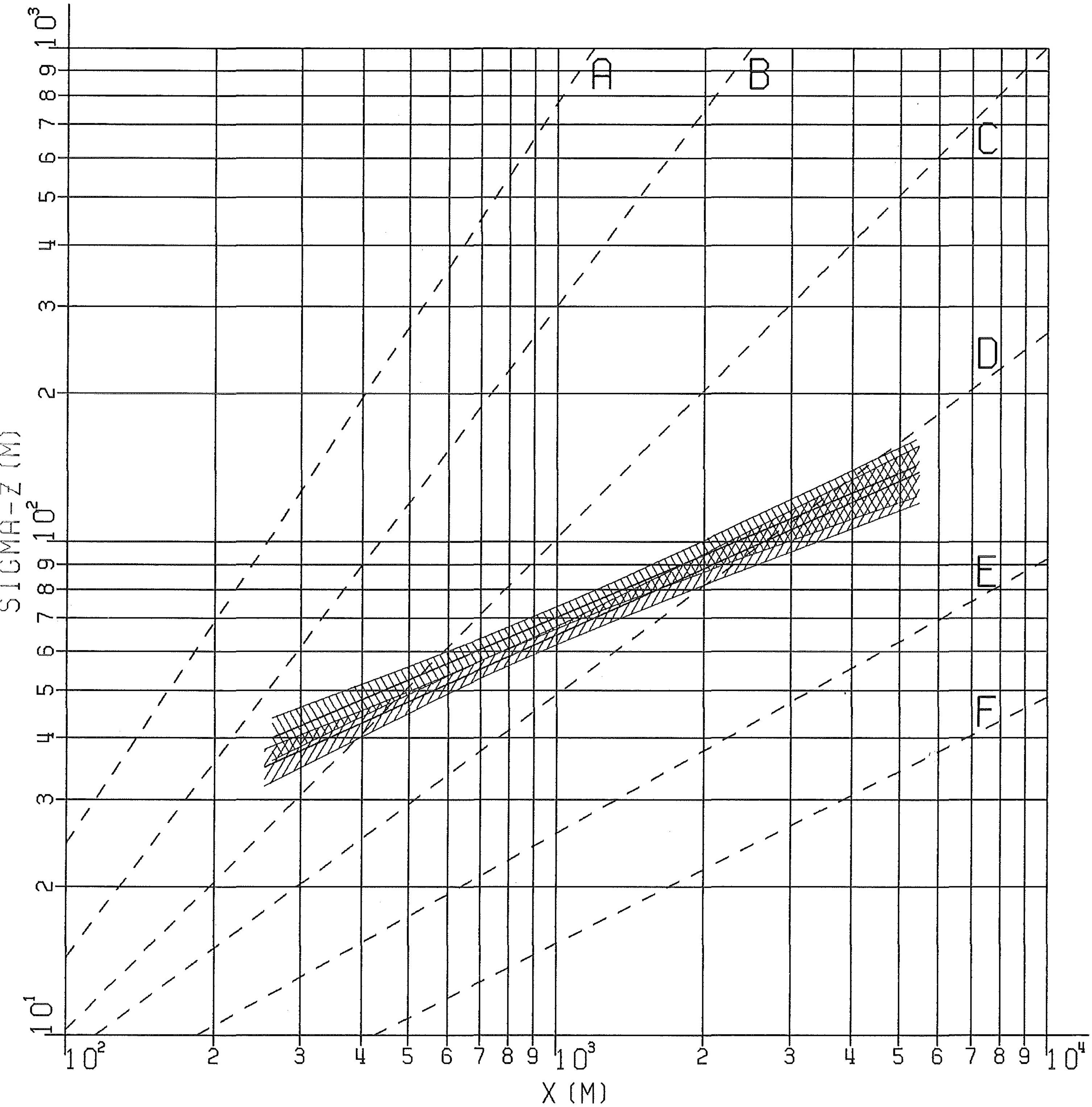

FIG. 59: VERTICAL DISPERSION PARAMETER
OF EXPERIMENT NO.70, PERIODS 1+2
H=160M, TRACER CFCL3
H=195M, TRACER CF2BR2
- - - - - COMBINED, SMOOTHED, AND CENTERED RESULTS

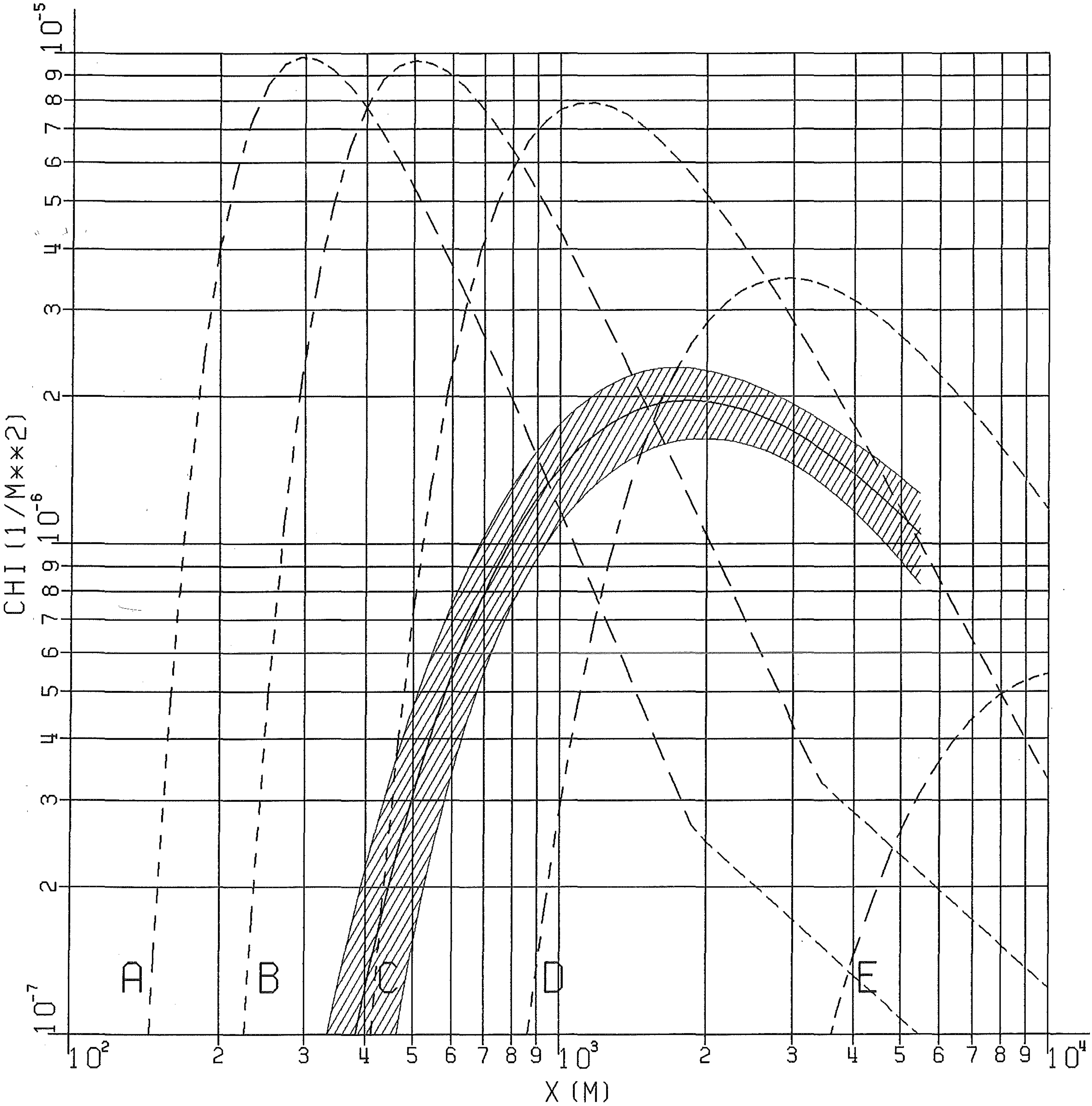

FIG. 60: NORMALIZED DIFFUSION FACTOR
OF EXPERIMENT NO.70, PERIODS 1+2
///////////// H=160M, TRACER CFCL3
– – – – – COMBINED, SMOOTHED, AND CENTERED RESULTS

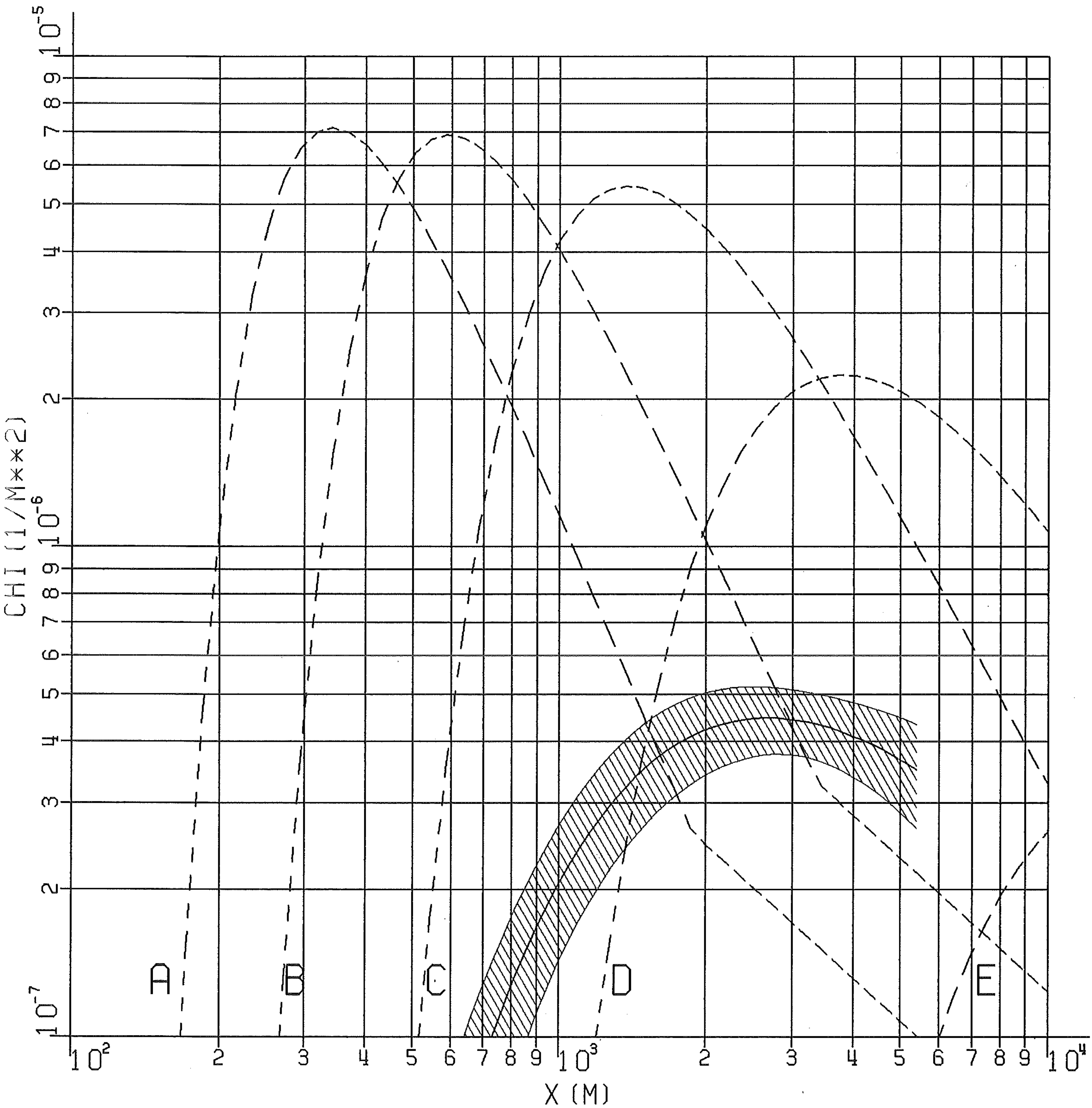

FIG. 61: NORMALIZED DIFFUSION FACTOR
OF EXPERIMENT NO.70, PERIODS 1+2
H=195M, TRACER CF2BR2
- - - - - COMBINED, SMOOTHED, AND CENTERED RESULTS

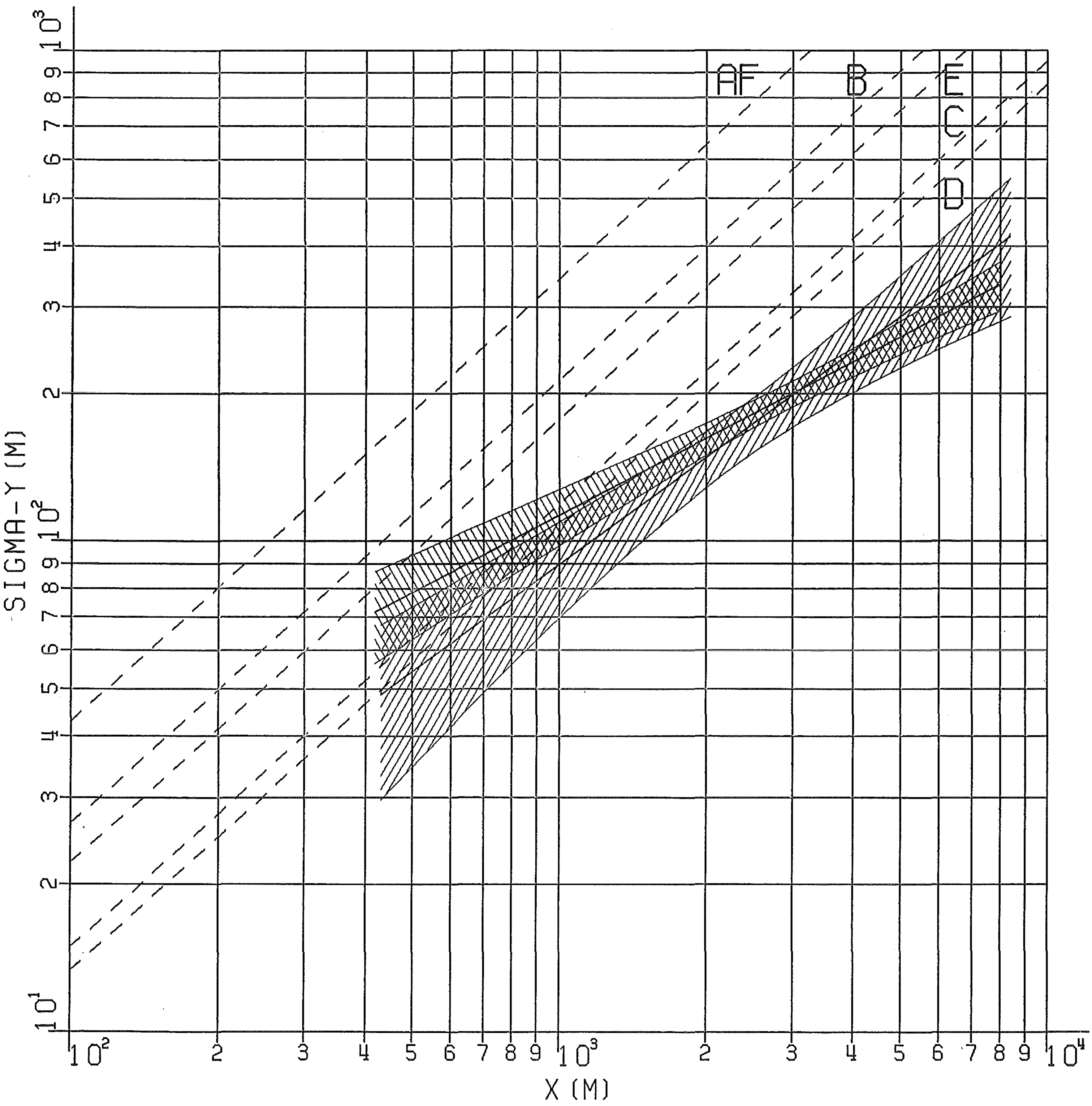

FIG. 62: HORIZONTAL DISPERSION PARAMETER
OF EXPERIMENT NO. 72, PERIODS 1+2

H=160M, TRACER CFCL3

H=160M, TRACER CFCL3 (JRC ISPRA)

----- COMBINED, SMOOTHED, AND CENTERED RESULTS

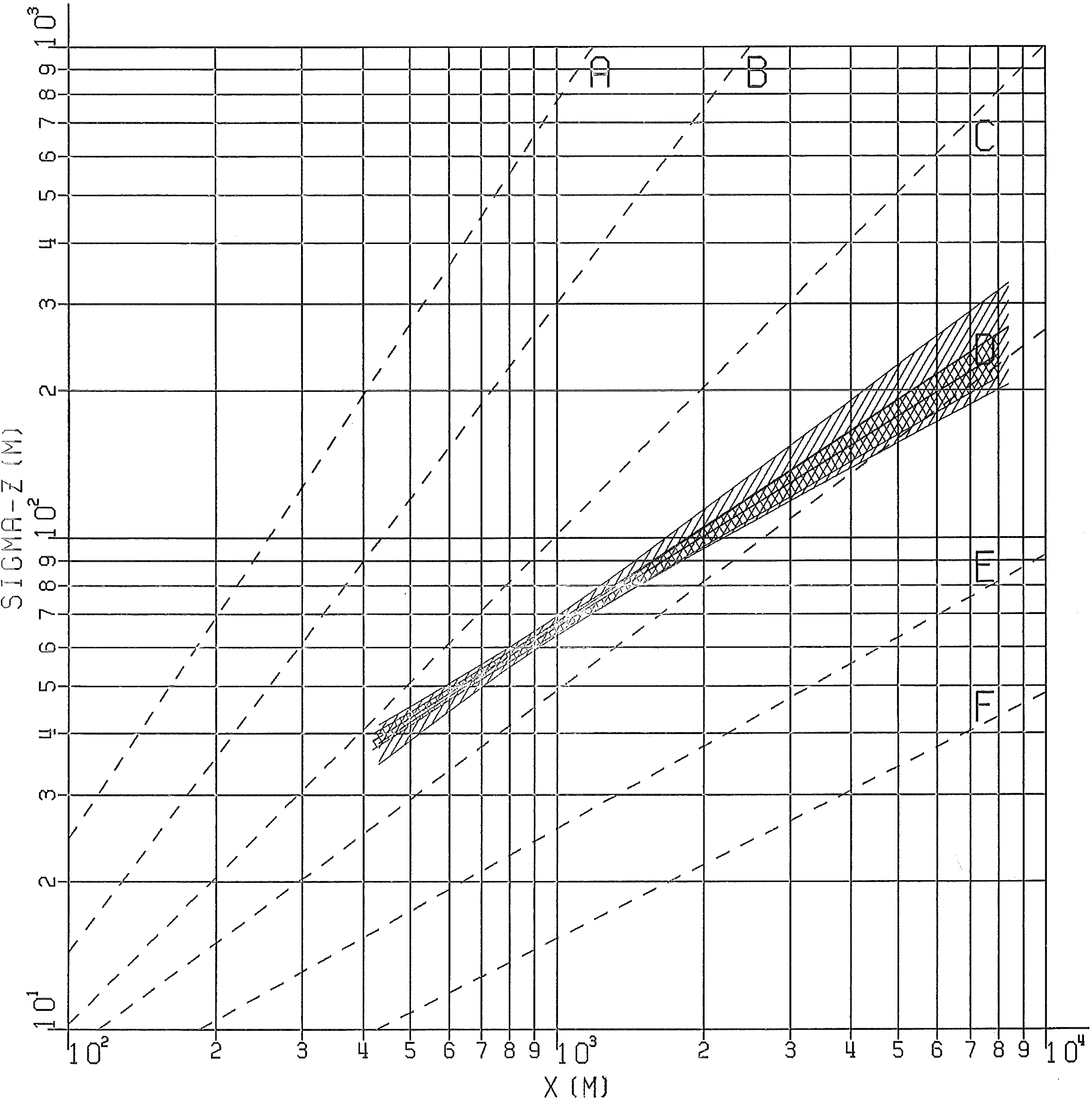

FIG. 63: VERTICAL DISPERSION PARAMETER
OF EXPERIMENT NO.72, PERIODS 1+2
H=160M, TRACER CFCL3
H=160M, TRACER CFCL3 (J R C ISPRA)
- - - - - COMBINED, SMOOTHED, AND CENTERED RESULTS

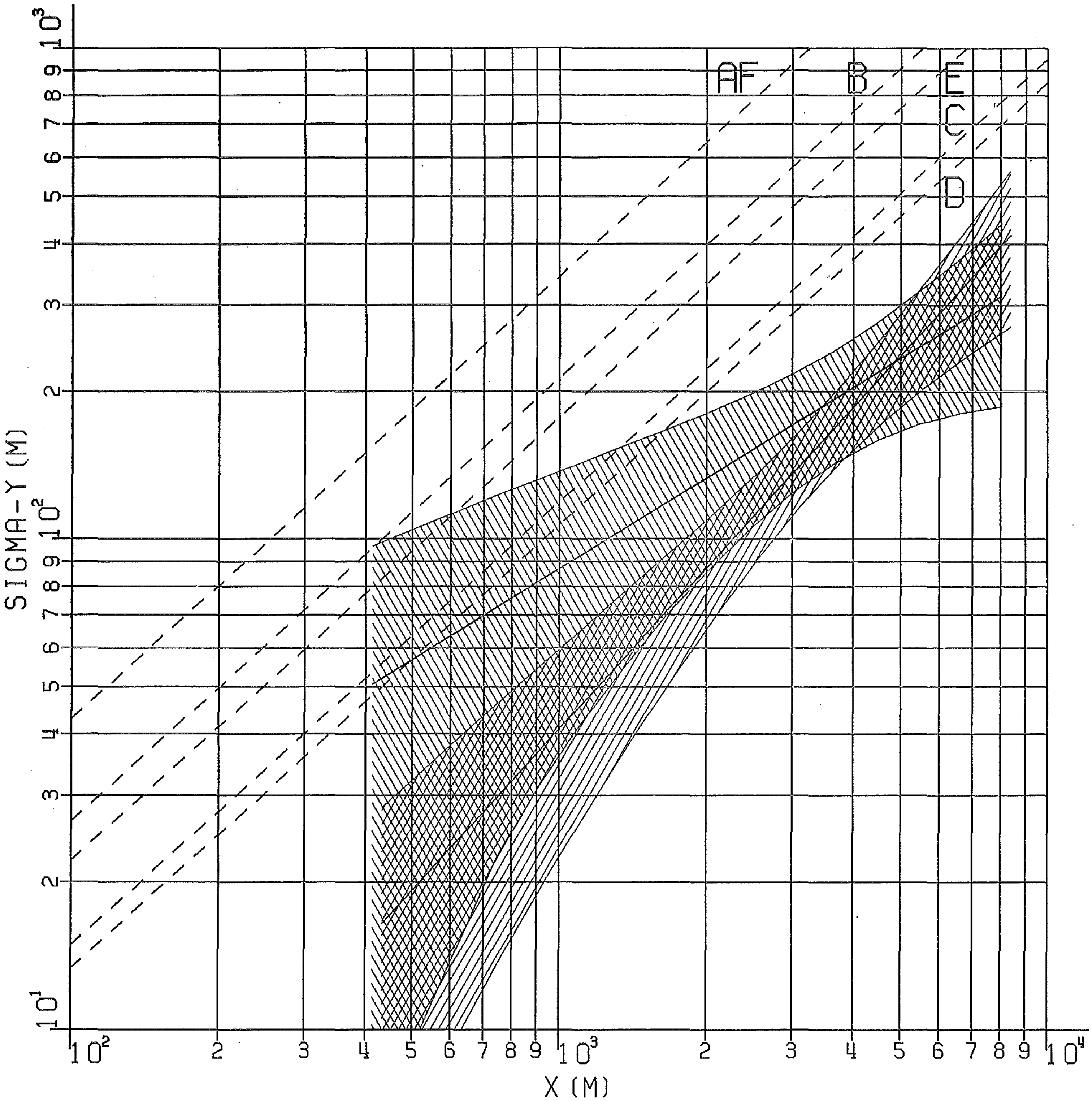

FIG. 64: HORIZONTAL DISPERSION PARAMETER
OF EXPERIMENT NO.72, PERIODS 1+2

//////////// H=195M, TRACER CF2BR2

\\\\\\\\\\\\ H=195M, TRACER SF6

- - - - - COMBINED, SMOOTHED, AND CENTERED RESULTS

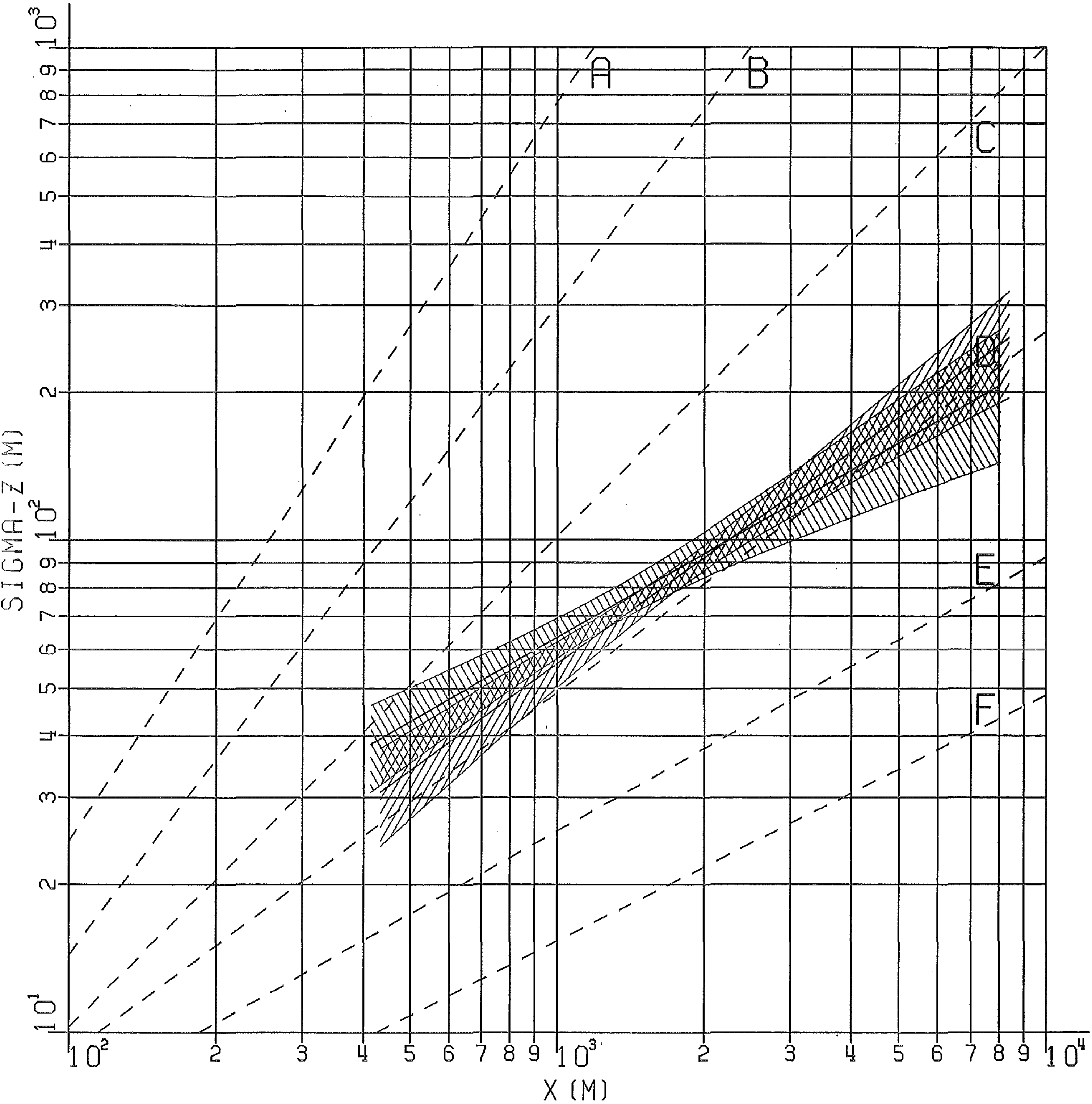

FIG. 65: VERTICAL DISPERSION PARAMETER
OF EXPERIMENT NO.72, PERIODS 1+2
////////// H=195M, TRACER CF2BR2
\\\\\\\\\\ H=195M, TRACER SF6
- - - - - COMBINED, SMOOTHED, AND CENTERED RESULTS

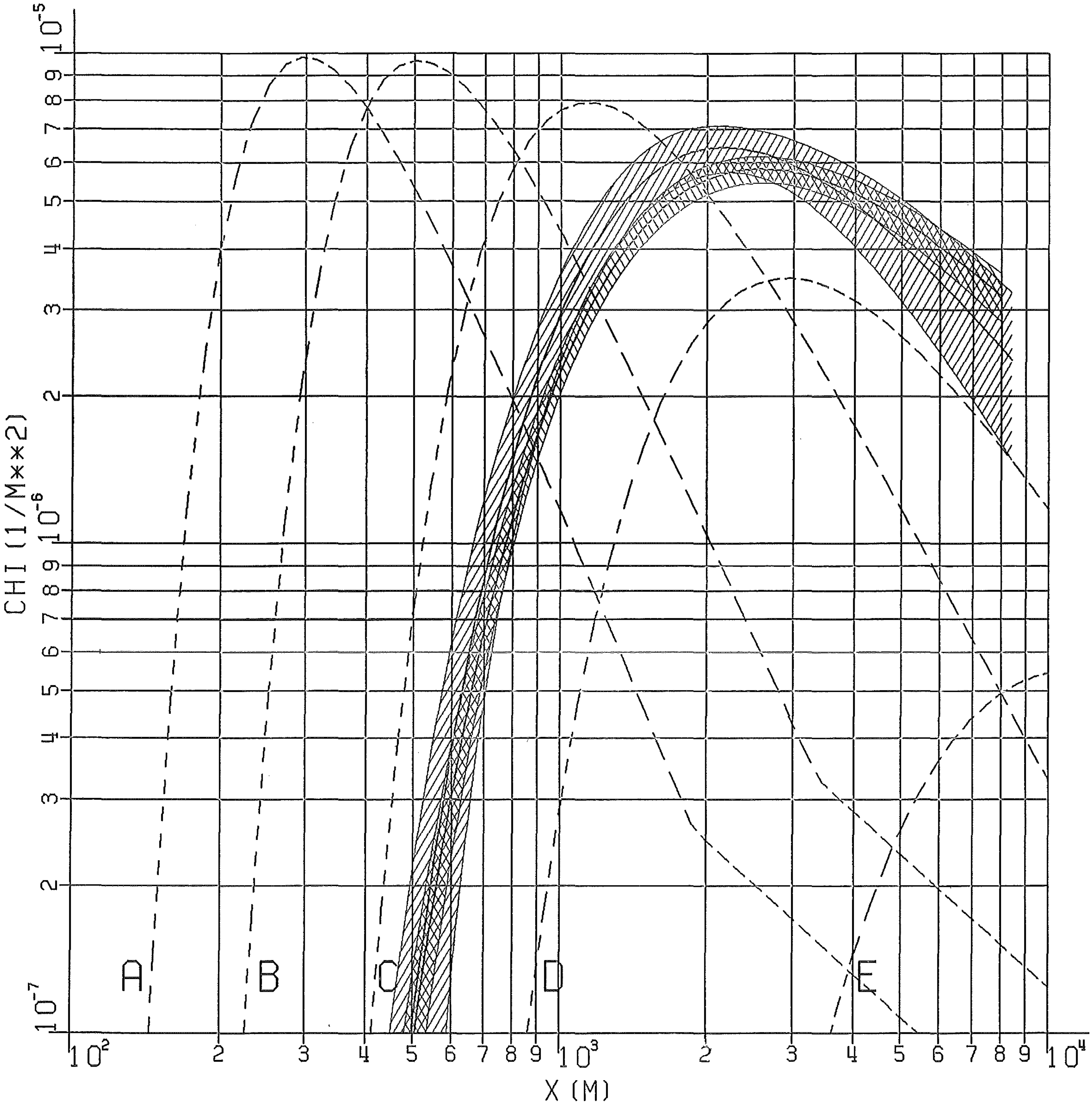

FIG. 66: NORMALIZED DIFFUSION FACTOR
OF EXPERIMENT NO.72, PERIODS 1+2

H=160M, TRACER CFCL3
H=160M, TRACER CFCL3 (JRC ISPRA)
- - - - - COMBINED, SMOOTHED, AND CENTERED RESULTS

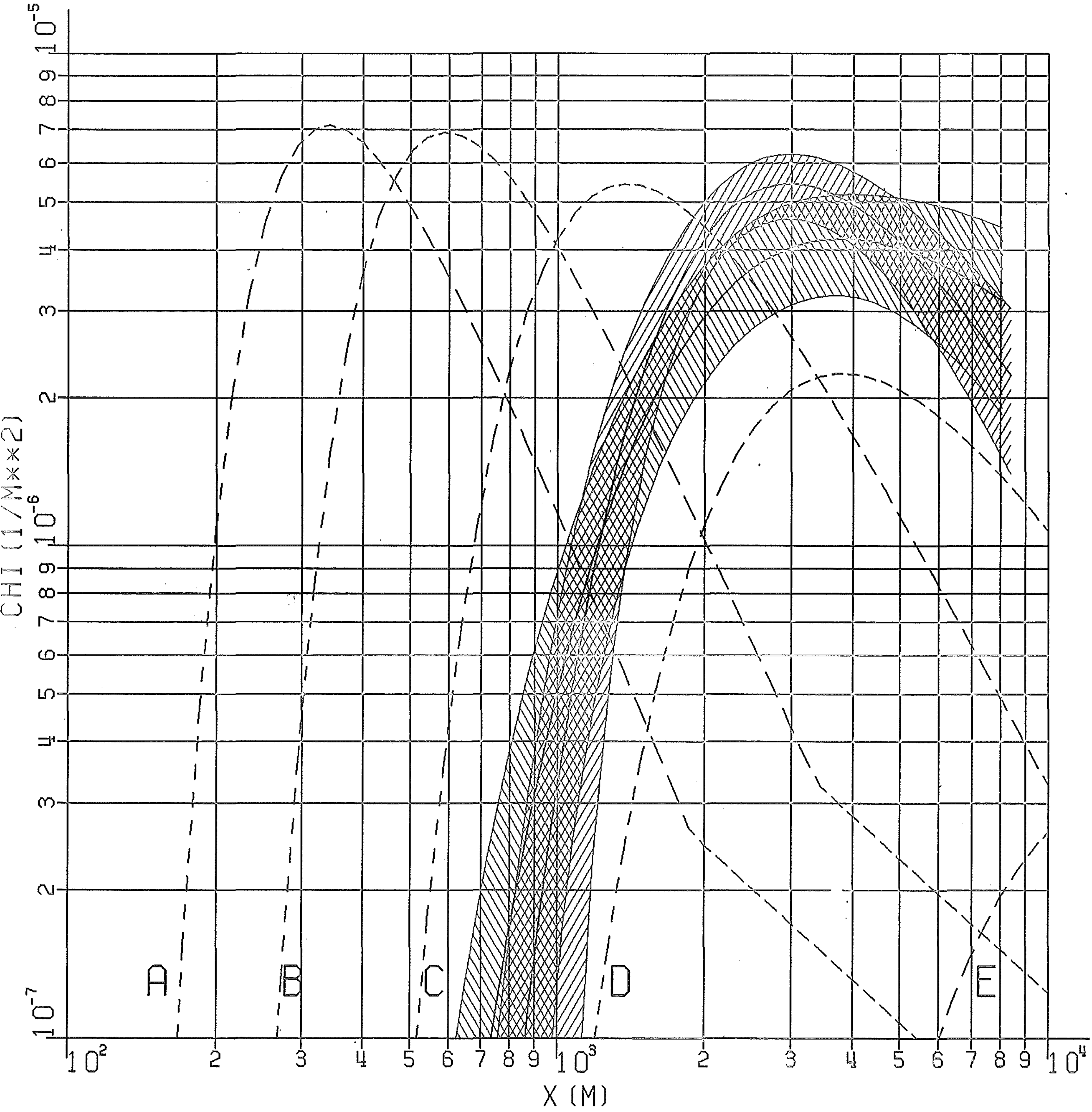

FIG. 67: NØRMALIZED DIFFUSIØN FACTØR
ØF EXPERIMENT NØ.72, PERIØDS 1+2

/////////////// H=195M, TRACER CF2BR2

\\\\\\\\\\\\\\\\ H=195M, TRACER SF6

- - - - - CØMBINED, SMØØTHED, AND CENTERED RESULTS

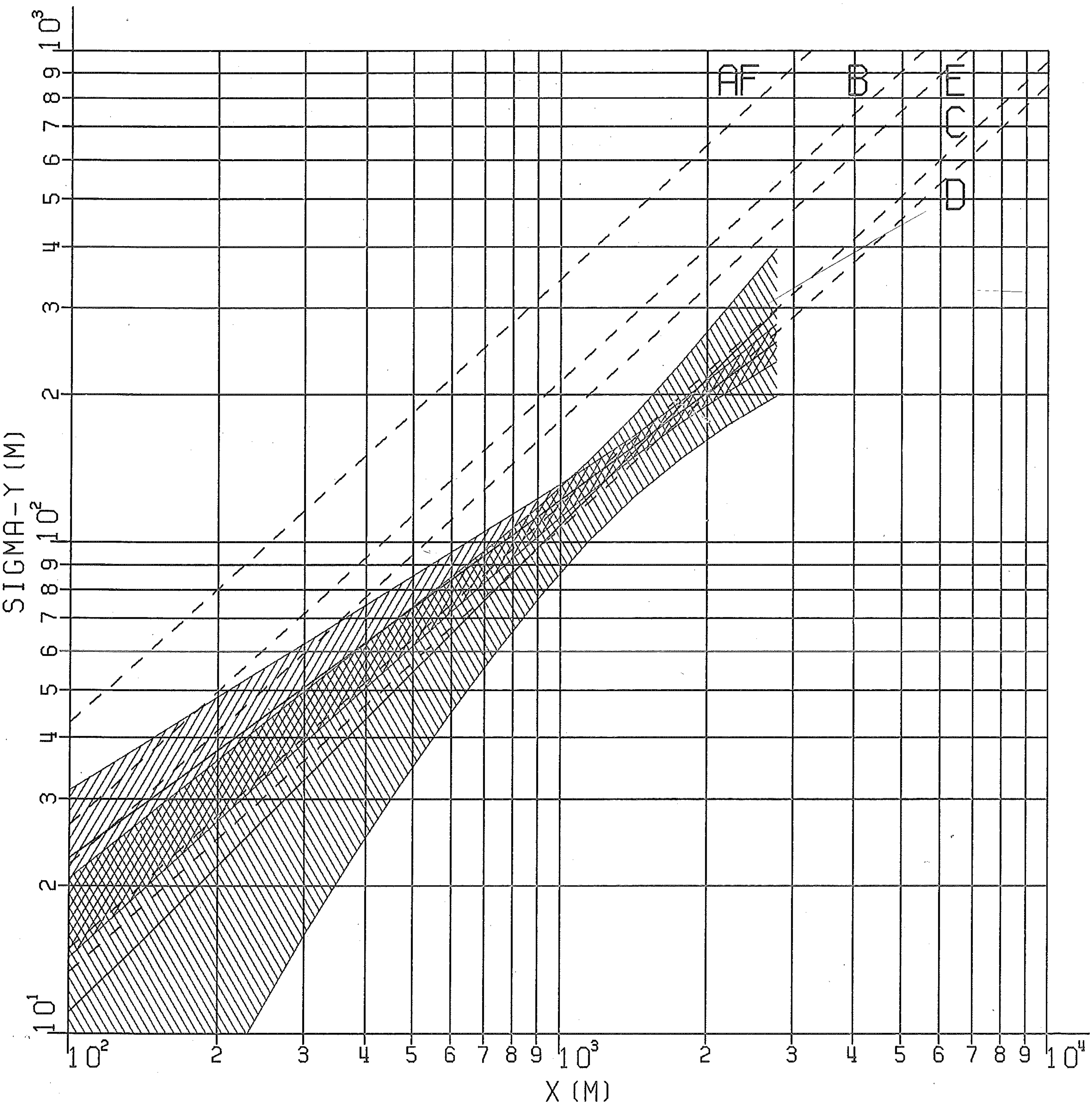

FIG. 68: HORIZONTAL DISPERSION PARAMETER
OF EXPERIMENT NO.73, PERIODS 1+2

H=195M, TRACER CF2BR2

H=160M, TRACER CFCL3

- - - - - COMBINED, SMOOTHED, AND CENTERED RESULTS

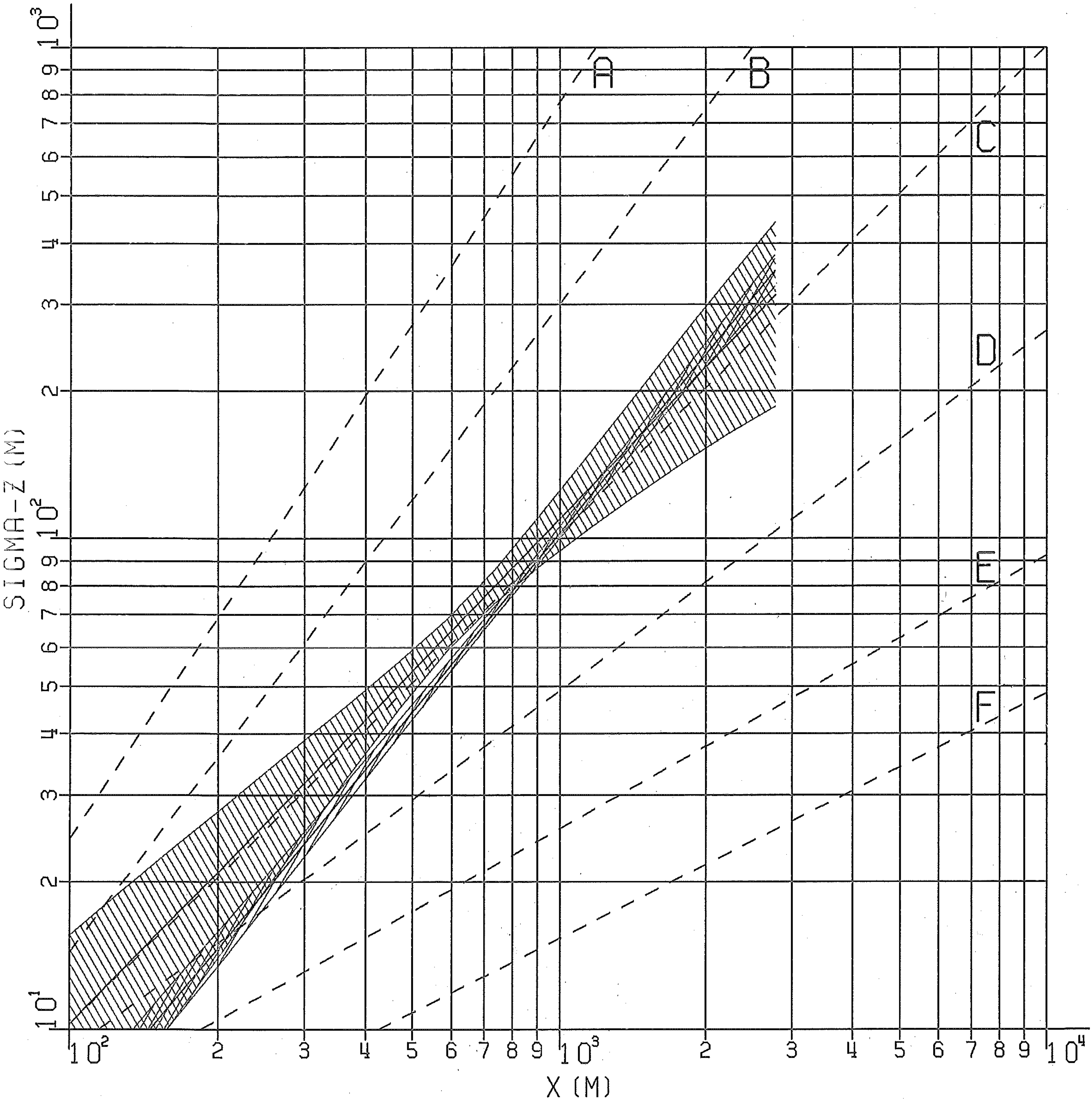

FIG. 69: VERTICAL DISPERSION PARAMETER
OF EXPERIMENT NO. 73, PERIODS 1+2

//////////// H=195M, TRACER CF2BR2

\\\\\\\\\\\\ H=160M, TRACER CFCL3

- - - - - COMBINED, SMOOTHED, AND CENTERED RESULTS

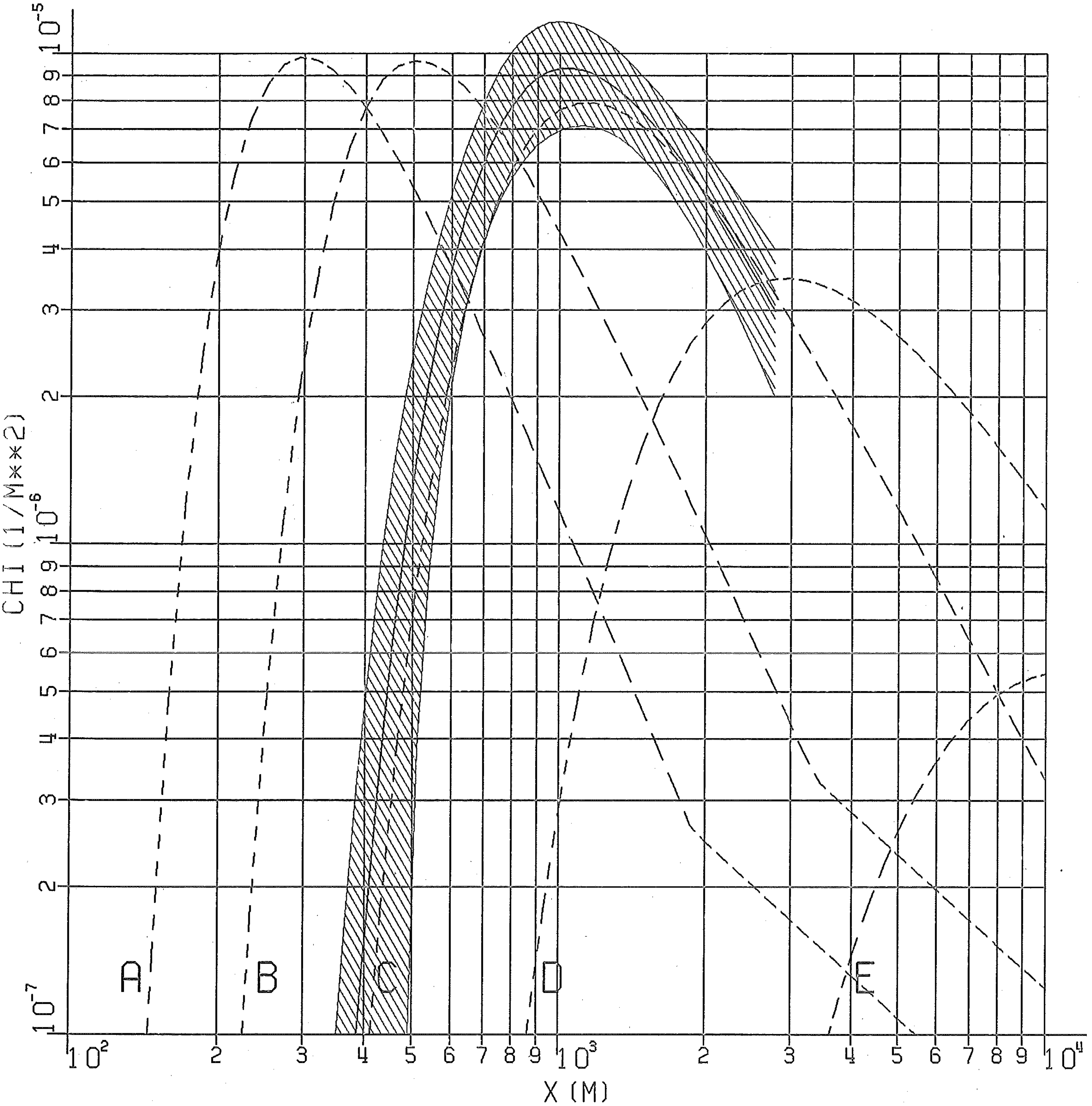

FIG. 70: NORMALIZED DIFFUSION FACTOR
OF EXPERIMENT NO.73, PERIODS 1+2
H=160M, TRACER CFCL3
- - - - - COMBINED, SMOOTHED, AND CENTERED RESULTS

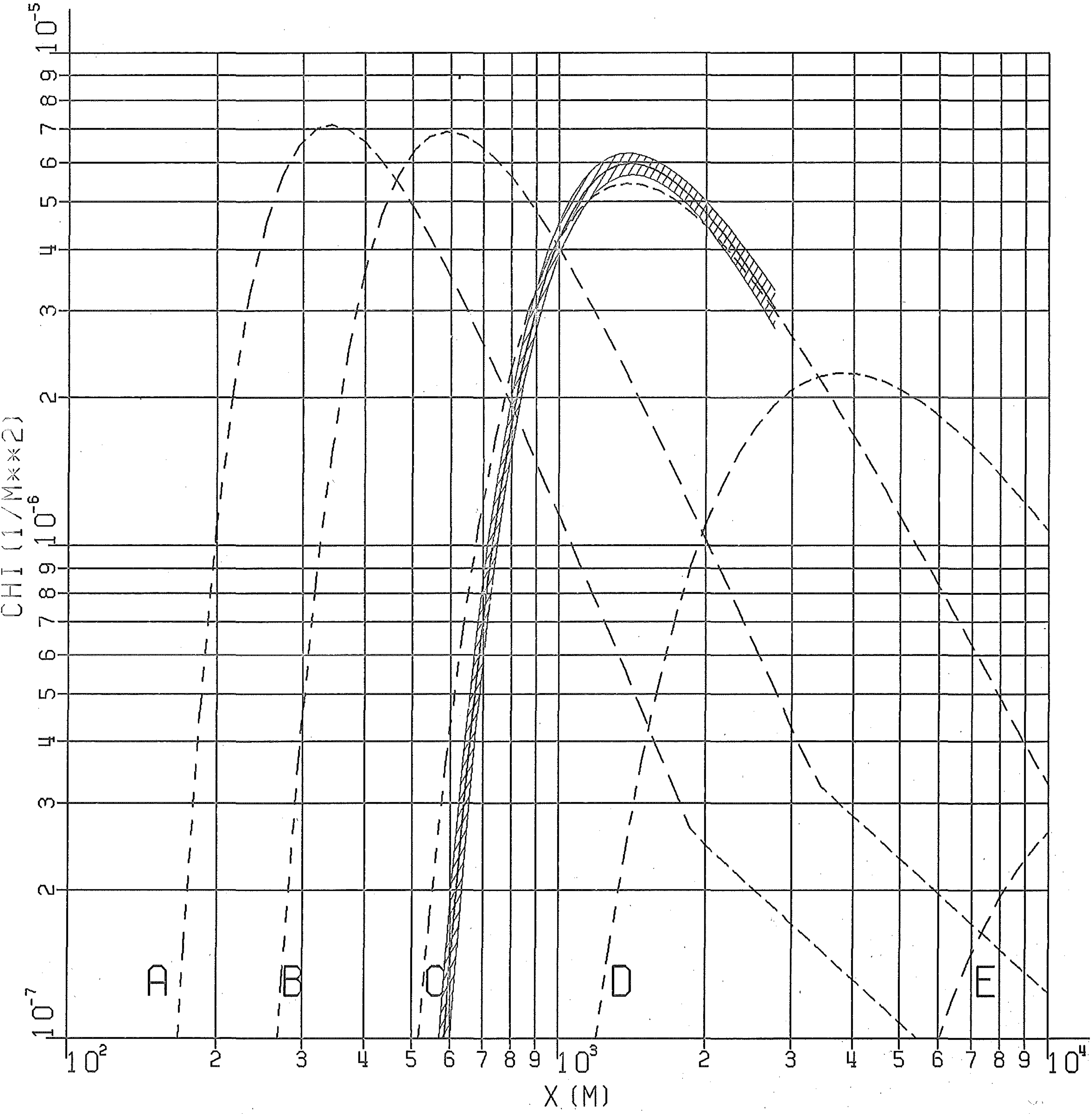

FIG. 71: NORMALIZED DIFFUSION FACTOR
OF EXPERIMENT NO.73, PERIODS 1+2
////////////// H=195M, TRACER CF2BR2
- - - - - COMBINED, SMOOTHED, AND CENTERED RESULTS

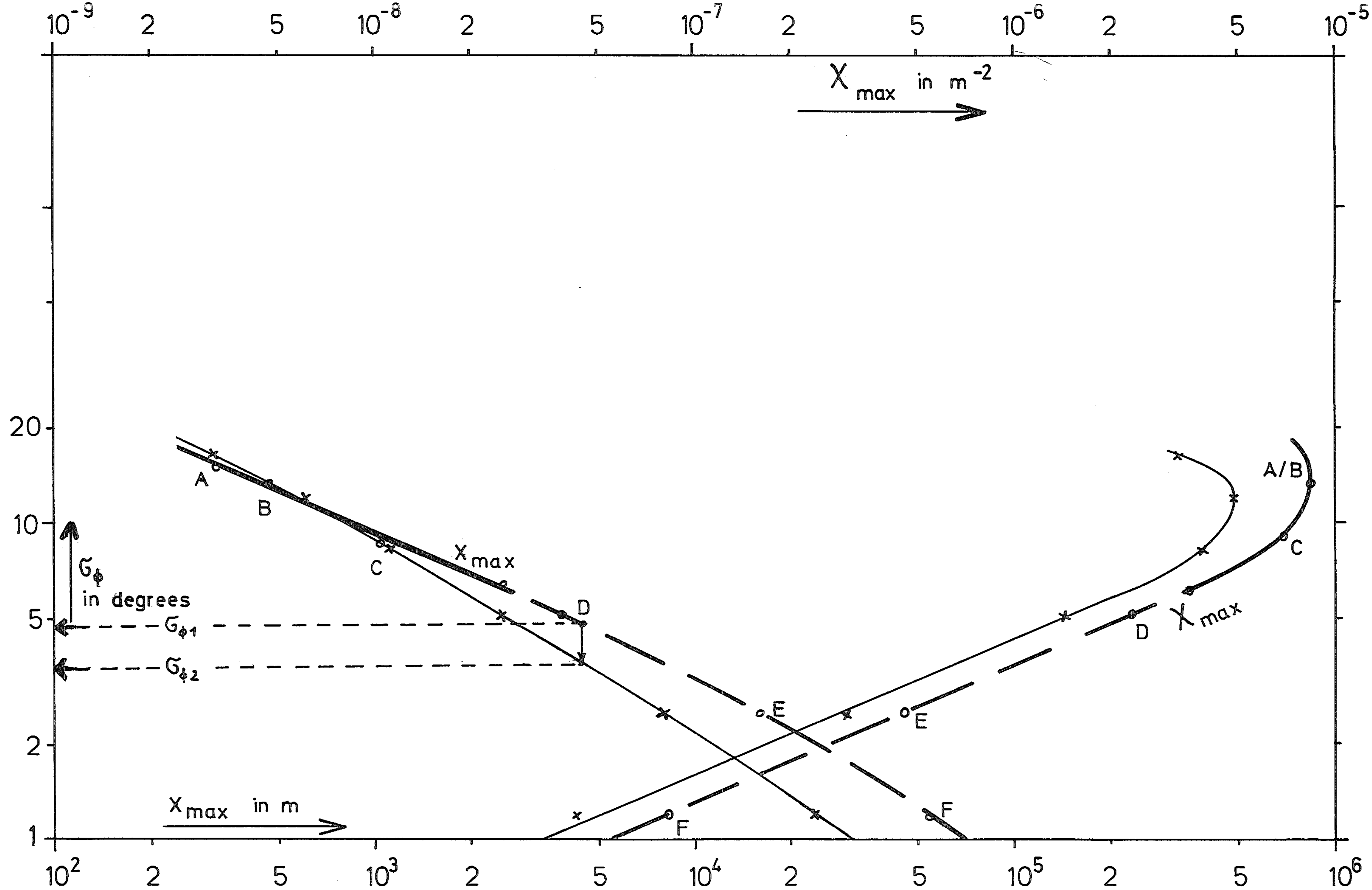

Figure 72: Standard deviation σ_ϕ of the vertical wind direction versus position x_{max} of the maximum of the normalized diffusion factor χ_{max} for a source height of 180 m

——— σ_y and σ_z from H = 60 m and 100 m [17]

▬▬▬ σ_y and σ_z from H = 160 m and 195 m

▬ ▬ ▬ extrapolated

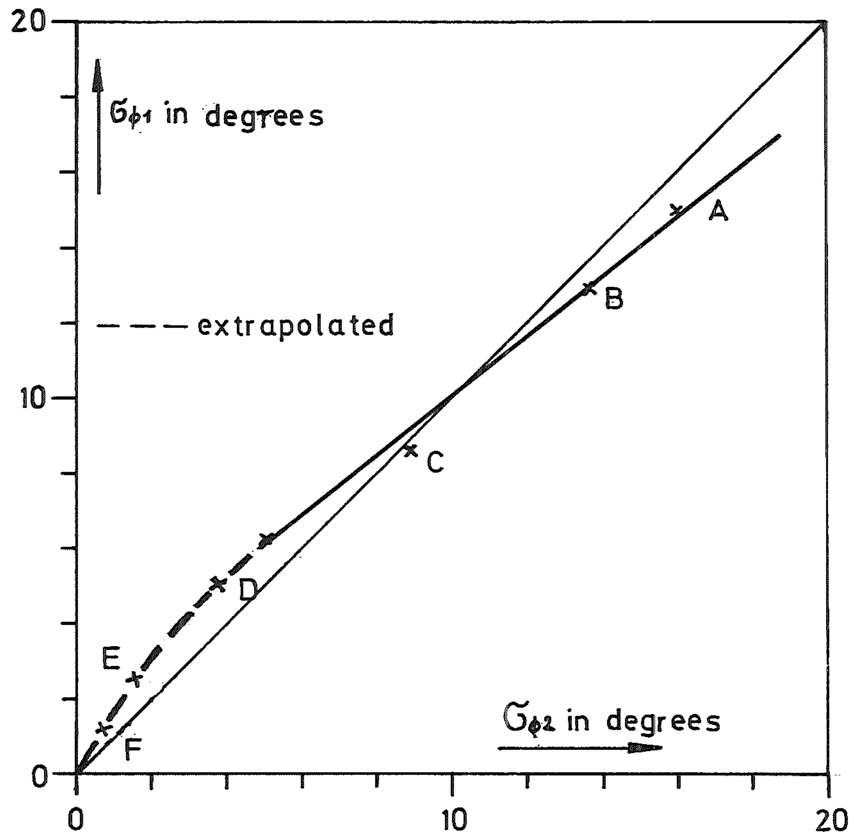

Figure 73: Relation of $\sigma_{\phi 1}$ (small source heights) and
$\sigma_{\phi 2}$ (great source heights)

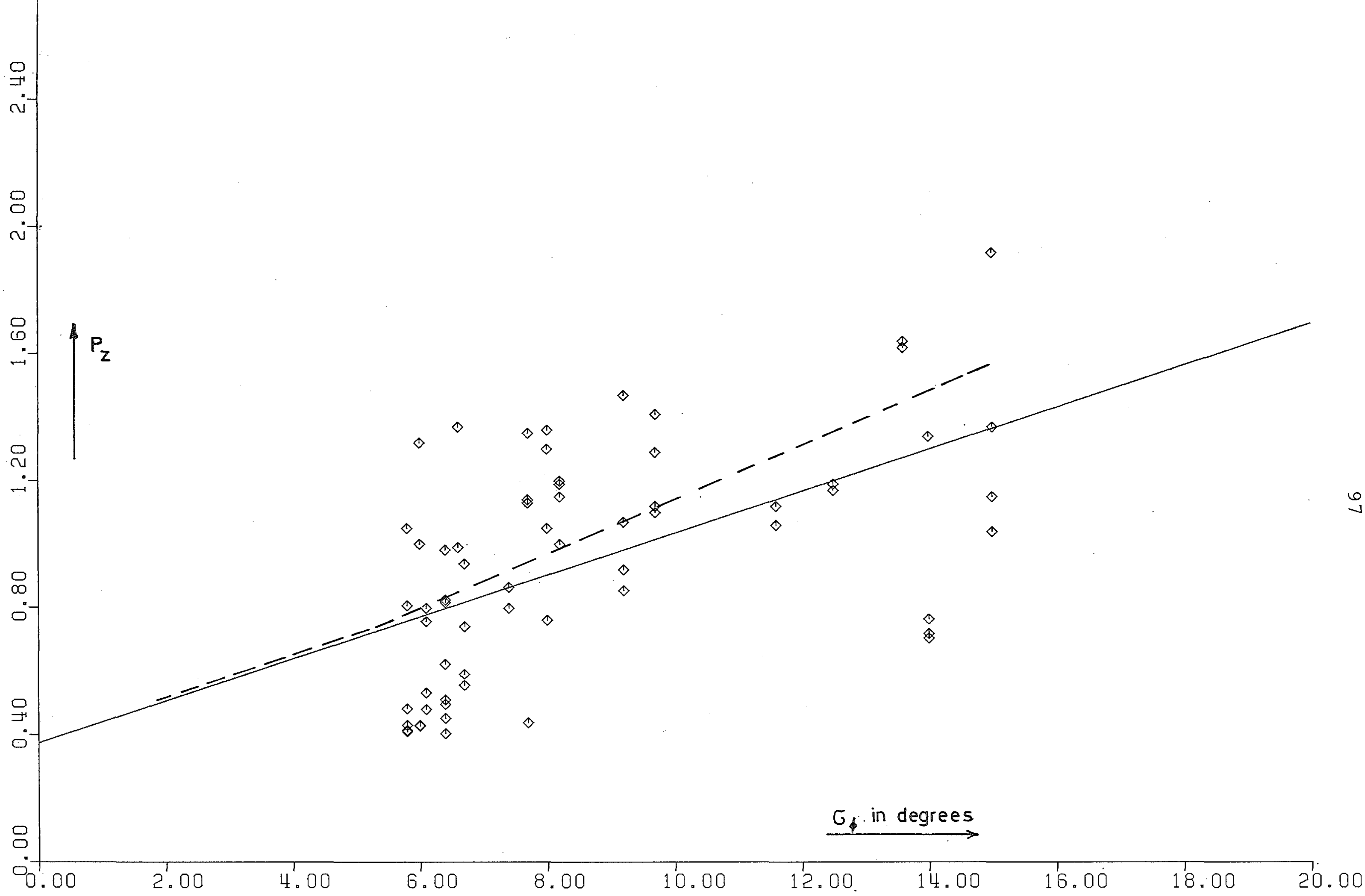

Figure 74: Scatter plot of p_z versus σ_ϕ of individual periods
——— linear regression with a correlation coefficient of 0.55
– – – derived from the results of the experiments with smaller source heights

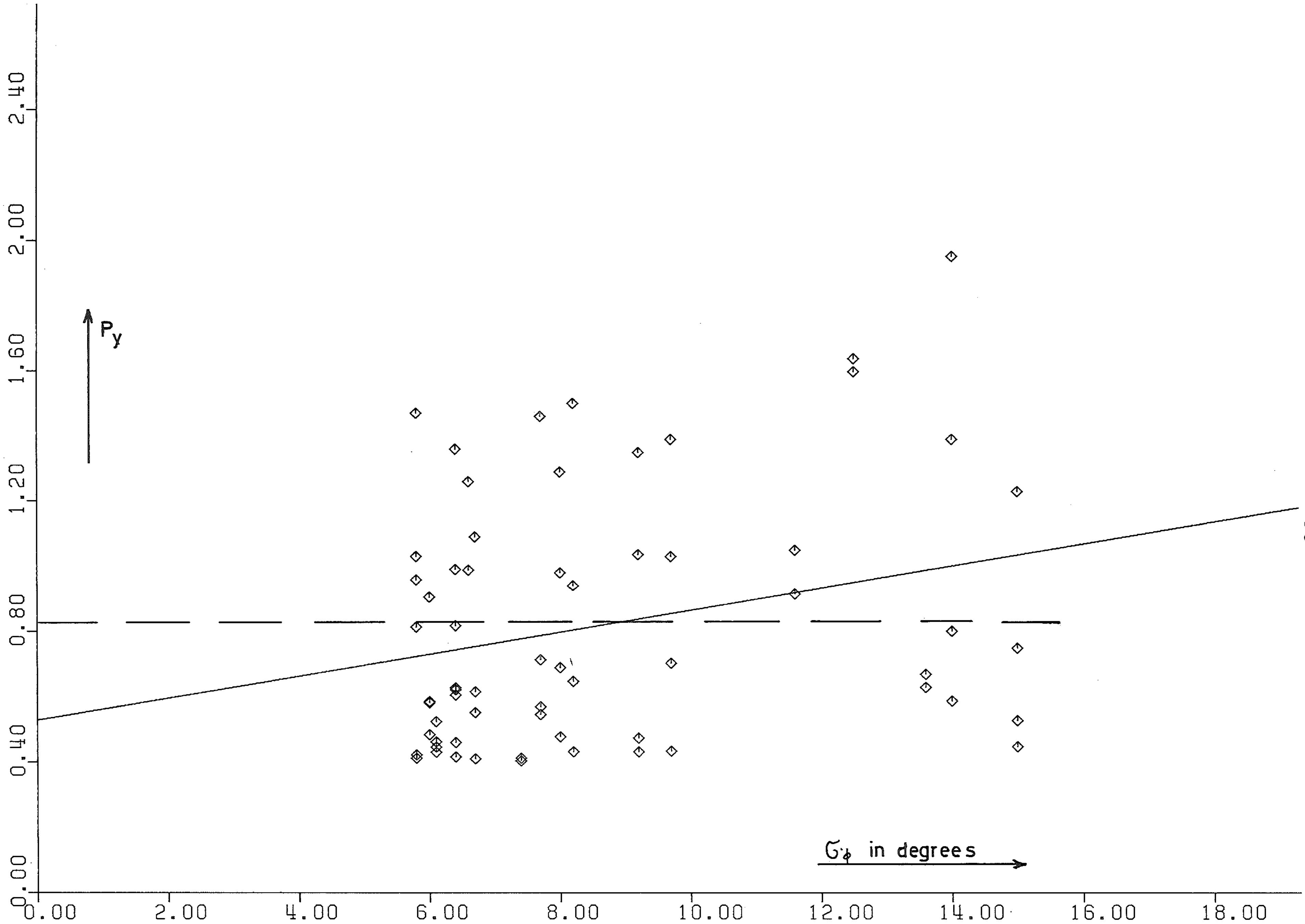

Figure 75: Scatter plot of p_y versus σ_ϕ of individual periods
——— linear regression
– – – – arithmetic mean value

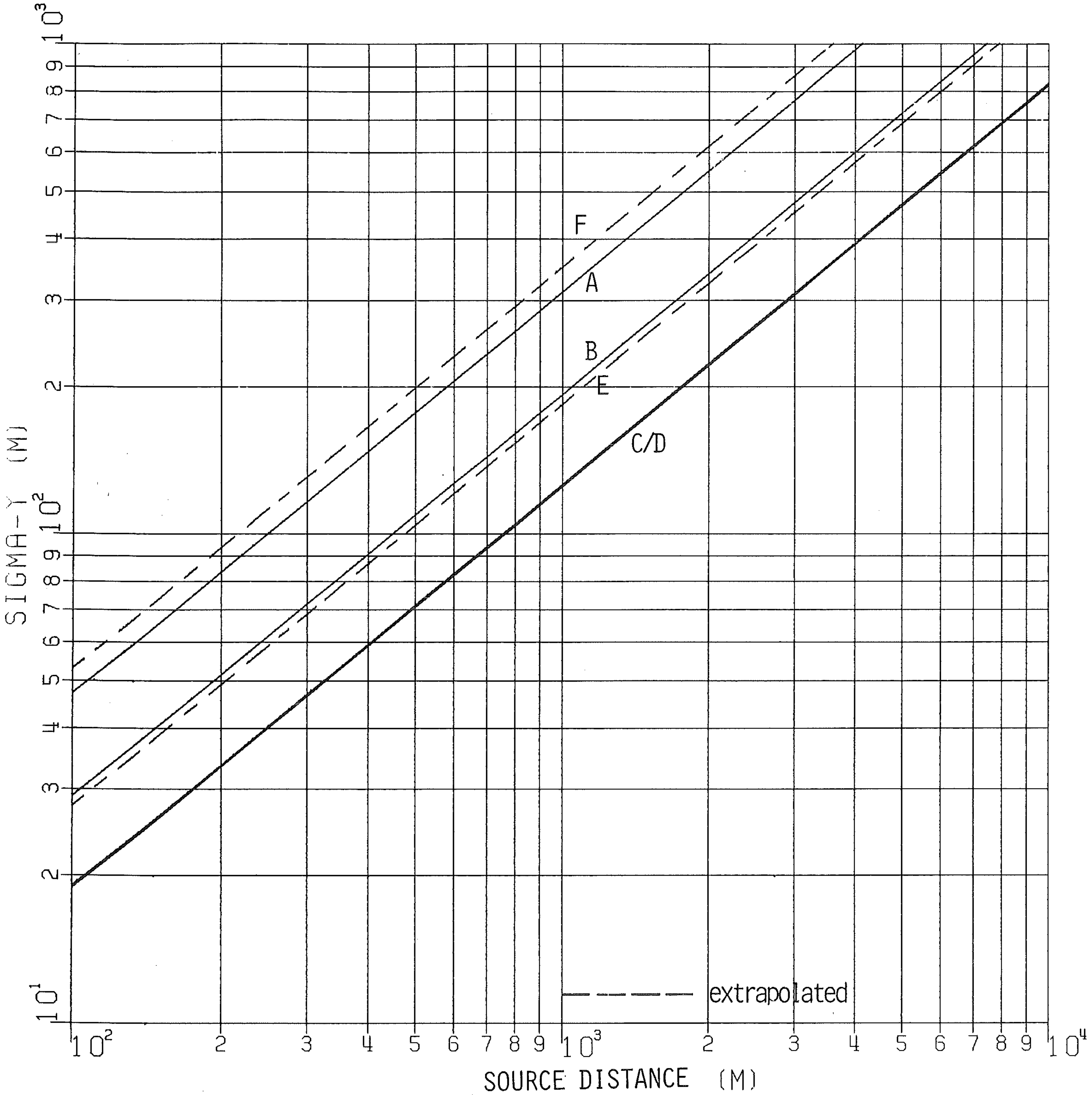

Fig. 76: Combined,smoothed,and centered horizontal dispersion parameters

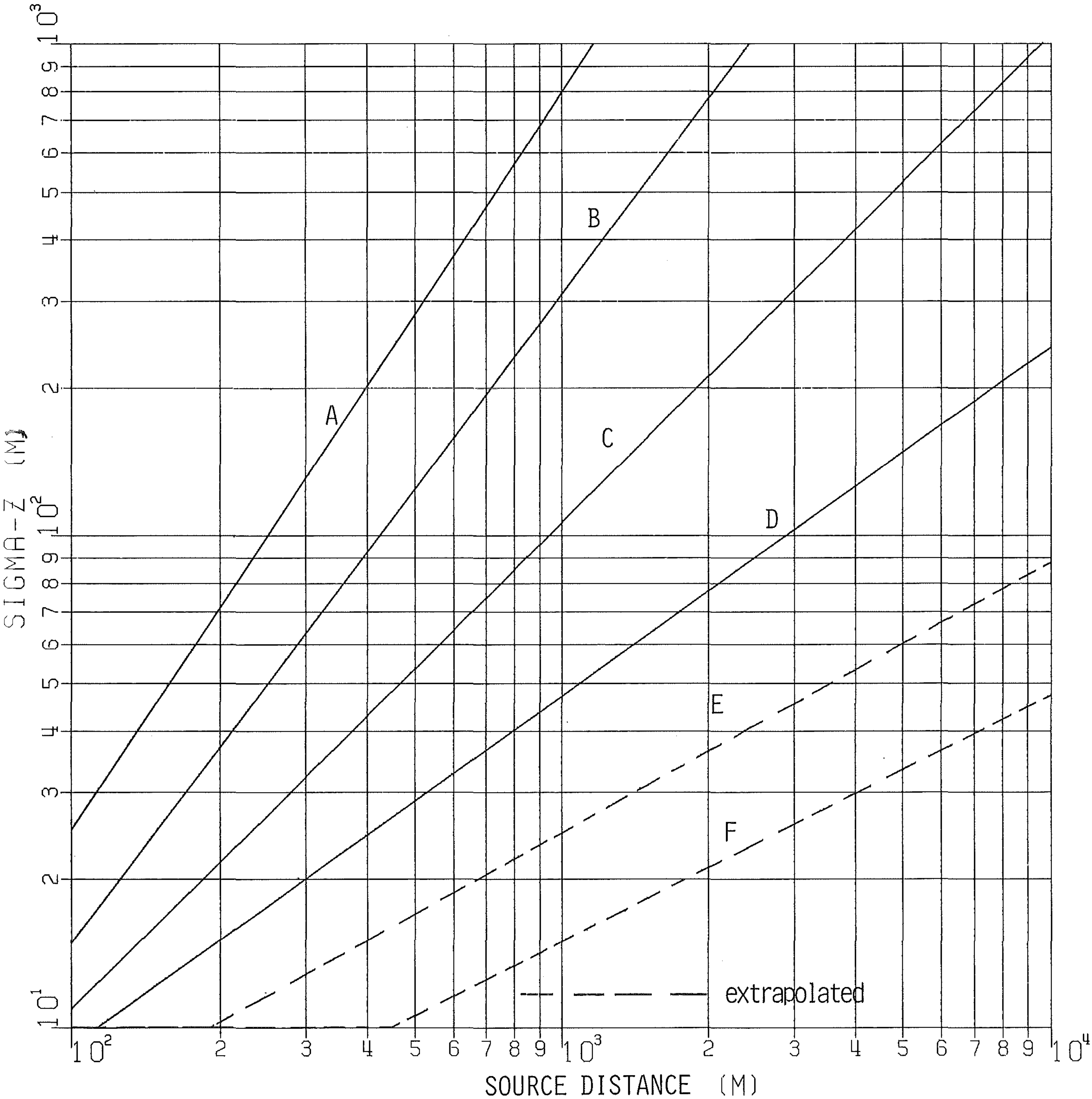

Fig. 77: Combined, smoothed, and centered vertical dispersion parameters

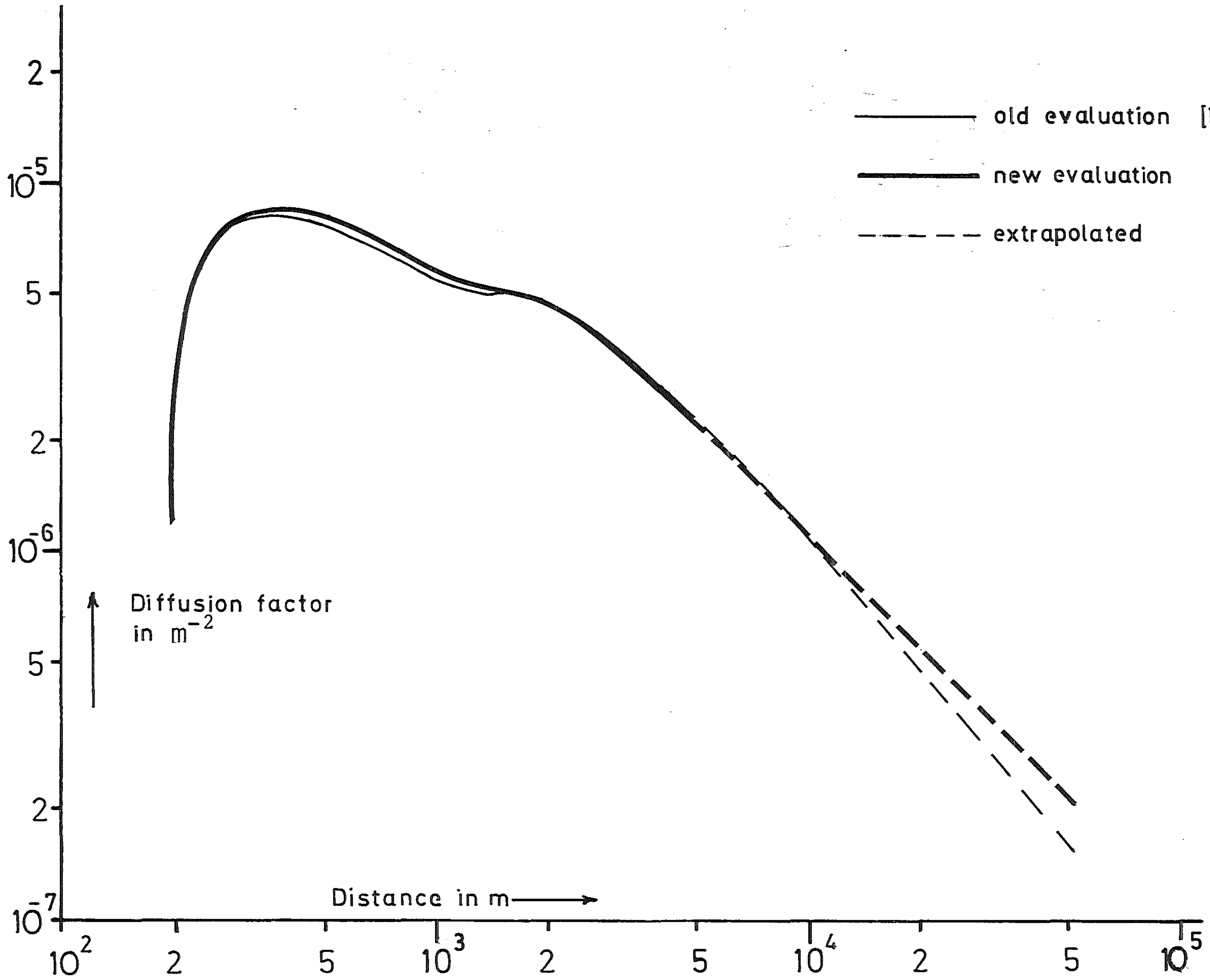

Figure 78: Normalized short-term diffusion factor

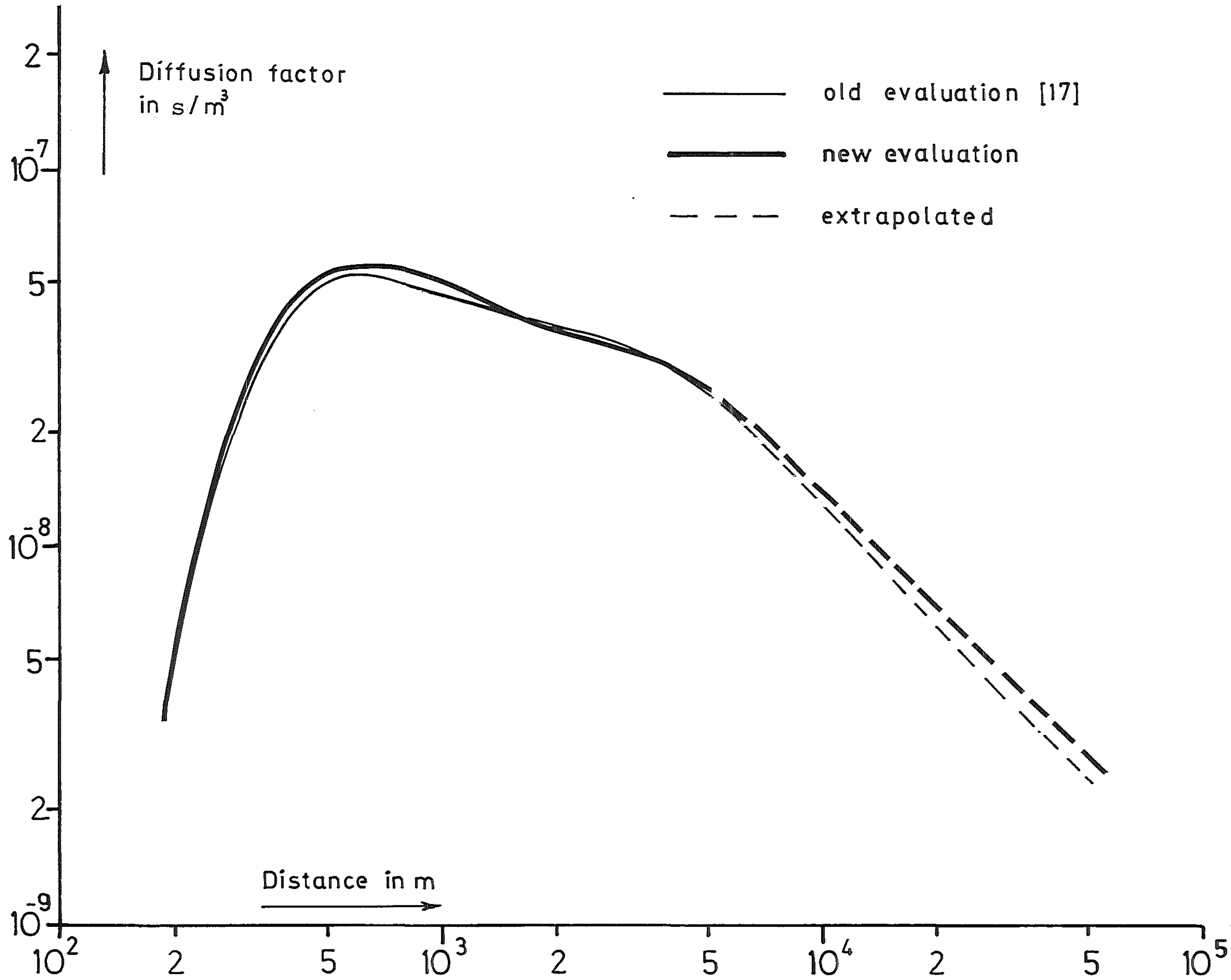

Figure 79: Maximum long-term diffusion factor